STUDIES OF THE PHYSICAL AND CHEMICAL PROPERTIES OF 1,4 DIOXANE AND THEIR RELEVANCE TO ADSORPTION AND TRANSDERMAL ABSORPTION

by

ALI JAFAR MAHDI

B.V. M. & S., University of Baghdad, 1982
M.Sc., University of Baghdad, 1988
B.A., University of Baghdad, 1999
M.S., Kansas State University, 2010

AN ABSTRACT OF A DISSERTATION

Submitted in partial fulfillment of the requirements for the degree

DOCTOR OF PHILOSOPHY

Department of Diagnostic Medicine and Pathobiology
College of Veterinary Medicine

KANSAS STATE UNIVERSITY
Manhattan, Kansas

2014

Abstract

1,4-Dioxane is a potentially carcinogenic solvent. It is a problematic groundwater contaminant because of its unique physical-chemical properties. It is found in a wide range of consumer products as a by-product contaminant. This research aimed to investigate contaminant properties and behavior of dioxane in the environment and also in the human body. The dioxane ability to decontamination by adsorption processes was evaluated with four adsorbents. The adsorption efficiencies of activated carbon (AC), metal oxide nanomaterials (TiO_2 and MgO), and diatomaceous earth (DE) were assessed in aqueous and vapor phases using infrared spectroscopy. AC showed the highest adsorptive capacity for dioxane at equilibrium in both phases. The rate and extent of dermal absorption are important in the analysis of risk from dermal exposure to dioxane. For this purpose, a new flow through diffusion system (FTDS) was developed by modifying a Bronaugh flow through diffusion cell with flow capacity in both the donor and receptor compartments and using attenuated total reflection Fourier transform infrared spectroscopy (ATR-FTIR) as the analytical technique. FTDS can provide 'real time' quantitative high-density permeation data over time and is characterized by the simplicity of its use and the low cost of test samples. The *in vitro* dermal absorption study of dioxane across human skin showed that the absorption parameters of dioxane were 1.16 ± 0.22 hr, 5.7 X 10^{-4} ± (0.62) cm/hr, 0.286 ± 0.035 mg/cm^2/hr, 4.8 X 10^{-5} (± 0.32) cm^2/hr, and 1.99 ± 0.086 mg for lag time, permeability, steady-state flux, diffusivity, and total amount absorbed over 8 hr, respectively. The study of the effect of the surfactant sodium lauryl sulphate and solvent systems water, ethanol, propylene glycol, and ethyl acetate on permeation profiles revealed that these solvents and surfactants increased the permeation of dioxane significantly. The FT-IR spectra of stratum corneum treated with solvents showed that there was broadening of the CH_2 asymmetric

stretching vibration of the CH_2 peak near 2920 cm^{-1} only in samples treated with ethanol. The lipid extract precipitates were detected and were mostly composed of the stratum corneum lipid part.

STUDIES OF THE PHYSICAL AND CHEMICAL PROPERTIES OF 1,4 DIOXANE AND THEIR RELEVANCE TO ADSORPTION AND TRANSDERMAL ABSORPTION

by

ALI JAFAR MAHDI

B.V. M. & S., University of Baghdad, 1982
M.Sc., University of Baghdad, 1988
B.A., University of Baghdad, 1999
M.S., Kansas State University, 2010

A DISSERTATION

Submitted in partial fulfillment of the requirements for the degree

DOCTOR OF PHILOSOPHY

Department of Diagnostic Medicine and Pathobiology
College of Veterinary Medicine

KANSAS STATE UNIVERSITY
Manhattan, Kansas

2014

Approved by:

Major Professor
Deon van der Merwe

Copyright

Abstract

1,4-Dioxane is a potentially carcinogenic solvent. It is a problematic groundwater contaminant because of its unique physical-chemical properties. It is found in a wide range of consumer products as a by-product contaminant. This research aimed to investigate contaminant properties and behavior of dioxane in the environment and also in the human body. The dioxane ability to decontamination by adsorption processes was evaluated with four adsorbents. The adsorption efficiencies of activated carbon (AC), metal oxide nanomaterials (TiO_2 and MgO), and diatomaceous earth (DE) were assessed in aqueous and vapor phases using infrared spectroscopy. AC showed the highest adsorptive capacity for dioxane at equilibrium in both phases. The rate and extent of dermal absorption are important in the analysis of risk from dermal exposure to dioxane. For this purpose, a new flow through diffusion system (FTDS) was developed by modifying a Bronaugh flow through diffusion cell with flow capacity in both the donor and receptor compartments and using attenuated total reflection Fourier transform infrared spectroscopy (ATR-FTIR) as the analytical technique. FTDS can provide 'real time' quantitative high-density permeation data over time and is characterized by the simplicity of its use and the low cost of test samples. The *in vitro* dermal absorption study of dioxane across human skin showed that the absorption parameters of dioxane were 1.16 ± 0.22 hr, 5.7 X 10^{-4} ± (0.62) cm/hr, 0.286 ± 0.035 mg/cm^2/hr, 4.8 X 10^{-5} (± 0.32) cm^2/hr, and 1.99 ± 0.086 mg for lag time, permeability, steady-state flux, diffusivity, and total amount absorbed over 8 hr, respectively. The study of the effect of the surfactant sodium lauryl sulphate and solvent systems water, ethanol, propylene glycol, and ethyl acetate on permeation profiles revealed that these solvents and surfactants increased the permeation of dioxane significantly. The FT-IR spectra of stratum corneum treated with solvents showed that there was broadening of the CH_2 asymmetric

stretching vibration of the CH_2 peak near 2920 cm^{-1} only in samples treated with ethanol. The lipid extract precipitates were detected and were mostly composed of the stratum corneum lipid part.

Table of Contents

List of Figures

List of Tables

Acknowledgements

I would like to express my deepest and sincere gratitude to my doctorate advisor Dr. Deon van der Merwe who provided me with advising, and was a main reason of research completion. I greatly appreciate the freedom he gave me and the opportunity to pursue my research in my own way.

I would like to extend the highest gratitude to Dr. Gary Anderson the director of the Veterinary Diagnostic Laboratory-Kansas State University who provided invaluable guidance and support throughout the process

I would also like to sincerely thank my academic advisory committee members Dr. Steven Galitzer the director of the department of Environmental Health and Safety - Kansas State University and Dr. Saugata Datta for their expert advice and for carefully evaluating my dissertation.

I would like to give my sincere thanks to Lori Blevins the Toxicology lab manager who helped me along the way of my work.

I am grateful to my friend Raghavendra G. Amachawadi for his professional, personal guidance and help while walking on the same path together for our degrees.

Many thanks to Marsin Al Shamary, a graduate student at Massachusetts Institute of Technology (MIT) for her help.

A special gratitude and appreciation goes to my wife Samira and children Ahmed and Hind for their unlimited sacrifice, support, love, encouragement, and patience.

CHAPTER I

Chapter 1 - Introduction and Literature Review

Introduction

In recent years, concerns about environmental contamination by 1,4-dioxane (dioxane) has steadily increased due to its probable carcinogenicity. The present usage and historic disposal practices have increased its contribution as a major contributor to groundwater contamination throughout the United States and elsewhere. Dioxane imposes greater challenges for its characterization and treatment because of its unique physical-chemical properties and behavior in the environment. The presence of dioxane as a by-product contaminant in cosmetics, detergents, and shampoos that contain ethoxylated ingredients is also partly increasing this concern. Approximately, 22% of all the cosmetics and cleaning products may be contaminated with dioxane as reported by Environmental Working Group researchers (EWG, 2007). Studying behavior or properties of dioxane is of great interest to risk assessors. Developing procedures or methods to contain and mitigate contamination and remediate or decontaminate indoor and outdoor environments is so crucial to the success of dioxane risk management. Furthermore providing accurate data about the routes by which individuals are exposed and the parameters to quantitatively evaluate possible exposures are necessary for successful risk assessment.

Our studies are an attempt to highlight some aspects of dioxane properties and behavior in the environment and in a human body. This dissertation was performed:

- to investigate the potential ability of dioxane for decontamination by adsorption processes from water and air.
- to understand the principles of dioxane transdermal absorption from water and chemical mixtures.

To accomplish these objectives, a group of porous and non-porous adsorbents were used in aqueous and gas conditions at equilibrium. The equilibrium adsorption data were analyzed by the Freundlich model of adsorption. A new flow through system was developed to provide high density data sets for dermal absorption measurement. The transdermal absorption of dioxane was assessed in human skin from water, solvents, and surfactant solutions. Generally, data on the absorption of dioxane in humans following dermal exposure are limited and arte insufficient to create a comprehensive understanding about its transport behavior across the skin. It is hoped that the findings of the current investigations will offer suitable and reliable data to allow the accurate assessment of risk following dermal exposure to dioxane.

Literature Review

Dioxane Adsorption

Dioxane Background

Dioxane Properties

Dioxane (1,4-diethylene dioxide) is a volatile, colorless liquid with a mild, ethereal odor. It is heterocyclic ether chemical, $C_4H_8O^2$ (figure 1.1). The compound is also known by many synonyms such as *p*-dioxane, diethylene oxide, 1,4-diethylene oxide, and 1,4-dioxacyclohexane. Dioxane has two oxygen atoms as a part of its ring structure. The oxygen atoms occur directly opposite each other to form symmetrical ether linkage and resulti in two functional groups in one molecule. The structure of dioxane makes it very stable and fairly resistant to reaction with acids, oxides, and oxidizing agents. This stability, under a wide variety of conditions, makes dioxane very suitable for use as an organic solvent.

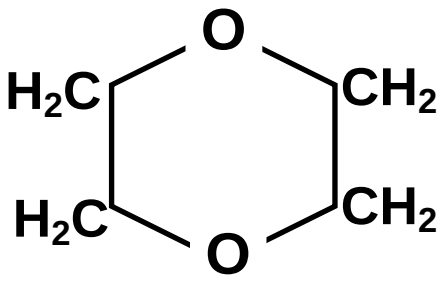

Figure 1.1: 1,4-Dioxane Structure

The ring of dioxane is resistant for breakdown except in the existence of highly concentrated acids and strong oxidizers and under conditions of high temperature and pressure (Reid & Hoffman, 1942). Dioxane has good solubility in water, and this is related to the polarity it attains when a pair of dioxane rings create a dimer with two intermolecular hydrogen bounds. The two remaining oxygen atoms are available for interaction with water molecules. Dioxane is completely miscible with water and most organic solvents, and water is totally soluble in dioxane. The oxygen molecules of dioxane have electrons available for sharing. Therefore, the two oxygen atoms make dioxane hydrophilic and extremely soluble in water (Mazurkiewicza & Tomasik, 2006). Although the ether functional groups are not capable of hydrogen bonding to each other, the electronegative oxygen atoms have a partial negative charge capable of interacting with the O-H dipoles of water molecules (Vallombroso, 2001). Compared to other solvents and according to the classical rankings of solvecy, pure dioxane has intermediate degree of solvency. However, its unusually high dipole moment in aqueous solution allows it to act as an efficient water-structure breaker, which provides dioxane a higher solvency than predicted (Mohr *et al.*, 2010). Table 1.1 provides a list of some physicochemical properties of dioxane.

Table 1.1: Properties of 1,4-dioxane

Property	**Value**
Molecular weight	88.106 Da
Density	1.028 gm/cm^3
Vapor pressure	5.08 kPa at 25 ºC, 15.8 kPa at 50 ºC, 42.2 kPa at 75 ºC
Boiling point	102.2 ºC
Heat of vaporization	98.6 cal/g
Freezing point	11.85 ºC
Flash point	12 ºC
Polarity	16.4
Solubility	Miscible
Acid dissociation constant	pK_a = -2.92
Ultraviolate light absorption	180 nm
Henry's Law Constant (K*H* dimensionless)	1.96×10^{-4}
Octanol-Water Partition Coefficient log(K_{ow})	-0.27
Organic Carbon Partition Coefficient log(K_{oc})	1.23

Sources: (Mohr *et al.*, 2010, Zenker *et al.*, 2004, Howard, 1990)

Dioxane Uses

Physical-chemical properties of dioxane make it very versatile and useful in a variety of applications. Until 1995, dioxane was used as a stabilizer for the solvent 1,1,1-trichloro-ethane (TCE), whose usage was stopped because of its ozone depletion potency (ECB, 2002). It is used extensively as a processing solvent in the manufacturing and chemical processing of detergents, cleaning agents, adhesives, cosmetics, varnishes, pharmaceuticals, fumigants, emulsions, deodorants, polishing compounds, fats, lacquers, resins, oils, waxes, paints, dyes, plastics, rubber, cellulose acetate, and pesticides. Soaps and cosmetics containing ethoxylated surfactants may also contain dioxane (Mohr *et al.*, 2010). It is also used as an extraction medium for animal

and vegetable oils and as a laboratory chemical (eluent in chromatography) and in plastic, rubber, pharmaceuticals/insecticides and herbicides (BUA, 1991). Moreover, dioxane is formed as an undesired by-product in many industrial processes, particularly through the synthesis of polyester, and it is also found as a by-product of the ethoxylation process in cosmetics, detergents, and shampoos (ASTDR, 2012).

In food, residues of dioxane may be found in manufactured food additives such as polysorbate 60 and polysorbate 80 and in some emulsifiers used in frozen dairy products and other frozen desserts (Marzulli *et al.*, 1981, Guo & Brodowasky, 2000). It is also found as a natural component in numerous foods like tomatoes, shrimp, and coffee (Stickney *et al.*, 2003).

Dioxane Occurrence

The amounts of dioxane in the ambient environment have been studied extensively. Many investigations have reported the existence of dioxane in monitoring samples of ambient air. Measurements of dioxaine in ambient air samples performed at 45 locations in 12 cities were collected by the U.S. EPA between 1979 and 1984 and showed concentrations ranging between below detection and 30 $\mu g/m^3$ (mean 0.44 $\mu g/m^3$) (USEPA, 1993). In a study conducted in New Jersey in 1981, the geometric mean of dioxane concentration in air samples collected from industrial areas ranged from 0.04 to 0.07 $\mu g/m^3$ and dioxane was detected in 51% of the samples (Harkov *et al.*, 1981). The same locations of New Jersey were resampled in 1982, and the results pointed to a decline of dioxane concentrations, where the geometric means of these samples ranged from 0 to 0.01 $\mu g/m^3$; 20% of samples were positive with a maximum value of 5.31 $\mu g/m^3$ (Harkov *et al.*, 1984). No information on the ambient levels of dioxane in air is available for the recent years. Since the use of dioxane has dropped in recent years, current levels of

dioxane in ambient air are likely to be less than levels reported in the 1980s or in earlier periods (ASTDR, 2012).

Occurrence of dioxane in water has been reported in many countries. In Japan, the outcome of nationwide surveys showed that the dioxane concentration in surface water are ranging between below detection and 35 μg/L in 1990, between below detection and 19 μg/L in 1994, and between below detection and 42 μg/L in 1997 (WHO, 2005). In another surveys on ground and surface water, dioxane was found in 87% of samples at levels up to 95 μg/L (Abe, 1999). In the United States, municipal water supplies were reported to contain 1 μg/L of dioxane in the 1970s (Kraybill, 1978). Results from other nationwide surveys on dioxane in water have revealed varied ranges of concentrations. The New Hampshire Department of Environmental Services found 67 locations at which dioxane was detected in groundwater at an average of 243 μg/L (Mohr *et al.*, 2010). In California, dioxane was determined to have concentration of 1.1–109 μg/L in groundwater, whereas drinking water samples from homes in Connecticut had maximum dioxane concentrations of 26 μg/L in untreated water in one residential well and 12 μg/L in treated water from another residential well (ASTDR, 2012). In a drinking water well in Massachusetts, a concentration of 2,100 μg/L was reported (Burmaster, 1982). In Canada, dioxane was detected in groundwater near landfills at concentrations <1 μg/L between 1983 and 1986. however, the concentrations were much higher in groundwater beneath a landfill, where it was 500 μg/L (ECB, 2002).

Dioxane Environmental Contamination

Releases to The Environment

Dioxane may enter the environment during its production, processing, handling, transporting, and formulation. Additionally, dioxane may remain as an impurity in many end-products (ECB, 2002). Historically, dioxane has been released into environment because of its use as a TCE stabilizer. Currently, this source of release is anticipated to be very low because the use of TCE has been stopped (ASTDR, 2012).

The amount of dioxane released to the environment in the United State can be evaluated by keeping track of the quantities reported in the Toxics Release Inventory (TRI) of U.S. EPA since 1988. However, these datasets are sometimes inaccurate because only certain types of facilities are required to report. Nevertheless, TRI data are still useful for providing approximate annual amounts, sites and the final disposition of dioxane releases. For example, in 2007, TRI data estimated that a total of 182,338 pounds (82,693 kg) of dioxane were released to the environment from 44 reporting facilities in 21 states, where 125,341pounds (56,854 kg) were released into the air, 56,996 pounds (25,853 kg) into water, 596 pounds (270 kg) onto land, and 2,200 pounds (998 kg) were released in other ways. In addition, an estimated 2,794 pounds (1,267 kg) were transferred off-site (TRI, 2013).

In general, TRI data showed that a total of 18,786,142 pounds (8,161,797 kg) of dioxane have been released into the environment in the United States between 1988 and 2012. Total on-site disposal or other releases were 11,717,373 pounds (5,108,123kg) and 7,068,768 pounds (3,053,673kg) for total off-site disposal or other releases. Total releases of dioxane to air and water were 6,522,259 pounds and 4,273,124 pounds, respectively (TRI, 2013). Releases of

dioxane to air and water have decreased significantly in last the decade. Releases to air reported in the TRI database have decreased from a high of 841,790 pounds in 1989 to 87,910 pounds in 2012. Discharge to water reported to TRI database increased from 203,320 pounds in 1988 to 652, 296 pounds in 1993, and then declined to 18,826 in 2012 (TRI, 2013, Mohr *et al.*, 2010). TRI data for estimated annual releases and disposal of dioxane are represented in figure 1.2. The releases of dioxane as a by-product can by assessed from production of plastic, manufacturing of alkyl ether sulphates, ethoxylated surfactants and textiles (Mohr *et al.*, 2010).

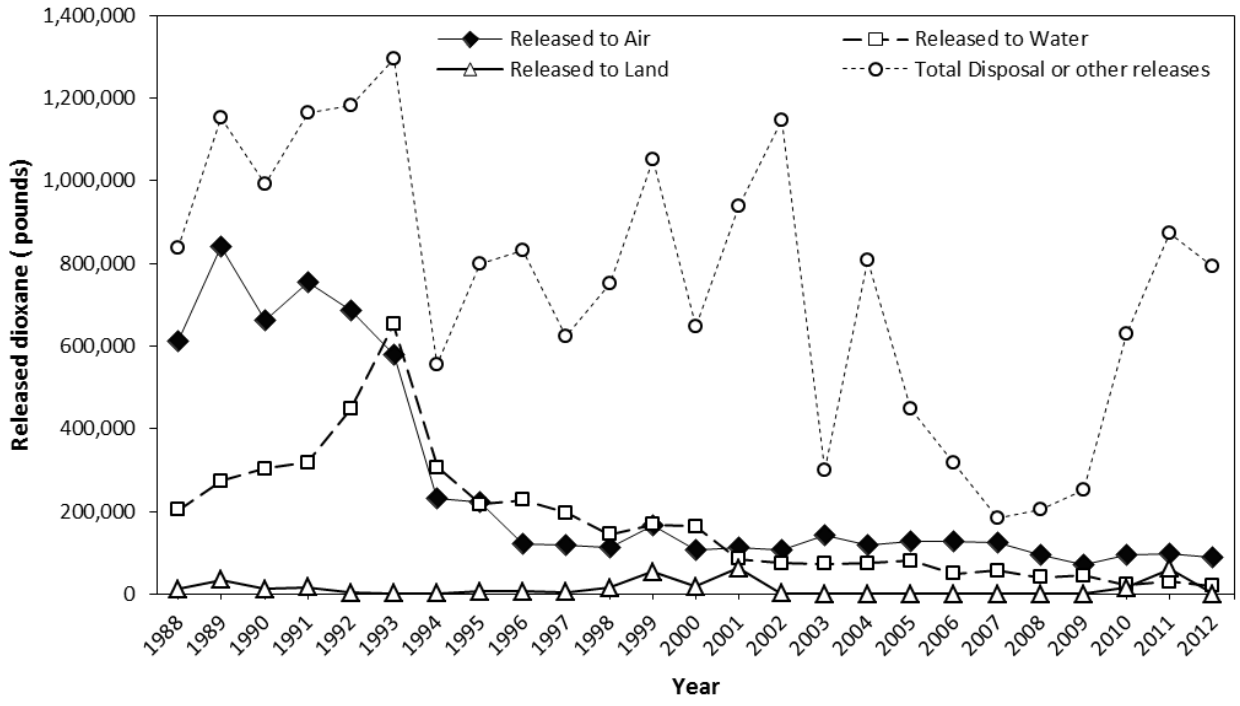

Figure 1.2: Estimated releases and disposal of dioxane in USA from 1988 through 2012.

Source: TRI – USEPA site (*http://www.epa.gov/triexplorer*)

Sources of Contamination

The sources of contamination in the environment caused by dioxane can be classified into two types of sources, point and nonpoint sources of contamination.

- *Point sources of contamination*: Point sources of contamination include spills and previous land disposal practices. Dioxane is often detected in landfill leachate, groundwater beneath municipal and industrial landfills, and in landfill gas and landfill gas condensate. But, not all landfills are implicated in releases of dioxane. Landfills are most likely to involve as point sources of dioxane contamination. Usually, landfills implicated in groundwater contamination by dioxane those that are receiving solvent wastes, household products associated with methyl chloroform, paint filters, laboratories chemical wastes, industrial sludge from ink and textile manufacturing, adhesive products used in celluloid film processing, vapor degreasing still bottom, and resin production (Mohr *et al.*, 2010).

  The mean concentrations of dioxane in leachate of landfill sites are widely variable. U.S. EPA surveys reported that the concentration of dioxane in leachate from municipal landfills was ranged between 11 and 323 ppb, and the average concentration at hazardous waste landfills was between 466 and 7611 ppb (USEPA, 2000). The concentration of dioxane was also reported to be 0.62 $\mu g/m^3$ and 0.33 g/m^3 in landfill gas in many sites throughout the United States (ECB, 2002).

- *Nonpoint sources of contamination:* Nonpoint sources of dioxane's contamination, usually, come from wastewater effluent discharged to waterways. A by-product (impurity) daioxane in end use of some products like in domestic detergents, shampoo, and personal care products, which mostly come from household discharges to be released

to sewers along with surfactants (Abe, 1999). Dioxane, as an impurity is formed during the manufacture of alkyl ether sulphates and some ethoxylated compounds. About 80% of this can be removed by a stripping process. Therefore, dioxane (as an impurity) may be released as stripper condensate and discharged to the drainage system, where it is diluted by other waste streams and arrive at the sewer as trade waste (NICNAS, 1998).

Dioxane has been detected in raw wastewater in the United States and Japan. In the United State, dioxane was found at 1 ppb in effluents from the North Side and Calumet sewage treatment plants on the Lake Michigan Basin, in discharges into Lake Michigan near Chicago (Konasewich *et al.*, 1978), and in North Carolina in the Haw River (Dietrich *et al.*, 1988). It was also detected in samples from raw wastewater (3 ppb) and treated wastewater effluent (2 ppb) in Ann Arbor, Michigan (Skadsen *et al.*, 2004). In Japan, dioxane was found at 0.2 to 0.56 ppm in tested effluent from a wastewater-treatment plant in Kanagawa Prefecture. The source of dioxane was assumed to be come from households discharging shampoo, liquid dish washing and laundry soap (Abe, 1999).

Dioxane Behavior in Environment

Discharging industrial wastes into the environment are generally associated with degradation of water quality and hazard to human and ecological health. Numerous compounds in industrial effluents decay with time because of biodegradation, physical removal, or chemical reaction to less harmful by-products. The tendency of chemicals to volatilize, hydrolyze, photo-oxidize, adsorb, and biodegrade plays an important role in their behavior in the environment, such as their diffusion or migration through soil, water, and air, and in which phase the chemical is present (liquid, gas, or solid) (Mohr *et al.*, 2010).

Dioxane is resistant to hydrolysis because it does not have functional groups that are susceptible to hydrolysis. Hydrolysis of dioxane is not expected to occur in the environment, as ethers are generally classified as resistant to hydrolysis (Aus, 1999, Wolfe & Jeffers, 2000).

Photooxidation of dioxane in the atmosphere is the primary loss mechanism and mostly occurs with OH radicals, whereas the photolysis reaction occurs with ozone molecules (Grosjean, 1990). Dioxane also is resistant to photolysis and not expected to undergo direct photolysis in aqueous media because it does not adsorb light in the environmental spectrum (i.e., >290 nm), but it may undergo indirect photolysis by aqueous hydroxyl radicals near the water surface (Anbar & Neta, 1967). However, some studies have found that direct photolysis of liquid dioxane at 185 nm produces formaldehyde, glycol monovinyl ether and ethylene, and at 147 nm (in the gas-phase) gives formaldehyde and ethyleneas the principal products (BUA, 1991).

The vapor pressure of dioxane at 25 ºC (37 mm Hg) presumes volatilization is conceivable. However, the low Henry's law constant for dioxane of $4.8x10^{-6}$ atm^3 m/mole indicates that the transfer of this contaminant from water to air is insignificant (Thomas, 1990). Based on this Henry's law constant, the volatilization half-life is estimated as 7 days. Volatilization from dry and moist soil surfaces may occur under vapor pressure of 38.1 mm Hg (Daubert & Danner, 1985). Even though volatilization of dioxane could exist, hazards to human health from inhalation exposures are anticipated to be low under normal environmental circumstances (ASTDR, 2012).

Dioxane is relatively resistant to biodegradation. Laboratory studies have shown that indigenous microorganisms in soil and waste water are typically unable to degrade this compound (Zenker *et al.,* 2004). However, biodegradation has been reported in many studies in

both pure and mixed cultures. For example, partial degradation of dioxane in a pure culture of *Mycobacterium vaccae* was shown but not to grow on the compound (Burback & Perry, 1993). Similarly, biodegradation of dioxane was reported as the sole carbon and energy source by a *Rhodococcus* strain (Bernhardt & Diekmann, 1991). A study on wastewater treatment plant effluent showed no degradation of dioxane in cultures of sewage microorganisms exposed for 1 year at concentrations ranging from 100 to 900 ppm (Klecka & Gonsior, 1986). In another investigation, microorganisms existing in sludge of municipal or industrial effluent were unable to degrade dioxane during 48 hours of exposure to concentrations ranging between 10 and 100 ppm (DCC, 1989).

The high solubility (4.31×10^5 mg L^{-1}), low log octanol-water partition coefficient (K_{ow} = -0.27), and a low organic carbon partition coefficient (K_{oc} = 1.23) of dioxane hints at a very high mobility in soil. Therefore without a substantial degradation process, dioxane is susceptible to leaching from soil into aquifers. Dioxane is not adsorbed to suspended sediments or soil as a result of any particular interaction with the surface of soil minerals; however, it can get trapped in the interfacial region of clay soil because of its strong hydrophilicity. This may show a lower mobility for dioxane in clay soil than predicted (Zhang *et al.*, 1990). In most chlorinated solvents which have been contaminated aquifers, dioxane has migrated significantly beyond the associated solvent plumes. The plumes of dioxane can persist after the source has been removed or controlled, and they have been documented to measure twice the length of the associated solvent plumes and to affect an area up to six times greater (Walsom & Tunnicliffe, 2002).

No data are available about bioaccumulation or bioconcentration of dioxane. Dioxane bioaccumulation is expected to be very low because of its low log K_{ow} and high hydrophilicity,

and it is assumed that dioxane will not bioconcentrate in plants, aquatic organisms or animals. Additionally, dioxane is not biomagnified to any extent in prey organisms (VCCEP, 2007a).

The Toxicology of Dioxane

Data of dioxane health effect are very limited in human. Wherefore, toxicity of dioxane has been estimated by considering studies in animal models and available limited data from human exposures. Investigations of toxicity in human are mostly based on these contain of case reports of accidental or occupational intoxication, limited epidemiological studies of occupational workers, and volunteer studies of acute inhalation exposure. Data from human and laboratory animal studies, taking together identify potential adverse health effects that may be created from exposure to dioxane. Inhalation and ingestion routes have been reported as the primary exposure routes of dioxane intoxication. Inhalation exposures to dioxane are mostly associated with occupational settings. Although, there are no data regarding the health effects of human exposure via the oral route, usually, oral exposures in humans may come from consumption of contaminated drinking water (Mohr *et al.*, 2010).

The liver and kidneys are the target organs for dioxane toxicity, and the data in laboratory animals suggest that it takes place regardless of the route of exposure. Many studies in animals have provided detailed descriptions of hepatic and renal pathology in many species with different dioxane concentrations and different routes of exposure. Generally, various degrees of hepatocellular and renal degeneration and necrosis have been the main changes seen (ASTDR, 2012).

Toxicokinetics

Dioxane metabolism and kinetics involve the understanding of how dioxane is absorbed, distributed, metabolized, and excreted within the body following exposure by oral, dermal or inhalation routes. The toxicokinetics of dioxane are described by using data of human and animal studies in addition to computer modeling and *in vitro* testing. The data of dioxane toxicokinetics in humans are very limited, but they are well explained in laboratory animals exposed through oral, skin, inhalation, and intravenous routes. In animals, radiolabelled dioxane has been used to study the distribution of the chemical throughout the body. In both humans and animals, dioxane is metabolized to β-hydroxyethoxy acetic acid (HEAA) by mixed-function oxidase enzymes; under acidic conditions HEAA can be converted to 1,4-dioxane-2-one. Both of these metabolites are quickly and predominantly excreted via kidney to the urine (ASTDR, 2012).

Absorption

Dioxane is well absorbed following oral and inhalation exposure. Rapid absorption of dioxane after inhalation exposure has been demonstrated in workers and human volunteers, by measuring concentration of dioxane and HEAA in blood and urine (Young *et al.*, 1976, Young *et al.*, 1977). Similar results were found in laboratory animals' studies for inhalation exposure (Young *et al.*, 1978a, Young *et al.*, 1978b).

Absorption associated with oral exposures was evaluated in animals. Gastrointestinal absorption was almost complete in male rats orally administrated with 10–1,000 mg/kg of radiolabeled dioxane, given as a single dose or as 17 consecutive daily doses (Young *et al.*, 1978a, Young *et al.*, 1978b). No human data are available to assess absorption of dioxane via oral exposure.

Dermal absorption information of dioxane are limited in humans and animals. However, an *in vitro* study has been conducted on human skin in which dioxane penetrated excised skin 10 times more under occluded conditions than unoccluded. Radiolabeled dioxane was used with lotion which was applied to the excised skin in occluded and unoccluded diffusion cells. The study also reported detecting rapid evaporation, which further decreased the small amount available for skin absorption in occluded and unoccluded diffusion cells (Bronaugh, 1982a). Another study in monkeys, dermal absorption was reported to be low from a menthol or skin lotion vehicle. The ability of the chemical to penetrate the skin was evaluated by examination of radiolabel in urine (Marzulli *et al.*, 1981).

Distribution

No data are available for the distribution of dioxane in human and animals after oral, inhalation, or dermal exposures. The only related data regarding distribution of dioxane is that described in investigations involving intraperitoneal exposure of animals. Intraperitoneal injection of labeled dioxane in male rats showed that the tissue distribution was mostly even through renal, hepatic, skeletal muscles, colon, and lung tissues, with blood concentrations higher than tissues (Woo *et al.*, 1977b). Another study in rats found that after intraperitoneal injection, the time to reach maximum accumulation of radiolabel was shorter for liver and kidney than for blood or the other tissues. Tissue to blood ratios for kidney, liver and brain were less than one, while the testes had a ratio greater than one (Mikheev *et al.*, 1990). The principles of physiologically based pharmacokinetic (PBPK) modeling study reported that dioxane could be transferred to milk in lactating mothers (Fisher *et al.*, 1997).

Metabolism

The exact metabolic pathways of dioxane are not known. However, many studies have reported that HEAA is the main product of dioxane metabolism. Only one study identified 1,4-dioxane-2-one as a major metabolite (Woo *et al.*, 1977b). But, there is some question about this compound as an ultimate metabolite, and its presence in the sample was believed to result from the acidic conditions (pH of 4.0 - 4.5) of the analytical assays. HEAA can be converted to 1,4-dioxane-2-one, and under alkaline conditions, the reverse reaction takes place (Braun & Young, 1977). Generally, HEAA may be generated from oxidation of dioxane via:- (a) diethylene glycol. (b) directly to 1,4-dioxane-2-one . (c) 1,4-dioxane-2-ol. A proposed metabolic scheme for dioxane in rats is presented in figure 1.3 (Woo *et al.*, 1977a).

1,4-Dioxane oxidation was shown to be mediated by the cytochrome P450 (CYP450 enzyme in the liver). CYP450 induction with phenobarbital or Aroclor and suppression with 2,4-dichloro-6-phenylphenoxy ethylamine or cobaltous chloride were effective in significantly increasing and decreasing, respectively, the presence of HEAA in the urine of male rats (Woo *et al.*, 1977a, Woo *et al.*, 1978). Oxidation to diethylene glycol and HEAA pathway seems to be the most probable, because diethylene glycol was found as a minor metabolite in rat urine following a single 1,000 mg/kg gavage dose of dioxane (Braun & Young, 1977). Furthermore, intraperitoneal injection of 100–400 mg/kg diethylene glycol in rats resulted in urinary elimination of HEAA (Woo *et al.*, 1977a). Metabolism of dioxane in humans to the ultimate metabolite (HEAA) is extensive following inhalation exposure. In a study on adult male volunteers exposed to 50 ppm reported that over 99% of the dioxane was excreted after 6 hours as HEAA instead of the parent compound (Young *et al.*, 1977). In a another study, the ratio of HEAA to

dioxane in the urine of humans following a exposure for 7.5 hour to 1.6 ppm dioxane was 118:1, hinting nearly complete metabolism at this exposure concentration (Young *et al.*, 1976).

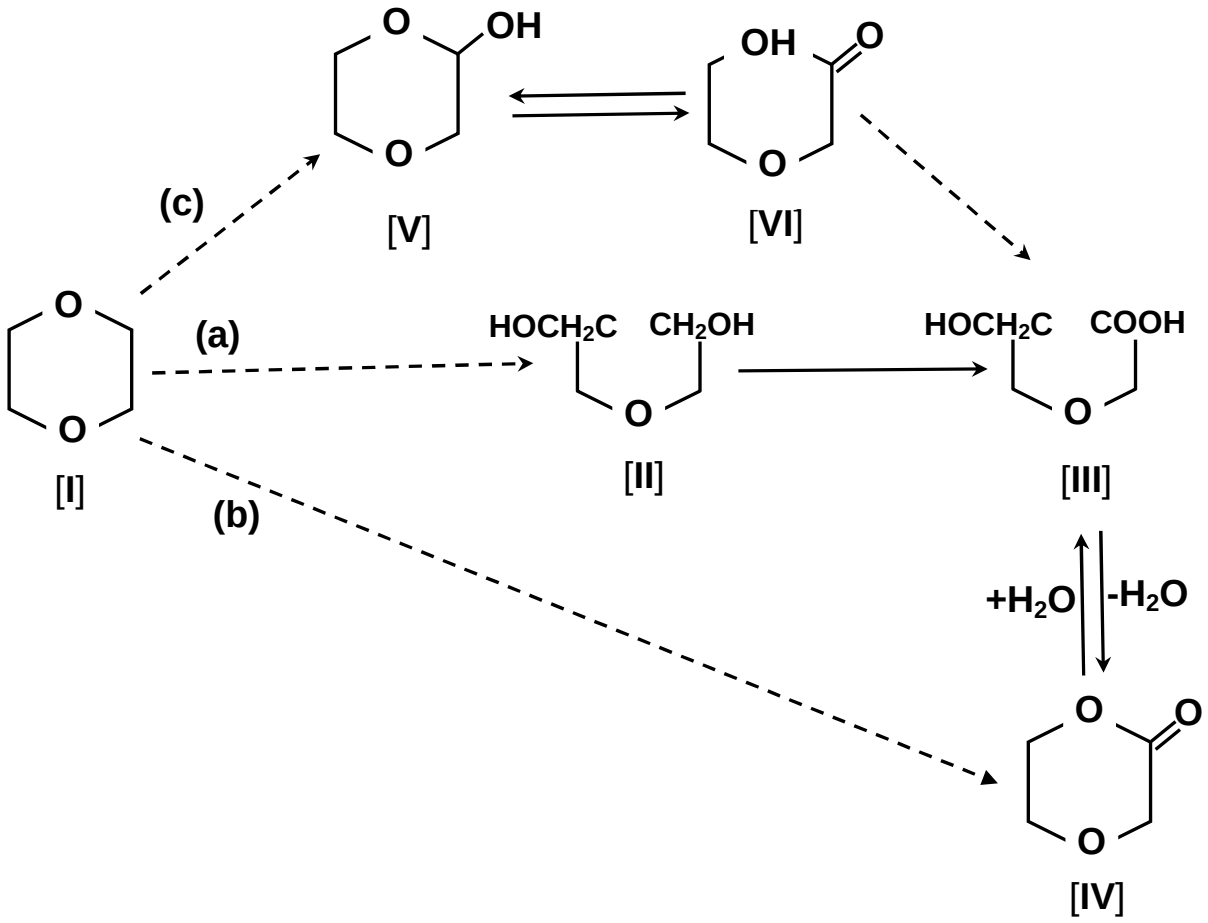

Figure 1.3: Suggested metabolic pathways of dioxane in the rat. I = dioxane; II = diethylene glycol; III = β-hydroxyethoxy acetic acid (HEAA); IV = 1,4-dioxane-2-one; V = 1,4-dioxane-2-ol; VI = β-hydroxyethoxy acetaldehyde. Note: Metabolite [V] is a likely intermediate in pathway b as well as pathway c. The proposed pathways are based on the metabolites identified; the enzymes responsible for each reaction have not been determined. The proposed pathways do not account for metabolite degradation to the labeled carbon dioxide (CO_2) identified in expired air after labeled 1,4-dioxane exposure.

Source: (Woo et al., 1977a)

Excretion

Dioxane is mainly execrated as HEAA in urine. However, the expiration of dioxane in breath increases at higher doses due to metabolic saturation. In workers exposed to a time-weighted average of 1.6 ppm for 7.5 hours, 99% of dioxane excreted in urine was in the form HEAA metabolite (Young *et al.*, 1976). In adult male volunteers exposed via inhalation to 50 ppm dioxane for 6 hours, the excretion half-life was 59 minutes (Young *et al.*, 1977). There is no information about excretion of dioxane in humans following oral exposures. Excretion of dioxane in rats has been mainly through urine. As in humans, half-life of excretion in rats exposed to 50 ppm dioxane for 6 hours was 1.01 hours. Urinary excretion was 76% to 99% depending on the administrated dose following oral exposure, where the urinary excretion decreased as a dose increased. Excretion of dioxane through respiration increased with increasing dose (Young *et al.*, 1978a, Young *et al.*, 1978b).

After a single intravenous dose of 10 mg/kg of dioxane in rats, 4% of the dioxane was excreted in the urine as dioxane, 92% as HEAA, and 1% was excreted in the exhalation air (Young *et al.*, 1978a).

Health Effects of Dioxane

Many reports have described dioxane as having adverse effects due to acute and chronic exposure. The human data mostly consist of case reports of occupational intoxication, volunteer studies, and epidemiological studies of workers occupationally exposed to dioxane. The source

of health effects data in animals mostly comes from short or long-term toxicity studies in laboratory due to many exposure routes.

Acute Exposure

Earlier case reports of acute occupational poisoning with dioxane pointed out that exposure to high concentrations caused toxicity in the liver, kidney, and central nervous system (Barber, 1934, Johnstone, 1959b). The first record of adverse health effects resulted from acute exposure to dioxane date from 1933, when factory workers were exposed to high (unspecified) concentrations of dioxane through inhalation. Some of patients who displayed signs of liver changes, increased urinary protein and increased white blood cell counts. Five deaths occurred within a period of 2 weeks of the onset of illness. Postmortem findings suggested that hemorrhagic nephritis and centrilobular necrosis of the liver may have been responsible for lethality (Barber, 1934). Another case was documented in which a worker who died following exposure by inhalation and direct dermal contact to high levels of dioxane (between 208 to 650 ppm). The post-mortem examination showed lesions in the liver, kidneys, brain, and pulmonary system. However, the effects could not be easily separated from the effects due to high consumption of alcohol (Johnstone, 1959b). Human volunteer studies showed that acute inhalation exposure to >200ppm of dioxane for several minutes caused irritation of nose, eyes, and throat (Silverman *et al.*, 1946). Following six hours exposure to 50ppm dioxane eye irritation was also seen (Young *et al.*, 1977). In a study of six individuals exposed to 2,000 ppm dioxane vapors for three minutes, there were no clinical symptoms or nasal discomfort, but one out of four individuals exposed to 1,000 ppm for five minutes complained of constriction of the throat (Fairley *et al.*, 1934). The exposure of 12 volunteers to 20 ppm dioxane for two hours yielded no significant

respiratory effects during exposure or up to three hours after exposure (Ernstgard *et al.*, 2006). The available epidemiological studies in occupational workers exposed to dioxane have not provided evidence of effects in humans (Buffler *et al.*, 1978, Thiess *et al.*, 1976).

The acute and short-term toxicity investigations of dioxane in laboratory animals have been conducted with different routes of exposure including oral, dermal, inhalation, and intravenous or intraperitoneal injection. Generally, early studies have provided information on lethality of high concentrations of dioxane in many species (rabbits, rats, guinea pigs, mice, cats, and dogs). These studies also have indicated that the target organs are liver, kidney, and lungs in some cases. Exposure to 5,000 ppm of dioxane was lethal to rabbits, rats, and mice, while 10,000 ppm was lethal to guinea pigs (Fairley *et al.*, 1934). Clinical symptoms of central nervous system depression also were shown, including paralysis, coma, narcosis, and death (Nelson, 1951, Laug *et al.*, 1939, Schrenk & Yant, 1936, de Navasquez, 1935). The established LD_{50} for acute exposure in rats via the oral route is 5,200 ppm. The LC_{50} for rats through the inhalation route is 46 gm/m^3 (USEPA, 1996).

Chronic Exposure

The chronic exposure database for dioxane in humans is limited. In an occupational study to assess health effects in 74 German workers exposed to dioxane concentrations ranging between 0.006 and 14.3 ppm for an average of 25 (12 to 41) years in a factory for dioxane production. The clinical evaluation of the workers showed evidence of abnormal liver functions where serum glutamate-oxalacetic transaminase (SOGT), serum glutamate pyruvate transaminase (SGPT), alkaline phosphatase, and gamma

glutamyltransferase were increased. No liver enlargement or icterus was noticed. Renal function tests and urinalysis were normal in exposed workers. No signs of hepatic or renal disease were found and no cancer was detected (Thiess *et al.*, 1976). Other studies in humans suggested that chronic exposure to dioxane may play a role in renal failure and death (Yaqoob & Bell, 1994, Buffler *et al.*, 1978).

Subchronic and chronic toxicity studies have been conducted in laboratory animals to identify potential health effects associated with long-term exposure. The majority of these studies have been with oral drinking water exposure. Long-term inhalation studies were limited and insufficient to describe the inhalation risks of dioxane. Subchronic toxicity studies have generally considered histopathological changes to be evidences of organ-system toxicity. The most reported histopathological changes of subchronic toxicity in rats and mice were renal cortical degenerations and necrosis, hemorrhage, hepatocellular degeneration, hepatocyte swelling, and nuclear enlargement of nasal and bronchial epithelium (JBRC, 1998, Stott *et al.*, 1981, Fairley *et al.*, 1934). Whereas, chronic studies have reported that the pathological changes were hepatocyte with enlarged with hyperchromic nuclei, hepatomegaly, glomerulonephritis, gastric ulcers, pneumonia, arthritis, atrophy of nasal olfactory epithelium, nasal inflammation, delayed ossification of the sternebrae and reduced fetal body weights (JBRC, 1998, Giavini *et al.*, 1985, NCI, 1978, Kociba *et al.*, 1974b, Argus *et al.*, 1973, Argus *et al.*, 1965).

Carcinogenicity Effects

Limited data are available regarding cancer and exposure to dioxane in humans. Survey on 74 workers exposed to concentrations of dioxane ranged between 0.006 and 14.3 ppm for an average duration of exposure of nearly 25 years. Two of twelve deaths were

attributed to cancer which had been reported (Thiess *et al.*, 1976). In an occupational investigation of 165 workers exposed irregularly to low level (0.1 - 17 ppm) of dioxane in a manufacturing and processing facility at least one month during a 21-year period showed no apparent excess of total cancer deaths (Buffler *et al.*, 1978). Limited retrospective studies on 80 workers who inhaled dioxane with potential exposure of 0.18 to 184 mg/m^3 for several years showed no evidence of occupational disease or an increased cancer occurrence comparing to the general population (NIOSH, 1977). In three epidemiologic studies on workers exposed to dioxane, the observed number of overall death rate and the cancer death rate did not differ significantly from the expected deaths (ASTDR, 2012).

Long-term exposure studies in laboratory animals have reported that dioxane can cause liver and kidney damage and induces hepatocellular and nasal tumors. Moreover, in rats nasal adenomas and carcinomas were also reported, accompanied by non-neoplastic lesions in the nasal cavity. These lesions were also observed in mice, but in mice dioxane did not induce an increased incidence of nasal tumors (Kano *et al.*, 2009, NCI, 1978, Kociba *et al.*, 1974a, Argus *et al.*, 1973, Argus *et al.*, 1965).

Based on evidence in humans and experimental animals, and due to the inadequate evidence for the carcinogenicity of dioxane in humans and sufficient evidence for the carcinogenicity of dioxane in experimental animals the International Agency for Research on Cancer (IARC) has assessed dioxane as being a Group 2B carcinogen (possibly carcinogenic to humans) (IARC, 1999). Under the Guidelines for Carcinogen Risk Assessment, dioxane is “likely to be carcinogenic to humans” based on evidence of liver carcinogenicity in several 2-year bioassays conducted in many laboratory animal

species (USEPA, 2005). Lifetime cancer risk of 1 in 100,000 has been assessed by the U.S. EPA for people drinking-water contaminated with 30 µg/L dioxane (USEPA, 2013a). Based on both non-threshold and threshold approaches, the World Health Organization (WHO) has issued a guideline value for drinking-water quality of 50 µg/L dioxane (WHO, 2008).

The genotoxic effects of dioxane has been tested using *in vitro* assay systems with non-mammalian eukaryotic organisms, prokaryotic organisms, and mammalian cells, and also examined *in vivo* assay systems using many strains of rats and mice. In most of *in vitro* and *in vivo* systems studies, dioxane was nongenotoxic or weakly genotoxic (USEPA, 2013b).

Remediation of Dioxane

Technologies that are effective for treating chlorinated solvents are often not appropriate for treating dioxane because the properties of dioxane vary from those of chlorinated solvents. The physical and chemical properties of dioxane pose challenges for removing dioxane from water. Because of its high miscibility and low degree of partitioning to organic matter in soil, dioxane is well suited to removal by groundwater extraction. However, the low Henry's Law constant of dioxane poses other challenges for clean-up technologies like air stripping. The low adsorptive capacity of dioxane also limits the efficiency of treatment by granular activated carbon (USEPA, 2006).

Many techniques are used for clean-up of dioxane contaminated sites. The technologies range from simple *in-situ* development of natural microorganisms to costly advanced oxidation processes. Some remediation technologies have consensus on their potential for success, but other technologies do not have universal acceptance, like air stripping and activated carbon adsorption.

The most common techniques are advanced oxidation processes, specialized sorbents, and bioremediation (Mohr *et al.*, 2010).

- *Advanced oxidation processes* use hydroxyl radicals, which are powerful oxidizers, to successively oxidize organic contaminants to carbon dioxide, water, and residual chloride. Two common processes include photo-induced oxidation using UV light with hydrogen peroxide and hydrogen peroxide with ozone. Hydroxyl radicals are released from hydrogen peroxide added to contaminated water because of UV light. Hydroxyl radicals are also generated when ozone is added to hydrogen peroxide with or without UV light (USEPA, 2006).
- *Specialized sorbents:* many types of sorptive media have been tested to assess their capacity to remove dioxane from water: surfactant-modified zeolite, surfactant-modified zeolite with zero-valent iron, macroporous polymers, granulated activated carbon (GAC), organoclays, and palladium-111, GACs made from agricultural by-products are common sorbents used for dioxane removal from water (Mohr *et al.*, 2010).
- Bioremediation: this method involves placing contaminants in extracted water in contact with microorganisms in attached or suspended growth biological reactors (USEPA, 2006). Bioremediation has historically been avoided because dioxane shows insignificant biological oxygen demand and is considered to be relatively nonbiodegradable. However,

recent studies have revealed that specific species of plants and microorganisms (like some strains of *Actinomycete* and *Pseudonocardia*) can successfully remediate dioxane (Zenker *et al.*, 2000).

Adsorption

Adsorption is the phenomenon marked by a natural tendency of components in a liquid or a gas phase (adsorbate) to attach as a monolayer or a multilayer at the surface of a solid material (adsorbent), and it may result from either physical or chemical interaction with the surface (Ruthven, 1984). The phenomenon of adsorption was discovered over two hundred years ago. Gases uptake by charcoal was first investigated by C. W. Scheele in 1773 and by Abb F. Fontana in 1777. In 1785, T. Lowitz found that charcoal can decolorize solutions by a surface adsorption mechanism (Ruthven, 1984). The site of adsorption is the place where the adsorbate and adsorbent come in contact with each other. The molecules or atoms of the adsorbent are held together by various forces which include electrostatic interactions, van der Waals interactions, hydrogen bound, charge transfer, ligand exchange, direct and indirect dipole-dipole interactions, hydrophobic bound, and chemisorption (Suthersan, 2002).

Atoms and molecules can attach themselves onto surfaces in two ways: physical interactions (physical adsorption) and chemical interaction (chemical adsorption).

Physical Adsorption: this adsorption takes place as a consequence of energy differences and/or electrical attractive forces by which the adsorbate molecules become physically attached to the adsorbent molecules (Everett, 1971). The atoms located inside the solid (adsorbent) are exposed to equal forces in all directions, while atoms on the surface are

exposed to unbalanced forces. The adsorbate adheres to the surface of the adsorbent only through van der Waals interactions. Van der Waals interaction is the sum of the attractive or repulsive forces between molecules or parts of same molecules, and it is the main forces governing the physical adsorption. Van der Waals forces on a solid surface arise due to London dispersion forces. The London dispersion force (LDF) is a force between two instantaneously induced dipoles. The LDF is a force resulting from two electrons in adjacent atoms occupying positions that make the atoms create temporary dipoles. An atom or molecule can form a temporary dipole when its electrons are distributed irregularly about the nucleus (Marsh & Rodriguez-Reinoso, 2006). In physical adsorption the attraction to the surface is weak but long range and the energy released upon accommodation to the surface is of the same order of magnitude as an enthalpy of condensation, and it is always exothermic. The physically adsorbed molecule keeps its identity and on desorption returns to its original form. Physical adsorption systems usually reach equilibrium rapidly; however, equilibrium may be slow if the transport process is rate-determining (Rouquerol *et al.*, 1999).

Chemical Adsorption: in this adsorption process, the adsorbate bonds to the adsorbent by the formation of a chemical bond with the surface. Chemical forces at the interface are more complicated than these in physical adsorption. The main chemical bonds involved in chemical adsorption are ionic bond, covalent bond, and co-ionic bond. The chemically adsorbed molecules are linked to reactive parts of the surface, and the adsorption is certainly restricted to a monolayer. This interaction is much stronger than physical adsorption. Generally, chemical adsorption has more strict requirements for the compatibility of adsorbate and surface site than physical adsorption. In chemical

adsorption, if the adsorbed molecule undergoes reaction or dissociation, its identity will be lost and cannot return to its original form by desorption. The energy of this adsorption is the same order of magnitude as the energy change in comparable chemical reaction. At low temperatures the chemical adsorption system cannot reach thermodynamic equilibrium because of insufficient thermal energy (Rouquerol *et al.*, 1999, Emmett & Brunauer, 1937).

Many factors affect adsorption and influence its capacity. The size of the adsorbate molecule impacts its potential to be adsorbed to the adsorbent surface. Large molecules have more locations where van der Waal's forces contribute to attraction of the adsorbate molecule to charged particles in adsorbent. This attraction usually occurs through temporary dipole generating from time-varying electron distribution or polarity induced by charges on particles. The electrons are attracted to the positive site in the temporary dipole in the adjacent adsorbent surface, leading to a net attraction of the adsorbate to the adsorbent surface (Mohr *et al.*, 2010). The smaller particle size of adsorbent gives higher adsorption rates. They reduce internal diffusion and mass transfer limitation to penetrate of the adsorbate inside the adsorbent (i.e., equilibrium is more easily achieved and nearly full adsorption capability can be reached) (Al-Anber, 2011, Ali, 2011). Surface area and porosity of the solid also influence adsorption processes. Higher surface area and porosity increase adsorption capacity. Polarity, ionization, contact time, hydrogen bonds, and water solubility are other factors which affect adsorption. Non-polar compounds are more prone to be adsorbed; more highly ionized molecules of adsorbate are adsorbed to a smaller degree than neutral molecules;

and highly soluble and miscible compounds (hydrophilic) are less prone to adsorption (Dragun, 1988).

Adsorption Isotherm

Upon contacting an amount of sold (adsorbent) with a compound (adsorbate) long enough, adsorption will occur and continue until equilibrium will be established between the compound in solution or gas and the same compound in the adsorbed state. At equilibrium a relationship occurs between the concentration (if liquid) and pressure (if gas) of the compound in solution or gas and the concentration or the pressure of the same compound in the adsorbed state (amount of compound adsorbed / unit mass of adsorbent). Adsorption equilibrium is commonly described by adsorption isotherms (the mathematical models to describe adsorption) whose parameters express the surface properties and affinity of the adsorbent, at a fixed temperature, and pH (Snoeyink, 1999). Usually, the mathematical correlation, which establishes an essential role towards the modeling analysis, operational design and applicable practice of the adsorption systems, is commonly depicted by graphically expressing the adsorbent-phase against its residual concentration or pressure (Ncibi, 2008). In general, the essential purpose of studying adsorption isotherms is to identify circumstances for which high adsorption capacities are attained and to estimate the shape of the curve relating the equilibrium concentration of an adsorbate on the surface of an adsorbent.

Isotherm Models

A wide variety of models for predicting the equilibrium distribution have been formulated over the years, such as Langmuir, Freundlich, Brunauer–Emmett–Teller, Redlich– Peterson, Dubinin–Radushkevich, Temkin, Toth, Koble–Corrigan, Sips, Khan, Hill, Flory–Huggins and Radke–Prausnitz isotherm. Most of those isotherms have built in terms of three fundamental

approaches (Kinetic consideration, thermodynamics, and potential theory) (De Boer, 1968, Myers & Prausnitz, 1965).

A variety of mathematical models have been suggested to describe adsorption phenomena. Some of them were developed with a theoretical basis to describe adsorption mechanisms, while others are just empirical or a simplification of more elaborate models. In some ranges of activity, adsorption isotherms can be come close to linear equations (Andrade *et al.*, 2011). The equations most commonly used to describe the curvilinear adsorption behavior of compounds are the linear, Langmuir, Freundlich, and Brunauer-Emmett-Teller isotherm, due to their relative simplicity.

Linear Isotherms

Linear isotherms is the simplest model to describe the relationship between mass of compound adsorbed/ mass (q) and equilibrium concentration of adsorbable compound in solution (c_{eq}).

$$q = a + b(c_{eq})$$

In this example, linear regression could be used to extrapolate the slope (b) and the intercept (a). Several adsorbates show linear isotherms at low concentrations or pressures (Hinrich *et al.*, 2002).

Langmuir Isotherms

The Langmuir model was primarily developed to describe gas solid-phase adsorption onto activated carbon. The model was based on three assumptions: (1) the adsorbed layer is made up of unimolecular layers; (2) All adsorption sites are identical and

independent; (3) the adsorption and desorption rate is independent of the population of neighboring sites (no interaction between adsorbate molecules) (Langmuir, 1916).

Graphically, it is characterized by a plateau, an equilibrium saturation point where once a molecule occupies a location, no more adsorption can occur. Furthermore, Langmuir theory has related rapid decrease of the intermolecular attractive forces to the increase of distance. The equation of this isotherms model is:-

$$x/m = \frac{aC}{1 + bC}$$

Where *x/m* is the weight of adsorbate divided by the weight of adsorbent, *a* and *b* (determined graphically) are constants, *C* the aqueous concentration or pressure of the adsorbate.

The Langmuir isotherm is usually linearized by inversion and so used to test whether it is obeyed by experimental data.

$$\frac{1}{x/m} = \frac{b}{a} + \frac{1}{aC}$$

Langmiur isotherm model has many limitations. It postulates that adsorption is unimolecular layer. But, formation of unimolecular layer occurs only under low pressure environments, and under high pressure environments the postulate breaks down. Therefore, the Langmuir isotherms model is valid under low pressure only. It presumes all the locations on the adsorbent surface are homogeneous and have identical affinity for adsorbate molecules, but in real conditions adsorbent surfaces are

heterogeneous. The model also disregards interactions between adsorbate/adsorbate molecules. This is impossible as weak force of attraction occurs even between molecules of same adsorbat (Rouquerol *et al.*, 1999).

Freundlich Isotherm

Freundlich isotherm model was developed for the adsorption of animal charcoal (Freundlich, 1906). It is the earliest model describing the non-ideal and reversible adsorption relationship, and is not limited to the formation of unimolecular layer. This empirical model can be applied to multimolecular layer adsorption, with non-uniform distribution of adsorption heat and affinities over the heterogeneous surface of adsorbent (Adamson & Gast, 1997).

Presently, Freundlich isotherm is usually applied in heterogeneous systems especially for organic substances or highly interactive species on activated carbon and molecular filters. The slope ranges between 0 and 1 is a measure of adsorption capacity or surface heterogeneity, becoming more heterogeneous as its value becomes closer to zero. A value below unity implies chemisorptions process where 1/n above one is an indicative of cooperative adsorption (Foo & Hameed, 2010). The Freundlich Isotherm is described by the following equation:

$$x/m = kC^{1/n}$$

Where *x/m* is the weight of adsorbate divided by the weight of sorbent (usually in µg/g or mg/g), *K* is a constant, C the aqueous concentration (usually in mg/ml), and *n* a constant.

To linearize the isotherm by taking the logarithm of expression to see if the experimental adsorption behavior of a substance obeys the Freundlich isotherm or K_d model,

$$log\ x/m = log\ k + 1/n\ log\ C$$

Freundlich equation has many limitations. It is completely empirical and has no theoretical basis; it fails at higher pressure or concentration to describe adsorption; and the constants ‘k’ and ‘n’ are temperature dependents, they differ with temperature (Adamson & Gast, 1997).

Brunauer–Emmett–Teller (BET) Isotherm

BET isotherm (Bruanuer *et al.*, 1938) is a theoretical model which represents a fundamental milestone in interpretation of multi-layer adsorption isotherms, particularly the types II and III. It most extensively applied in the gas–solid equilibrium systems (Adamson & Gast, 1997). This model assumes that the adsorbed molecules stay put, same enthalpy for any layer, equal energy of adsorption for each layer except for the first layer, and a new layer can form while another is still not finished (Rouquerol *et al.*, 1999).

BET equation and has the form:

$$q = \frac{B * Ceq * b}{(Cs \quad Ceq) * \left[1 + (B \quad 1) * \left(\frac{Ceq}{Cs}\right)\right]}$$

For linear form of equation:

$$\frac{Ceq}{(Cs - Ceq)} = \frac{1}{Bb} + \left(\frac{(B-1)}{Bb}\right)\left(\frac{Ceq}{Cs}\right)$$

Where, *B*= a term for the energy of interaction with surface; *b* = monolayer capacity; *Cs* = concentration of solute at saturation; *Ceq* = concentration of solute at equilibrium.

Adsorbents

Activated Carbon

Activated carbon is a member of a family of carbons extending from carbon blacks to nuclear graphite. All types come from organic origin sources but with various carbonization and manufacturing processes. Activated carbon is solid, porous adsorbent, black carbonaceous substance distinguished by the absence of both impurities and an oxidized surface from elemental carbon (Marsh & Rodriguez-Reinoso, 2006).

Historically, activated carbon had been used by Egyptians about 1500 BC as an adsorbent for medical purposes and also as a purifying material. In ancient India, Hindus had used charcoal to purify their drinking water. In Japan, at old Kashiwara Jingu, Nara temple, a well for underground water constructed in the 13th century AD was found equipped with a charcoal filter at the bottom. In the 18th century, during the Napoleonic era in France, wood char and later bone char were used for first time in refining beet sugar (Suzuki, 1990). The first industrial production of activated carbon started in 1900 and it was used in sugar industries (Bansal & Goya, 2005).

Activated carbon can be prepared from a large number of natural and synthetic precursors such as coconut, wood, peat, coal, tar, and sawdust (Rouquerol *et al.*, 1999). It has a large

surface area and pore volume, making it appropriate for a wide variety of applications. It is used extensively for elimination of unwanted odor, color, tests, and impurities from waste water. It is also employed for air purification in inhabited locations and gas-phase application (Bansal & Goya, 2005).

Carbon is the main constituent (80 to 95%) of activated carbon, in addition to other elements such as nitrogen, hydrogen, oxygen, and sulfur. The typical composition of activated carbon is found to be 88% carbon, 6-7% oxygen, 1% nitrogen, 1% sulfur, 0.5% hydrogen with the balance representing inorganic ash constituents.

The porosity is the most important and essential property of activated carbon: the property that determines its usage. This porosity donates the surface area that provides the capacity to adsorb gases and vapors from compound gases and dissolved or dispersed materials from liquids. The total number of pores, their shape, and size determine the adsorption capacity and even the dynamic adsorption rate of the activated carbon. Porous structures are classified relative to their pore diameter or pore width. Pore sizes are commonly categorized into three groups; macro, meso, and micro. A macropore has diameter >1000 angstroms, a mesopore diameter is 100-1000 angstroms, and a micropore diameter is less than 100 angstroms (Roy, 1994). Several measurements are conducted after activated carbon production to describe the range of surface area, and pore distribution. Surface area is measured by the amount of liquid nitrogen adsorption volume at liquid nitrogen temperature. Pore volume distribution is measured by calculating the ratio of optical densities of standard molasses solution as decolorized by a sample of carbon and a reference of standardized decolorizing carbon. This value is called a molasses number, the higher numbers reflecting a larger percentage of macropores. The iodine number is the value of micropores percentage measuring, this value determines adsorption of iodine (in milligram) per

gram of carbon from 0.02 N iodine solution (Roy, 1994). The most commonly used activated carbon adsorbents have a specific surface area of 800-1500 m^2/g and a pore volume of 0.20-0.60 cm^3/g. The surface area in activated carbon is mostly contained in pores which have effective diameters less than 2 nm. The adsorption capacity of activated carbon is determined by its physical or porous structure but it is also strongly influenced by the chemical structure (Bansal & Goya, 2005).

Metal Oxide Nanoparticles

Nanomaterials are materials that exist at a scale of 10^{-9} meters (one nanometer is equaled to one-billionth of a meter). The extremely small size and some unique physical and chemical properties of nanomaterials have led to using them extensively in industrial, chemical, biomedical, and electronic applications. Nanomaterials can be available in different chemical forms such as metals, metal oxides, polymeric materials, ceramics, and more (Fryxell & Cao, 2012).

Different nanomaterials are being used as adsorbents to remove toxic pollutants from the environment. This is due their high surface area with large surface to bulk ratios, unusual shapes, high surface concentrations of reactive edge and corner, high percentage of their constituent atoms at a surface, and a wide range of Lewis acid-base properties and oxidation/reduction potentials (Volodin *et al.*, 2006). The surface area of nanoparticles ranges from 400 to 1000 m^2/g with about 10^{19} interfaces/cm^3. The surface area increases as the particle size decreases and the reactivity is considerably improved. The size of small crystallite in nanocrystals is quite remarkable. For instance, magnesium oxide prepared by the aerogel procedure has crystallite size ~ 4 nm, calcium oxide ~ 7 nm, titanium oxide ~ 10 nm, and zinc oxide ~ 8 nm. Whereas, the

surface area of magnesium oxide, calcium oxide, titanium oxide, and zinc oxide crystallite are ~500 m^2/g, ~150 m^2/g, ~100 m^2/g, and ~1 m^2/g, respectively (Ranjit *et al.*, 2005).

Nanoparticals of some metal oxides like oxides of magnesium, calcium, zinc, titanium, aluminum, and iron, have been exhibited to be highly efficient and active adsorbents for numerous toxic substances. In most cases, destructive adsorption occurs on the surface of the nanoparticals, so that the adsorbate is chemically broken up and thereby made nontoxic. The term "destructive adsorbent" is defined as the ability to efficiently adsorb and chemically destroy incoming adsorbate (Volodin *et al.*, 2006). Very high surface areas and higher reactivity compared to their bulk counterparts provide nanoparticals of metals oxides high adsorption capacity per mass adsorbent. This allows for the adsorption of relatively high amounts of some chemicals. Therefore, nanopartical adsorbents can have advantages over traditional adsorbents in areas that influence adsorption capacity: surface area and chemistry, and pore size distribution. One distinctive characteristic of nanometerscale structures is that, unlike macroscopic materials, they usually possess a high proportion of their component atoms at a surface. The bulk of an object decreases more rapidly than its surface area as the size reduces. This scaling tendency leads, in the most extreme case, to structures where almost every atom in the structure is interfacial (Ali, 2011).

Diatomaceous Earth

Diatomaceous earth or Diatomite is a loose, earthy or loosely cemented porous, pale-colored, soft, lightweight rock of sedimentary origin, mainly formed by fragments of skeletons of diatom algae (diatomea and radiolarian), with size ranges from 0.75 to 1500 μm. Typically, it is composed of 87–91% silicon dioxide (SiO2) with substantial quantities of alumina (Al2O3) and

ferric oxide (Fe2O3). Diatomite has its origin from a siliceous, sedimentary rock consisting mainly of the fossilized skeletal remains of diatom, a unicellular aquatic plant related to the algae (Paschen, 1986). Diatomite consists of a wide variety of shape and sized diatoms, typically from 10–200 μm, in a structure contains up to 80–90% voids (Lemonas, 1997). It is a highly porous structure, with good adsorption ability, chemical inertness, low density, and high surface area. The unique combination of physical and chemical properties of diatomite, make it applicable for a number of industrial uses as filtration media for various beverages and inorganic and organic chemicals, and for the removal of inorganic and organic pollutants (Michell & Atkinson, 1991, Al-Ghouti *et al.*, 2004).

Diatomite is widely used in filtering processes. It is used as a filter medium for swimming pools and fish tanks, in chemistry as a filtration aid to filter very tiny particles that pass through or block classical filter paper. In addition to this, it is used to filter drinking water, sugar, honey, and syrups without altering of their natural properties (Morsy & Bakr, 2010).

Results of many studies have shown that natural diatomite holds great potential to adsorb wide range of chemicals, such as the basic dye in solutions (Khraisheh *et al.*, 2004), BTEX (benzene, toluene, ethyl-benzene and xylenes), MTBE (methyl tertiary butyl ether) from aqueous solution (Aivalioti *et al.*, 2010), and heavy metals like lead, copper, and cadmium from wastewater (Morsy & Bakr, 2010). Diatomite possesses high liquid absorptive capacity. It can absorb 1.5 to more than 3 times its weight of water. Therefore, it is used widely as an absorbent for industrial spills and pet liter, as a mild abrasive in polishes, and as an insulation material (Antonides, 1997).

Fourier Transform Infrared Spectroscopy (FT-IR)

Fourier Transform Infrared Spectroscopy (FT-IR) is a powerful technique for recognizing types of chemical bonds in a molecule by creating an infrared absorption spectrum that is like a molecular "fingerprint". It can be utilized to provide useful information on molecular identity and structure. FT-IR is used to determine qualitative and quantitative features of IR-active molecules in organic or inorganic solid, liquid or gas samples (Rees, 2010).

FT-IR Spectrometer acquires broadband near infrared (NIR) to far infrared (FIR) spectra. Absorption takes place during transferring of the energy of the beam of light to the molecule. The molecule becomes excited and transfers to a higher energy state. The energy transfer occurs in the form of electron ring shifts, vibrations of molecular bond, rotations, and translations. Infrared is commonly concerned with stretching and vibrations (Smith, 2011). Energy of infrared photons are enough to effect groups of atoms to vibrate with respect to the bonds that link them. Similar to electronic transitions, these vibrational transitions relate to distinct energies, and infrared radiation can be absorbed by molecules only at certain wavelengths and frequencies. Chemical bonds vibrate when exposed to infrared radiation at specific frequencies, and they absorb the radiation at frequencies that match their vibration modes. Some bonds absorb infrared radiation strongly than others, and some bonds do not absorb at all. In order for a vibrational mode to absorb infrared radiation, periodic change in dipole moments must be involved. Energy absorption from a spectrum infrared radiation transferring through or reflecting off a chemical produce a pattern of energy absorption that is associated with the functional groups and the structural arrangement of molecules in the chemical. Measuring the amplitudes and frequency of radiation absorption generates a spectrum that can be utilized to identify functional groups and compounds (Griffiths & De Haseth, 2007).

FT-IR spectroscopy has many basic advantages and disadvantage over a classical dispersive infrared instrument.

These advantages are:

- Multiplex advantage (Fellgett advantage): A complete spectrum can be collected rapidly and many scans can be averaged in a shorter time than one scan on most dispersive instruments.
- Throughput advantage (Jacquinot advantage): the ability to complete the same signal/noise ratio as a dispersive instrument in a much shorter time
- Precision advantage (Connes advantage): the frequency scale of laser spectrum is known very accurately (high resolution) and is very stable (Sun, 2009).

The disadvantages are:

- FT-IR instruments do not measure spectra, they measure interferograms. Interferograms are not easy to interpret without first performing a Fourier transform to generate a spectrum.
- Because of multiplex advantage (source noise limited) applies, all regions of spectrum are observed simultaneously. Hence, the noise will be speared throughout the spectrum in an FT-IR system, if it take places in on part of the infrared radiation from the source (Smith, 2011).

Dermal Absorption

Human Skin

Skin is the largest organ of human body, making up to 16% of body weight, with a total area of 1.9 m^2 to form a physical barrier to the external environment (REF). Skin performs many vital functions, including protection against external physical and chemical assailants like micro-organisms, solar radiation, and toxic agents. Also, skin plays an important role in thermoregulation, control of excess water loss from the body, neural sensation, mechanical support, immunological surveillance, and others stressors (Kanitakis, 2002).

Skin is composed of three layers: the epidermis, dermis, and hypodermis (subcutaneous tissue). The epidermis is the external layer primarily consists of layers of keratinocytes in addition to melanocytes, Langerhans cells, and Merkel cells. The dermis layer is a supportive connective tissue between the epidermis and underlying subcutaneous tissue. It is basically made up of the fibrillar structural protein known as collagen and contains hair roots, sweet glands, blood and lymph vessels, nervous cells, and fibers. The hypodermis is a layer of loose connective tissue that lies beneath the dermis (Kanitakis, 2002, Riviere, 2005).

Epidermis

The epidermis is the outer layer of skin which forms both the physical and chemical barrier between the interior body and exterior environment. Anatomically, the epidermis is made up of stratified squamous epithelium. The main cells of the epidermis are the keratinocytes which are derived from ectoderm, forming the outermost layer of the skin. It is composed mainly of two types of cells: keratinocytes and dendritic cells. The keratinocytes vary from the dendritic cells

by owning intercellular bridges and ample amounts of stainable cytoplasm (Murphy, 1997). The thickness of the epidermis ranges from 0.05 mm on the eyelids to 2 mm on the soles of the feet and palms of the hand. The epidermis normally is separated into four layers according to keratinocyte morphology and position as they differentiate into horny cells. The four divided layers of the epidermis are created by the differing stages of keratin maturation. The classification of epidermal layers (from the external surface to the lower layer) is as follows:

- Stratum corneum (horny layer).
- Stratum granulosum (granular cell layer)
- Stratum spinosum (spinous or prickle cell layer)
- Stratum basale (basal or germinativum cell layer)

The three lower layers that formed the living, nucleated cells of the epidermis are sometimes referred to as the stratum malpighii and rete malpighii. These three layers are also known as a "viable epidermis" (Murphy, 1997, Riviere, 2005, James *et al.*, 2006). The epidermis is a permanently renewing layer and provides rise to derivative structures. The basal cells of the epidermis undergo proliferation cycles that furnish for the renewal of the external epidermis. The epidermis is a dynamic tissue in which cells are continually engaged in unsynchronized movement (Chu, 2008).

The epidermis layer is composed of at least 80% of cells which are ectodermally derived keratinocytes. The cells are differentiated through their migration from the basal layer to the surface of the skin, resulting in keratinization. During the process of keratinization, the keratinocyte first passes through a synthetic phase followed by a degradative phase (Chu, 2008). In the synthetic phase, the cell builds up a cytoplasmic supply of keratin. In degradative phase of

keratinization, the cells lose their organelles and the contents are consolidated into a mixture of filaments and amorphous cell envelopes, and the cell finally is known as a corneocyte (James *et al.*, 2006). In addition to the keratinocytes, other types of cells exists, which are usually identified as nonkeratinocytes and contains the melanocytes, Merkel cells, and Langerhans cells that exist in the epidermis but do not contribute to the process of keratinization (Riviere, 2005).

Stratum Corneum

The stratum corneum is the outermost layer of the epidermis. It is composed of several layers of hexagonal-shaped, tightly packed, anucleate, without cytoplasmic organelles, flattened, non-viable cornified cells, and known as corneocytes. The corneocytes are dead cells that are constantly self-renewing through desquamation from surface, and balanced by cell divisions in the lower epidermis (Holbrook & Odland, 1975). The stratum corneum cell layer can differ in its density depending on how the filaments are packed. The stratum corneum cell layers may vary in thickness from one body site to another. In general, it consists of 10-30 layers of stacked corneocytes in most areas of skin, but with the area of the palms and the soles having the most. Each corneocytes is about 40 µm in diameter and 0.5µm thick, and shows the end stage of keratinocyte differentiation(Gawkrodger & Ardern-Jones, 2012). Each corneocyte is enclosed by an envelope protein and is filled with tight bundles of intracellular keratin proteins. It is water insoluble, thermodynamically stable, and can retain water. In the corneocyte, the shape and alignment of the keratin proteins, which stabilized by disulphide cross-linked macrofibres, add strength to the stratum corneum (Lynley & Dale, 1983).

Corneocytes are surrounded by a dense cross-linked protein layer, referred to as the cell envelope. They are embedded in a monolayer of lipids matrix which is chemically

linked to this densely packed cell envelope (Harding *et al.*, 2000). The corneocytes are arranged in the lipid matrix in what is known as the "brick and mortar" structure (Michaels *et al.*, 1975). This lipid matrix plays an important role in the stratum corneum as it serves as an interface between the hydrophilic structures of corneocytes and the lipophilic extracellular lipid matrix. Additionally, corneodesmosomes interconnect the corneocytes and provide cohesion to the stratum corneum (Bouwstra & Gooris, 2010). The proportion of lipid content in stratum corneum ranges between 1 to 11 percent in human skin (Raykar *et al.*, 1988). The major lipid classes in human stratum corneum (% weight of solvent extracted lipids) are ceramides (40-50%), cholesterol (20 - 33%), saturated long chain free fatty acids (7 -13%), cholesterol sulfate (0-7%) and cholesteryl esters (0–20 %) (Wertz *et al.*, 1987, Norlen *et al.*, 1998). Stratum corneum lipids are synthesized in stratum granulosum, where they are packaged into lamellar bodies pre-apical secretion into the intercellular spaces to compose the intercorneocyte lipid. In contrast to other lipid structures (like cell membranes), the stratum corneum does not have phospholipids. The lipophilic environment of intercellular (lipid matrix) domains with hydrophilic domains of corneocytes impart a degree of "*amphiphobicity*" upon the stratum corneum, donating partial protection against both lipophilic and hydrophilic penetrants (Chilcott & Price, 2008).

Ceramides are a class of polar lipids. A typical ceramide consists of polar head-group (sphingosine, phytosphingosine or 6–hydroxysphingosine moiety) containing several functional groups that can form lateral hydrogen bonds with adjacent ceramide molecules. The polar heads link covalently to acyl chains of varying length, the large proportion consisting of 24–26 carbons (relatively longer than the phospholipids of

plasma membranes), with a small fraction containing 16–18 carbons. (Motta *et al.*, 1993, Bouwstra *et al.*, 2002b, Bouwstra *et al.*, 2003).

Stratum corneum lipids are congregated into lamellae (bilayers, with periodicity of approximately 13 nm) organized parallel to the surface of the corneocytes (Bouwstra & Ponec, 2006). The ceramides are linked to lipid layer through connections between sphingosine chains and fatty acid chains in ceramides. Spaces between the layers are filled with free lipids and relatively short acyle chains mainly consisting of fatty acids and cholestrol. The cermides head groups are organized into dence hydrogen- bonded lattices to compose orthorhombic crystalline bilayers. Acyl chains are mutually attracted through Van der Waalas force (Bouwstra & Gooris, 2010).

In epidermis, corneocytes are interconnected to each other by protein structures called desmosomes. Desmosomes are the main adhesion compound in epidermis, attaching keratin intermediate filaments to the cell membrane and bridging neighboring corneocytes, and allowing cells to resist mechanical stress (McGrath & Uitto, 2010). A desmosome is around or oval structure with diameter of 0.2 to 1 µm and 15 to 20 nm in thickness. It consist of two opposing symmetrically halves with a central intercellular space of 30 nm containing a dense line, each one belonging to one of to adjacent cells and containing of an intercellular , transmembranal, and extracellular part. Plaques of electrondense material run along the cytoplasm parallel to the conncation region. Three bands can be recognized in plaques an electrondense band next to the plasma membrane, a less dense band, then a fibrillar area (Holbrook, 1994, Cozzani *et al.*, 2000, Loden & Maibach, 1999).

Stratum Granulosum

The stratum granulosum is composed of many layers of flattened cells lying parallel to the epidermal–dermal junction. These cells comprise irregularly shaped, nonmembrane-bound, electron-dense keratohyalin granules, and are responsible for additional synthesis and modification of proteins involved in keratinization (Riviere, 2005, Chu, 2008). The keratohyaline granules are necessary in the genesis of the interfibrillary matrix which keeps keratin filaments conjugated and the inner lining of the horny cells (Matoltsy, 1976). The enzymatic action of keratohyaline granules enhances production of soft keratin in the epidermis by providing periodic cutting of keratin filaments. On the contrary, keratohyaline granules do not exist in hair and nails. Therefore, the keratin in those structures is hard (Matoltsy, 1976, Schwarz, 1979).

Stratum Spinosum

The stratum spinosum is multi-layered containing several (5-10) layers of irregular polyhedral cells fitted closely together that sits beneath the stratum granulosum (McGrath & Uitto, 2010). The surface of the cells displays minute spiny projections. As basal cells proliferate and mature, they proceed towards the outer stratum of epidermis, at first creating the stratum spinosum. The desmosomes, which look microscopically as prickles, connect the cells to neighboring stratum spinosum cells and to the stratum basale cells. This layer is distinguished by having numerous tonofilaments which discriminate it morphologically from the other layers (Riviere, 2005).

Stratum Basale

Stratum basale is the innermost layer of the epidermis which lies with their long axis perpendicular to the dermis. It consists of a single layer of columnar or cuboidal dividing and non-dividing keratinocytes. The cells are attached to the basement membrane by hemidesmosomes and attached laterally to each other and to the stratum spinosum cells by desmosomes (Wolff & Wolff-Schreiner, 1976). Stratum basale is the primary site of mitotically active cells in the epidermis that provide growth to cells of the outer epidermal layers. Nevertheless, not all cells in this layer have the potential to proliferate (Jones, 1996)

Dermoepidermal Junction / Basement Membrane

The basement membrane is a thin extracellular matrix rich in laminin and collagen that separates the epidermis from the dermis. The membrane contains four component layers; the lamina lucida, the lamina densa, the subbasal lamina, and basal epithelial cell that comprises the hemidesmosomes, in addtion to a variety of fibrous structures (Briggaman & Wheeler, 1975). The basment membrane has important functions; it preserves dermoepidermal junction, acts as a selective barrier between the dermis and epidermis to some materials, plays an important role in wound healing and cell behavior, and acts as a target for immunologic and nonimmunologic injury (Monteiro-Riviere & Inman, 1995)

Dermis

The dermis lies under the basement membrane and comprises of dense irregular connective tissue with a matrix of collagen, elastic, and reticular fibers embedded in an amorphous ground

substance of mucopolysaccharides (Riviere, 2005). It is interspersed with blood vessels, nerves, lymphatics, sweat glands, sebaceous glands, hair follicles, and arrector pili muscles. The dermis can be divied into a thin papillary layer and a thicker reticular layer. The thin papillary layer comprises of loose connective tissue, which is in contact with the epidermis.Whereas, the reticular layer consists of irregular dense connective tissue with fewer cells and more fibers (Chu, 2008). The dermis provides protection to the body from mechanical stress, binds water, thermoregulatory functions, sensory functions, and supports and nourishs the epidermis (Monteiro-Riviere, 1991, Chu, 2008).

Hypodermis (Subcutis)

The hypodermis is the innermost and thickest layer of the skin. It is made up of loose connective tissue and fat that lies under the dermis. It supports to anchor the dermis to the underlying muscle or bone. The hypodermis is primarily composed of a kind of cells, called as adipocytes which are specialized in accumulating and storing fats. These cells are congregated in lobules divided by connective tissues. It serves as an energy reserve. Addtionally, the loose consistency of collagen and elastic fibers provides the skin flexibility and free movement over the underlying structures (Riviere, 2005, James *et al.*, 2006).

Dermal Absorption

Dermal (skin, percutaneous) absorption is a term that describs the transport of a substance from outer surface of the skin into the skin and systemic circulation (Scheuplein, 1967). The transport of substances through the skin is a complex process and depends on the architecture of outer layers of skin.

There are three main mechanisms by which dermal absorption occurs:

i. Intercellular absorption: The penetrant is transferred around the corneocytes in the intercellular lipid matrix. Where, therew is chemical transport through a long and tortuous route between neighboring corneocytes.

ii. Transcellular absorption: The penetrant is transferred equally through the keratin-packed corneocytes and intercellular lipid matrix by partitioning.

iii. Transfollicular absorption: The penetrant bypasses the corneocytes, diffusing down hair follicles and into sebaceous glands or through sweat ducts.

The intercellular and transcellular absorption are also known as bulk pathways and transfollicular absorption is known as shunt pathways. Shunt pathways are not thought to play crucial role in dermal absorption because of limited areas of these shunt, it is only 0.1-1.0% of the total area (Scheuplein, 1967, Michaels *et al.*, 1975, Chilcott & Price, 2008).

In literature, much has been written about the implications of stratum corneum for penetrant transport because of the complexity of this barrier and incomplete understanding. It is known that the stratum corneum offers the skin's primary diffusion barrier (Scheuplein & Blank, 1971). Associations of skin permeability coefficients and the physicochemical properties of a wide variety of penetrants have shown that skin can be well modeled as a simple lipid barrier to substances possessing at least moderate water and oil solubility (Michaels *et al.*, 1975, Johnson *et al.*, 1997). Many models have been suggested that try to present the intrinsic nature of the stratum corneum in relatively simple term. However, each model was designed with some assumptions for particular purposes. Many models for the lipid organization in stratum corneum have been proposed: the stacked monolayer model (Swartzendruber *et al.*, 1989), the domain mosaic model (Forslind, 1994), the single gel phase model (Norlen, 2001), the laminglass model (Norlen, 2003), and the sandwich model (Bouwstra *et al.*, 2000, Bouwstra *et al.*, 2002a).

The stacked monolayer model which proposed in 1989 describes the molecular arrangement in the intercellular lipid matrix for the first time. In this model, the ceramides are arranged in a planar arrangement and the linoleic moiety of ceramides is randomly distributed in the two broad layers neighboring the narrow central layer. Cholestrol is distributed nonrandomly between layers (Swartzendruber *et al.*, 1989).

The domain mosaic model postulated the presence of a continuous liquid phase from the superficial layers of the stratum corneum down to the viable epidermis. It was the first model to include the existence of a liquid phase in the stratum corneum. In this model the intercellular lipids matrix of stratum corneum are segregated into a single crystalline/gel domains bordered by "grain borders" where lipids are in the fluid crystalline state. The crystalline areas are effectively impermeable and the fluid areas provide channels through which particles can diffuse leading to tortuous diffusion pathways through the intercellular lipids. Such organization offers for an effective "water-tight" barrier that allows a minute and controlled loss of water to keep the corneocytes moistened. As well as the model provided an explanation for the necessary mechanical properties permitting bending and stress imposed on the skin surface (Forslind, 1994).

The single gel-phase model proposed that the intercellular lipids within the stratum corneum, exists as a single and coherent lamellar gel phase without domain boundaries. In this gel phase the hydrocarbon chains are packed in a hexagonal and an orthorhombic pattern. The cholesterol concentration is uneven throughout the gel and lipids in areas with low cholesterol concentration are strongly packed, producing a gel that is crystal-like in nature, whereas the gel in areas with high cholesterol concentration is more liquid in nature (Norlen, 2001).

In 2003, Norlen proposed the laminglass model. This model postulated that the ceramides form a separate crystalline monolayer with the sphingosine and the fatty acid part forming two tightly packed hydrocarbon chain matrices. The consecutive crystalline and liquid crystalline layers compose an arrangement like a laminglass, similar to the stacked monolayer model. This model provides high permeability and resistance to mechanical stress imposed on the skin surface (Norlen, 2003)

The sandwich model proposed that the lipids are organized in a tri-layer structure: two broad layers with a crystalline (orthorhombic) structure are separated by a narrow central lipid layer with fluid domains. This model provides an explanation for structural data found by X-ray diffraction, FT-IR and transmission electron microscopy (Bouwstra *et al.*, 2000, Bouwstra *et al.*, 2002b).

Mechanism of Skin Transport

Dermal absorption contains permeation through the epidermis and absorption by the capillary network at the dermal-epidermal junction. Dermal absorption takes place primarily through the stratum corneum intracellularly or intercellularly. Many factors influence the dermal absorption including skin, environmental, and solute factors (Kielhorn *et al.*, 2006, USEPA, 1992)

Permeation of a solute across the stratum corneum is fundamentally a process of diffusion in which active transport and facilitated transport do not play an essential role. The polar substances tend to diffuse through protein portions of the stratum corneum, whereas the nonpolar compounds tend to diffuse through the intercellular lipid matrix (Albery & Hadgraft, 1979). After the solute partitions into epidermis it transports to cutaneous blood and lymphatic system. If the blood flow is

not enough, solute may sequester in the viable epidermis, in the dermis, and in hypodermis (Kielhorn *et al.*, 2006).

Diffusion of a compound into a specific layer of skin like the stratum corneum is called permeation. Diffusion can be defined as the 'process by which matter is transported from one part of a system to another as a result of random molecular movement' (Crank, 1975). Diffusion of compound through a membrane can be described by Fick's first law.

$$J = -D\,(\Delta C/\Delta x)$$

Where J flux of a compound (J, mass/cm^2 per second) at a given time and position is proportional to the differential concentration change ΔC over a differential distance Δx, D is the diffusivity.

With some modifications, Fick's first law can be applied to describe the diffusion process of compound across skin layers. This equation can help in identifying the ideal parameters involved in the dermal absorption (Scheuplein & Blank, 1971, Dugard, 1977). Basically, dermal absorption includes three stage processes. First stage includes partitioning of the compound into the stratum corneum. The second stage involves diffusion of the compound across the stratum corneum. In the final stage, the compound partitions from the stratum corneum into the underneath tissue. Therefore, the process of partitioning must be examined and linked to Fick's First Law of diffusion. Adapted to skin absorption, Fick's First Law comes with the form of:

$$J = P*D*C/H$$

Where J is the flux (rate of transfer per unit area), P is partitioning coefficient between the skin and the vehicle, D is the diffusion coefficient of the compound, C is the concentration gradient through the skin, H is the diffusional path length or skin thickness.

Fick's first law equation for dermal absorption relies on the assumptions that the compound does not bind, the compound diffusion coefficient and diffusion are constant with position or composition (Crank, 1975). These assumptions would result in a steady portion of any dose absorbed per unit time regardless of the dose concentration. However, results of many studies have disagreed with the extrapolations of Fick's law because the portion of compound absorbed was not steady across range of compound's concentrations in donor solution (Blank, 1964, Billich *et al.*, 2005).

Diffusion through the stratum corneum is driven by a thermodynamic gradient, not a concentration gradient. Movements of the compound molecules are dependent on the energy gradients in their immediate location. In constant temperature, the molecule movement across the stratum corneum is achieved through the energy flow from higher energy areas to areas of lower energy. Thermodynamic gradients are formed from the lucid force of all the inter-molecular repulsive and attractive forces (Atkins, 1994). The movement of molecule within a certain condition can be quantified in terms of its thermodynamic activity which is considered the driving force for diffusion. In some environments, the thermodynamic gradient could be in the reverse direction to a concentration gradient and hence, diffusion will take place against the gradient of concentration (Chilcott & Price, 2008).

Modeling of Skin Absorption

Modeling of dermal absorption offers applicable alternatives to laboratory experimentation. Models are used to comprehend associated features and processes of dermal absorption, in addition to predict its kinetics so that protective measures can be designed and implemented that minimize the risk of dermal absorption of toxic chemicals. Modeling of

compound transport across skin plays an important role in two major areas; assessments of dermal exposure to hazardous materials and in transdermal drug delivery (USEPA, 1992, Poet *et al.*, 2000, McDougal & Boeniger, 2002). Models can be categorize into two common categories: (i) quantitative structure-activity relationship (QSAR) models, (ii) mathematical models (Fitzpatrick *et al.*, 2004).

QSAR models are statistically derived linear and non-linear relationships between different physicochemical or structural properties of compound and the steady-state flux. In other words, QSAR basically includes three parts: (i) Modeling the activity or property (ii) descriptors of the physicochemical properties or molecules structural features, and (iii) a statistical procedure to create the relationship between activity and structure. Efficacy and safety concerns also distinguish QSAR models in irritation, skin sensitization, metabolism, chemical effects, and clearance. Therefore, these models are involved at a number of levels in chemical safety (Potts & Guy, 1995, Sartorelli *et al.*, 1998, Fitzpatrick *et al.*, 2004). In 1992, Potts and Guy proposed QSAR model based on Flynn (proposed a number of algorithms to predict K_p) dataset by using a combination of the octanol-water partition coefficient, K_{ow}, and the molecular weight or molecular volume as physicochemical descriptors as being both mechanistically relevant and competent of offering an appropriate explanation of these data (Flynn, 1990, Potts & Guy, 1995). QSAR models for skin permeability have many limitations which mostly relate to the modeling processes. These models are hindered by the insufficient high quality data comparable to absorption data (Fitzpatrick *et al.*, 2004). A steady-state permeability coefficient of QSAR does not predict absorption over time frames outside the steady-state part of the absorption/time curve. QSAR models are available only for permeability coefficients from aqueous vehicles, and the

predictions from aqueous vehicles cannot be extrapolated to predict the impacts of other solvents or formulations (Moss *et al.,* 2002, Cronin, 2005).

A number of mathematical models have been developed to simulate the effects of compounds partitioning into skin and the transport across the skin over time. Generally, most of these models have used either diffusion based or compartmental equations. Mathematical models have been established for measuring the skin absorption for a variety of exposure conditions. Mathematical models are varied in their degree of ability to describe or represent the processes associated with skin absorption perfectly. However, some of models are frequently experienced as being more complex than practically useful. In the simplest models, skin is considered as a single pseudo-homogeneous membrane. In more complex models, further layers of skin are included like the viable epidermis and dermis (Roberts & Anissimov, 2005).

Some of models have been developed that simulate the pathways of compounds through stratum corneum. Michaels and coworkers (Michaels *et al.*, 1975) modeled the steady-state behavior of the stratum corneum as "brick and mortar" where the brick represented the aqueous protein phase in the keratinocytes and the mortar represented the intercellular lipid phase. This model presumed that the transport was the sum of steady permeation, via the lipid matrix and protein phase and across the intercellular lipid matrix via a tortuous pathway. Flynn (Flynn, 1990) stated that diffusion of compound through the protein in the corneocytes of the stratum corneum is a thermodynamically and kinetically impossible passageway because the density and compactness of the keratin. Whereas, Scheuplein (Scheuplein, 1967) developed dermal absorption models based on transport through appendages. Scheuplein compared diffusion through appendages with diffusion through stratum corneum. It was found

that the appendages allowed greater diffusion at early times and the stratum corneum allowed greater diffusion at longer times.

Other models have been developed which are defined as physiologically-based pharmacokinetic (PBPK) models. These models do not consider the certain routes of dermal diffusion, but are developed to explain the rate of compound's diffusion via the skin and/or into the circulatory system using experimental observations and lumped-capacitance models (Clifford, 2004). PBPK models are based on mathematical descriptions of body compartments, tissues and partitioning processes, chemical transport and metabolism which effect the skin distribution, absorption and elimination of chemicals (Krishnan & Andersen, 1994). Potts and Guy (Potts & Guy, 1995) developed a PBPK model which can offer an algorithm to predict permeability from the chemical's physical properties. Multiple regression analyses were conducted using former data of the permeability coefficient for varied compounds, and the molecular volume and the hydrogen bond activity parameters were determined to be significant. Nevertheless, this model is only effective for polar compounds. Another PBPK model was adopted by Poet and coworkers (Poet *et al.*, 2000) to evaluate dermal permeability values and to predict exhaled concentrations of the chemical trichloroethylene. Good agreement was found between predicted and observed concentrations of trichloroethylene, however, the significance of the many features and processes were not clarified.

Measurements of Skin Absorption

Dermal absorption investigations are performed to determine the amount at which a compound is capable of penetrating the skin barrier. Information about a compound's dermal absorption rate is mostly of interest to regulatory agencies for risk assessment, therapeutics evaluations, and development of topically applied preparations. Estimation of chemical dermal absorption value is generally derived from experimental data *in vivo* or *in vitro*, or both. Such data provide direct or indirect evaluation of dermal absorption of a test substance across skin (Chilcott & Price, 2008).

In vivo Methods

The *in vivo* methods provide data about the extent of dermal uptake in addtion to the systemic absorption of the test chemical. The principle purpose in conducting *in vivo* methods in place of *in vitro* methods are that the *in vivo* methods employ a physiologically and metabolically intact system. *In vivo* absorption models can be used to measure dermal absorption directly or indirectly and commonly provide data relatively similar to those under which exposure is expected in a real environment (Bunge & McDougal, 1999). In the direct methods a compound is measured in the blood, tissue or body excretion by using strips of tape from stratum corneum, or evaluated through biological or pharmacological responses (USEPA, 2007). These methods are generally complicated and time consuming (Zendzian, 2000). While, in indirect models skin absorption is concluded from the diminishing of the compound on the dermal surface (Bunge & McDougal, 1999, Chilcott & Price, 2008).

For dermal absorption prediction in humans, different animal species models have been used with variable degrees of association (Wester & Maibach, 1992). The most common

animal species used for predicting human dermal absorption are laboratory rodents, however, other animal models such as swine, rabbits, guinea pigs, dogs, and rhesus monkeys(Bartek *et al.*, 1972, Bronaugh *et al.*, 1985, Hikima *et al.*, 2002) have also been used. Althogh, the *in vivo* methods for dermal absorption studies show reliable and promising results, they are always challenged by ethical considerations and country specific legislations (Chilcott & Price, 2008).

In vitro Methods

In vitro methods are developed to estimate the penetration of compound into and subsequent permeation through the skin into receptor fluid and can use non-viable skin to estimate penetration and permeation only or fresh, metabolically active skin to concurrently measure permeation and dermal metabolism (Kielhorn *et al.*, 2006). *In vitro* absorption methods provide a valid alternative of skin absorption assessment for many important aspects of dermal exposure. The *in vitro* technique is less expensive than *in vivo* technique, can be utilized with skin from different animal species in addition to the human skin, and can be employed to assess highly toxic or corrosive compounds without concern for ethical or legitimate considerations (USEPA, 2007, Chilcott & Price, 2008). The infinite dose and finite dose, two different type of *in vitro* techniques have been used to assess skin absorption, and the infinite dose technique is the most frequently used (Franz, 1975, Sartorelli *et al.*, 2000). *In vitro* models include different techniques (i) diffusion cells, (ii) isolated perfused tubed-skin preparation, and (iii) stratum corneum binding (USEPA, 1992).

Diffusion Cells

Diffusion cells are of two types; upright (vertical) or side-by-side (horizontal) type. The receptor chamber volumes are about 0.5–10 cm^3 with surface areas of exposed membranes of about 0.2–2 cm^2. Vertical diffusion cells are suitable for evaluating dermal absorption from semisolid preparations applied on the skin membrane surface and are best for simulating *in vivo* exposure scenarios (Brain *et al.*, 1998). Whereas, horizontal diffusion cells are suitable for evaluating mechanisms of diffusion across skin (Bronaugh, 2004). Diffusion cells can be classified into two types based on acceptor fluid status: whether it is confined to the receptor chamber (Static diffusion cell) or passes through (flow-through diffusion cell) the receptor chamber (Franz, 1975, Bronaugh, 1995). Either the vertical or the horizontal diffusion cells can be used in static or flow-through mode.

Static Diffusion Cells

Static diffusion cells are also known Franz-type diffusion cells. These cell systems are relatively simple in design and any type or any amount of vehicle containing the test compound can be spread on skin. The receptor fluid below the skin is manually collected by removing aliquots periodically for analysis and substituted with equal volumes of fresh receptor fluid (Franz, 1975). Because this process requires the immersion of both surfaces of the skin, it may result in much hydration and skin damage, thereby altering the permeability of the skin (Gummer & Maibach, 1991).

To simulate *in vivo* skin condition, it is important to create a known skin temperature in each diffusion cell. Therefore, the static diffusion cells can be designed in jacketed and non-jacketed models. In the jacketed model, heated water is circulated across the jacket to control the temperature of the diffusion cell. Whereas, the non-jacketed model may

be placed in a water bath or into dry heated blocks (Chilcott & Price, 2008). Receptor chamber fluid is important to be sufficiently stirred, because insufficient stirring may limit the rate of partitioning of compound through the skin into the receptor chamber, which resulting in skin absorption underestimation (Franz, 1975). Another important factor to be considered, is the solubility of the test chemical in the receptor fluid, which may impact the sink capacity and then the sampling frequency or receptor chamber dimensions (Brain *et al.*, 1998)

Flow-Through Diffusion Cells

Flow-through diffusion cells are distinguished by a changing receptor fluid continuously, which mimics, more or less, *in vivo* condition. The movement of receptor fluid is usually driven by a peristaltic pump, enabling an accurate and steady flow rate across each cell. However, some of the low-cost diffusion cells can use gravity to flow the receptor fluid by siphoning, but the flow rate induced by siphoning is more unsteady and needs an internal calibration (Chilcott & Price, 2008). A flow-through diffusion cell system was developed by Bronaugh and Stewar (Bronaugh & Stewart, 1985) in 1985. The cells were constructed using Teflon and contained a glass window in the bottom for viewing the receptor contents and at least 5 mL/hr which is a flow rate suggested of getting accurate results.

Different types of receptor fluid are used in diffusion cells. With nonviable skin, a buffered saline solution can be used. However, to maintain the viability of skin in the diffusion cells, physiological solution such as HEPES-buffered Hanks' balanced salt solution is required (Collier *et al.*, 1989). Saline solution, as a receptor, may be appropriate for studying hydrophilic chemicals dermal absorption. But, lipophilic

chemicals need a receptor fluid that more closely resembles the lipophilic properties of blood (USEPA, 1992), therefore, modifications of the receptor fluid are sometimes required to enhance the partitioning of lipophilic chemicals through skin into the receptor fluid to mimic the *in vivo* conditions. Earlier studies have suggested some substances to be added to the receptor fluid such as 3-5% of bovine serum (Bronaugh *et al.*, 1986), surfactants (Bronaugh & Stewart, 1984), and organic solvents (Scott & Ramsey, 1987). Selected receptor fluid and the flow rates are varied with the test compound, they are based on the solubility considerations and the volume of the receptor chamber (Skelly *et al.*, 1987).

References

Abe, A., 1999: Distribution of 1,4-dioxane in relation to possible sources in the water environment. Sci Total Environ, 227, 41-47.

Adamson, A. W. and A. P. Gast, 1997: Physical Chemistry of Surfaces. sixth ed., Wiley Interscience, New York.

Aivalioti, M., I. Vamvasakis and E. Gidarakos, 2010: BTEX and MTBE adsorption onto raw and thermally modified diatomite. J. Hazard. Mater., 178, 136-143.

Al-Anber, M. A., 2011: Thermodynamics Approach in the Adsorption of Heavy Metals. cahpter in ,Thermodynamics - Interaction Studies - Solids, Liquids And Gases edit by Moreno-Pirajan, J. C. INTECH. ISBN: 9789533075631, pp 737-762.

Al-Ghouti, M. A., M. A. M. Khraisheh and M. Tutuji, 2004: Flow injection potentiometricstripping analysis for study of adsorption of heavy metal ions onto modified diatomite. Chem. Eng. J., 104.

Albery, W. J. and J. Hadgraft, 1979: Percutaneous absorption: *In vivo* experiments. The Journal of pharmacy and pharmacology, 31, 140-147.

Ali, M. H., 2011: Ammonia gas adsorption on metal oxide nanoparticles. Master of Science Thesis, College of Engineering, Kansas State University, Manhattan, Kansas.

Anbar, M. and P. Neta, 1967: A compilation of specific bimolecular rate constants for the reactions of hydrated electrons, hydrogen atoms and hydroxyl radicals with inorganic and organic compounds in aqueous solution. Int. J. Appl. Radial Isntop., 16, 227-242.

Andrade, R. D., R. Lemus and C. E. Perez, 2011: Models of Sorption Isotherms for Food: Uses and Limitations. Vitae-Revista De La Facultad De Quimica Farmaceutica, 18, 324-333.

Antonides, L. E., 1997: Diatomite. U.S. Geological Survey, http://minerals.usgs.gov/minerals/pubs/commodity/diatomite/250497.pdf

Argus, M. F., J. C. Arcos and C. Hochligeti, 1965: Studies on the carcinogenic activity of protein-denaturing agents: hepatocarcinogenicity of dioxane. J Natl Cancer Inst, 35, 949-958.

Argus, M. F., R. S. Sohal, G. M. Bryant, C. Hoch-Ligeti and J. C. Arcos, 1973: Dose-response and ultrastructural alterations in dioxane carcinogenesis. Influence of methylcholanthrene on acute toxicity. Eur J Cancer, 9, 237-243.

ASTDR, 2012: Toxicological Profile for 1,4-Dioxane. U.S. Department of Health and Human Services Public Health Service, Agency for Toxic Substances and Disease Registry., http://www.atsdr.cdc.gov/toxprofiles/tp187.pdf.

Atkins, P., 1994: Physical chemistry. W.H. Freeman and Company, New York.

Aus, 1999: Australian SIDS Initial Assessment Report (OECD).

Bansal, R. C. and M. Goya, 2005: Activated Carbon Adsorption. CRC Press, ISBN: 978-0-8247-5344-3.

Barber, H., 1934: Haemorrhagic nephritis and necrosis of the liver from dioxan poisoning Guy's Hospital Reports, ISSN: 0017-5889 84, 267-280

Bartek, M. J., J. A. LaBudde and H. I. Maibach, 1972: Skin permeability *in vivo*: comparison in rat, rabbit, pig and man. The Journal of investigative dermatology, 58, 114-123.

Bernhardt, D. and H. Diekmann, 1991: Degradation of dioxane, tetrahydrofuran and other cyclic ethers by an environmental Rhodococcus strain. Appl Microbiol Biotechnol, 36, 120-123.

Billich, A., H. Vyplel, M. Grassberger, F. P. Schmook, A. Steck and A. Stuetz, 2005: Novel cyclosporin derivatives featuring enhanced skin penetration despite increased molecular weight. Bioorganic & medicinal chemistry, 13, 3157-3167.

Blank, I. H., 1964: Penetration of low-molecular-weight alcohols into skin. I. Effect of concentration of alcohol and type of vehicle. The Journal of investigative dermatology, 43, 415-420.

Bouwstra, J. A., F. E. Dubbelaar, G. S. Gooris and M. Ponec, 2000: The lipid organisation in the skin barrier. Acta dermato-venereologica. Supplementum, 208, 23-30.

Bouwstra, J. A. and G. S. Gooris, 2010: The lipid organization in human stratum corneum and model systems. Open Derm J, 4, 10-13.

Bouwstra, J. A., G. S. Gooris, F. E. Dubbelaar and M. Ponec, 2002a: Phase behavior of stratum corneum lipid mixtures based on human ceramides: the role of natural and synthetic ceramide 1. The Journal of investigative dermatology, 118, 606-617.

Bouwstra, J. A., P. L. Honeywell-Nguyen, G. S. Gooris and M. Ponec, 2003: Structure of the skin barrier and its modulation by vesicular formulations. Progress in lipid research, 42, 1-36.

Bouwstra, J. A., G. S. Pilgram and M. Ponec, 2002b: Does the single gel phase exist in stratum corneum? The Journal of investigative dermatology, 118, 897-898; author reply 899-901.

Bouwstra, J. A. and M. Ponec, 2006: The skin barrier in healthy and diseased state. Biochimica et biophysica acta, 1758, 2080-2095.

Brain, K. R., K. A. Walters and A. C. Watkinson, 1998: Investigation of skin permeation *in vitro*. In: Roberts MS & Walters KA eds. Dermal absorption and toxicity assessment. New York, Marcel Dekker, pp 161–187 (Drugs and the Pharmaceutical Sciences Vol. 91).

Braun, W. H. and J. D. Young, 1977: Identification of beta-hydroxyethoxyacetic acid as the major urinary metabolite of 1,4-dioxane in the rat Toxicology and Applied Pharmacology 39, 33-38.

Briggaman, R. A. and C. E. Wheeler, Jr., 1975: The epidermal-dermal junction. The Journal of investigative dermatology, 65, 71-84.

Bronaugh, R. L., 1982: Percutaneous absorption of cosmetic ingredients. In P Frost; SN Horwitz (Ed.),Principles of cosmetics for the dermatologist. St. Louis, MO: C.V. Mosby, pp. 277-284.

Bronaugh, R. L., 1995: Methods for *in vitro* skin metabolism studies. Toxicol Method, 5, 275-281.

Bronaugh, R. L., 2004: Methods for *in vitro* percutaneous absorption. In: Zhai, H. and Maibach, H. I. eds. Dermatotoxicology, 6th ed. New York, CRC Press, . pp 520–526.

Bronaugh, R. L. and R. F. Stewart, 1984: Methods for *in vitro* percutaneous absorption studies III: hydrophobic compounds. Journal of pharmaceutical sciences, 73, 1255-1258.

Bronaugh, R. L. and R. F. Stewart, 1985: Methods for *in vitro* percutaneous absorption studies IV: The flow-through diffusion cell. Journal of pharmaceutical sciences, 74, 64-67.

Bronaugh, R. L., R. F. Stewart and M. Simon, 1986: Methods for *in vitro* percutaneous absorption studies. VII: Use of excised human skin. Journal of pharmaceutical sciences, 75, 1094-1097.

Bronaugh, R. L., R. F. Stewart, R. C. Wester, D. Bucks, H. I. Mailbach and J. Anderson, 1985: Comparison of percutaneous absorption of fragrances by humans and monkeys. Food and chemical toxicology : an international journal published for the British Industrial Biological Research Association, 23, 111-114.

Bruanuer, S., P. H. Emmett and E. Teller, 1938: Adsorption of gases in multimolecular layers. J. Am. Chem. Soc., 60, 309–316.

BUA, 1991: 1,4-Dioxane/ed. by the GDCh Advisory Committee on Existing Chemicals of Environmental Relevance.

Buffler, P. A., S. M. Wood, L. Suarez and D. J. Kilian, 1978: Mortality follow-up of workers exposed to 1,4-dioxane. J Occup Med, 20, 255-259.

Bunge, A. L. and N. J. McDougal, 1999: Dermal uptake. In: Olin, SS, ed. Exposure to contaminants in drinking water. Estimating uptake through the skin and by inhalation. Boca Raton, FL: CRC Press. pp. 137-181.

Burback, B. L. and J. J. Perry, 1993: Biodegradation and biotransformation of groundwater pollutant mixtures by Mycobacterium vaccae. Appl Environ Microbiol, 59, 1025-1029.

Burmaster, D. E., 1982: The new pollution-groundwater contamination Environment, 24 6-36.

Chilcott, R. and S. Price, 2008: Principles and Practice of Skin Toxicology. John Wiley & Sons.

Chu, D. H., 2008: Overview of biology, development, and structure of skin. In K. Wolff, L.A. Goldsmith, S.I. Katz, B.A. Gilchrest, A.S. Paller, & D.J. Leffell (Eds.), Fitzpatrick's dermatology in general medicine (7th ed.). New York: McGraw-Hill., pp 57 -73.

Clifford, K. H., 2004: Probabilistic modeling of percutaneous absorption for risk-based exposure assessments and transdermal drug delivery. Statistical Methodology, 1, 47-69.

Collier, S. W., N. M. Sheikh, A. Sakr, J. L. Lichtin, R. F. Stewart and R. L. Bronaugh, 1989: Maintenance of skin viability during *in vitro* percutaneous absorption/metabolism studies. Toxicology and Applied Pharmacology, 99, 522-533.

Cozzani, E., M. Cacciapuoti, A. Parodi, R. Ghohestani and A. Rebora, 2000: Desmosomes and their autoimmune pathologies. European journal of dermatology : EJD, 10, 255-261.

Crank, J., 1975: The Diffusion Equations, in The Mathematics of Diffusion, 2nd edn (Crank, J.), Clarendon Press, Oxford. pp. 1 - 10.

Cronin, M. T., 2005: The prediction of skin permeability using quantitative structure–activity relationship methods, In (Ed) Riviere, J. Edmond, Dermal absorption models in toxicology and pharmacology. Boca Raton. pp 114- 134.

Daubert, T. E. and R. P. Danner, 1985: 1,4-Dioxane. In: Physical and thermodynamic properties of pure chemicals. New York, NY: Taylor & Francis.

DCC, D. C. C., 1989: Assessment of health and environmental effects of 1,4-dioxane and publications concerning 1,4-dioxane. Submitted to U.S. Environmental Protection Agency under TSCA Section 8E. OTS05166244.

De Boer, J. H., 1968: The Dynamical Character of Adsorption. second ed., Oxford University Press, London.

de Navasquez, S., 1935: Experimental tubular necrosis of the kidneys accompanied by liver changes due to dioxane poisoning Journal of Hygiene 35, 540-548.

Dietrich, A. M., D. S. Millington and Y. Seq, 1988: Specific identification of synthetic organic chemicals in river water using liquid-liquid extraction and resin adsorption coupled with electron impact, chemical ionization and accurate mass measurement gas chromatography-mass spectrometry analyses. J Chromatogr 436, 229-241.

Dragun, J., 1988: The Soil Chemistry of Hazardous Materials. Silver Spring,MD .The Hazardous Materials Control Research Institute.

Dugard, P., 1977: Skin permeability theory in relation to measurements of percutaneous absorption in toxicology. In: Marzulli FN & Maibach HI eds. Dermatotoxicology and pharmacology. Washington, DC, Hemisphere Publishing Corp., pp 525 – 550.

ECB, 2002: European Union Risk Assessment Report, 1,4-dioxane, CAS No: 123-91-1, EINECS No: 204-661-8. European Chemicals Bureau, Institute for Health and Consumer Protection, 21.

Emmett, P. H. and S. Brunauer, 1937: The Use of Low Temperature van der Waals Adsorption Isotherms in Determining the Surface Area of Iron Synthetic Ammonia Catalysts. J. Am. Chem. Soc., 59, 1553–1564.

Ernstgard, L., A. Iregren, B. Sjogren and G. Johanson, 2006: Acute effects of exposure to vapours of dioxane in humans. Hum Exp Toxicol, 25, 723-729.

Everett, D. H., 1971: Manual of Symbols and Terminology for Physicochemical Quantities and Units. International Union of Pure and Applied Chemistry Division of Physical Chemistry, IUPAC.

EWG, 2007: Environmental Working Group. EWG research shows 22 percent of all cosmetics may be contaminated with cancer-causing impurity . http://www.ewg.org/news/news-releases/2007/02/08/ewg-research-shows-22-percent-all-cosmetics-may-be-contaminated-cancer ((accessed 04.12.2014).

Fairley, A., E. C. Linton and A. H. Ford-Moore, 1934: The toxicity to animals of 1,4-dioxane. The Journal of Hygiene, 34, 486-501.

Fisher, J., D. Mahle, L. Bankston, R. Greene and J. Gearhart, 1997: Lactational transfer of volatile chemicals in breast milk. Am Ind Hyg Assoc J, 58, 425-431.

Fitzpatrick, D., J. Corish and B. Hayes, 2004: Modelling skin permeability in risk assessment--the future. Chemosphere, 55, 1309-1314.

Flynn, G. L., 1990: Physicochemical determinants of skin absorption. IN: Garrity, TR, Henry, CJ (Eds) Principles of route-to route extrapolation for risk assessment. Elsevier, New York, pp 93-127.

Foo, K. Y. and B. H. Hameed, 2010: Insights into the modeling of adsorption isotherm systems. Chemical Engineering Journal, 156, 2-10.

Forslind, B., 1994: A domain mosaic model of the skin barrier. Acta dermato-venereologica, 74, 1-6.

Franz, T. J., 1975: Percutaneous absorption on the relevance of *in vitro* data. The Journal of investigative dermatology, 64, 190-195.

Freundlich, H. M. F., 1906: Over the adsorption in solution. J. Phys. Chem, 57, 385–471.

Fryxell, G. E. and G. Cao, 2012: Environmental Applications of Nanomaterials: Synthesis, Sorbents and Sensors. Imperial College Press.

Gawkrodger, D. and M. R. Ardern-Jones, 2012: Dermatology: An Illustrated Colour Text. 5rd ed. Edinburgh, UK. ISBN 9780702051173. Elsevier Health Sciences UK.

Giavini, E., C. Vismara and M. L. Broccia, 1985: Teratogenesis study of dioxane in rats. Toxicol Lett, 26, 85-88.

Griffiths, P. and J. A. De Haseth, 2007: Fourier Transform Infrared Spectrometry. John Wiley & Sons, Inc., Hoboken, New Jersy. ISBN13: 9780470106297.

Grosjean, D., 1990: Atmospheric chemistry of toxic contaminants. 2. Saturated aliphatics: Acetaldehyde, dioxane, ethylene glycol ethers, propylene oxide. Air Waste Mgmt Assoc, 40, 1522-1531.

Gummer, C. and H. I. Maibach, 1991: Diffusion cell design. In: Bronaugh, R. L.; Maibach, H.I. eds.*In vitro* percutaneous absorption principles, fundamentals and applications. Boston, MA: CRC press, pp. 7-16.

Guo, W. and H. Brodowasky, 2000: Determination of the trace 1,4 Dioxane. Microchemical Jouranl 64, 174-180.

Harding, C. R., A. Watkinson, A. V. Rawlings and I. R. Scott, 2000: Dry skin, moisturization and corneodesmolysis. International journal of cosmetic science, 22, 21-52.

Harkov, R., R. Katz, J. Bozzelli and B. Kebbekus, 1981: Toxic and carcinogenic air pollutants in New Jersey volatile organic substances. In: McGovern JJ, ed. Proceedings from International Technical Conference Toxic Air Contamination. Pittsburgh, PA: Air Pollution Control Association

Harkov, R., B. Kebbekus, B. J.W., P. J. Lioy and J. Daisey, 1984: Comparison of selected volatile organic compounds during the summer and winter at urban sites in New Jersey. Sci Total Environ, 38, 259-274.

Hikima, T., K. Yamada, T. Kimura, H. I. Maibach and K. Tojo, 2002: Comparison of skin distribution of hydrolytic activity for bioconversion of beta-estradiol 17-acetate between man and several animals *in vitro*. European journal of pharmaceutics and biopharmaceutics : official journal of Arbeitsgemeinschaft fur Pharmazeutische Verfahrenstechnik e.V, 54, 155-160.

Hinrich, L., R. A. M. Bohn and G. A. O., 2002: Soil Chemistry John Wiley & Sons, Inc. ISBN13: 978-0471363392.

Holbrook, K., 1994: Ultrastructure of epidermis. In: Leigh IM, Watt FM, Lane EB, eds. Keratinocyte Handbook. Oxford: Oxford University Press. pp 3 - 43.

Holbrook, K. A. and G. F. Odland, 1975: The fine structure of developing human epidermis: light, scanning, and transmission electron microscopy of the periderm. The Journal of investigative dermatology, 65, 16-38.

Howard, P. H., 1990: Handbook of Environmental Fate and Exposure Data for Organic Chemicals. Chelsea, MI: Lewis Publishers, Inc.

IARC, 1999: International Agency for Research on Cancer ; 1,4-Dioxane. In: IARC Monographs on the Evaluation of Carcinogenic Risks to Humans, Vol. 71,Re-evaluation of some organic chemicals, hydrazine and hydrogen peroxide. International Agency for Research on Cancer, Lyon, France 71 part 2 589-602.

James, W. D., T. G. Berger and D. M. Elston, 2006: Andrews' diseases of the skin: Clinical dermatology (10th ed.). Philadelphia: Elsevier Saunders.

JBRC, 1998: Japan Bioassay Research Center. Two-year studies of 1,4-dioxane in F344 rats and BDF1 mice (drinking water) Technical Report .Kanagawa, Japan

Johnson, M. E., D. Blankschtein and R. Langer, 1997: Evaluation of solute permeation through the stratum corneum: lateral bilayer diffusion as the primary transport mechanism. Journal of pharmaceutical sciences, 86, 1162-1172.

Johnstone, R. T., 1959: Death due to dioxane? AMA Archives of Industrial Health, ISSN: 0567-3933, 20, 445-447.

Jones, P. H., 1996: Isolation and characterization of human epidermal stem cells. Clinical science, 91, 141-146.

Kanitakis, J., 2002: Anatomy, histology and immunohistochemistry of normal human skin. European journal of dermatology : EJD, 12, 390-399; quiz 400-391.

Kano, H., Y. Umeda, T. Kasai, T. Sasaki, M. Matsumoto, K. Yamazaki, K. Nagano, H. Arito and S. Fukushima, 2009: Carcinogenicity studies of 1,4-dioxane administered in drinking-water to rats and mice for 2 years. Food and chemical toxicology : an international journal published for the British Industrial Biological Research Association, 47, 2776-2784.

Khraisheh, M. A. M., Y. S. Al-Degs and W. A. M. Mcminn, 2004: Remediation of wastewater containing heavy metals using raw and modified diatomite. Chem. Eng. J., 99, 177-184.

Kielhorn, J., S. Melching-Kollmuss, I. Mangelsdorf and W. H. Organization, 2006: Environmental Health Criteria 235: Dermal Absorption. World Health Organization.

Klecka, G. M. and S. J. Gonsior, 1986: Removal of 1,4-dioxane from wastewater. Journal of Hazardous Materials, 13, 161-168.

Kociba, R. J., S. B. McCollister, C. Park, T. R. Torkelson and P. J. Gehring, 1974a: 1,4-dioxane. I. Results of a 2-year ingestion study in rats Toxicology and applied pharmacology, 30, 275-286

Kociba, R. J., S. B. McCollister, C. Park, T. R. Torkelson and P. J. Gehring, 1974b: 1,4-dioxane. I. Results of a 2-year ingestion study in rats Toxicology and Applied Pharmacology 30, 275-286

Konasewich, D., W. Traversy and H. Zar, 1978: Great Lakes Water Quality: Status report on heavy metal contaminants in the Lakes Erie, Michigan, Huron, and Superior Basins.

Kraybill, H. F., 1978: Carcinogenesis induced by contaminants in potable water. Bull NY Acad Med, 54, 413-427.

Krishnan, K. and M. E. Andersen, 1994: Physiologically based pharmacokinetic modeling in toxicology. In: Hayes, A. W. (ed.) Principles and Methods of Toxicology. Raven Press Ltd.,CRC press New York. ISBN: 9780203362839. pp 149-188.

Langmuir, I., 1916: The constitution and fundamental properties of solids and liquids. J. Am. Chem. Soc., 38, 2221-2295.

Laug, E. P., H. O. Calvery, H. J. Morris and G. Woodard, 1939: The toxicology of some glycols and derivatives Journal of Industrial Hygiene and Toxicology, 21, 173-201.

Lemonas, J. F., 1997: Diatomite. Am. Ceramic Soc. Bull., 76, 92-95.

Loden, M. and H. I. Maibach, 1999: Dry Skin and Moisturizers: Chemistry and Function Taylor & Francis, CRC Press. ISBM: 9780849375200 . pp 110-112.

Lynley, A. M. and B. A. Dale, 1983: The characterization of human epidermal filaggrin. A histidine-rich, keratin filament-aggregating protein. Biochimica et biophysica acta, 744, 28-35.

Marsh, H. and F. Rodriguez-Reinoso, 2006: Activated Carbon. Elsevier Science & Technology Books, ISBN: 0080444636.

Marzulli, F. N., D. M. Anjo and H. I. Maibach, 1981: *In vivo* skin penetration studies of 2,4-toluenediamine, 2,4-diaminoanisole, 2-nitro-p-phenylenediamine, p-dioxane and N-nitrosodiethanolamine in cosmetics. Food Cosmet Toxicol, 19, 743-747.

Matoltsy, A. G., 1976: Keratinization. The Journal of investigative dermatology, 67, 20-25.

Mazurkiewicza, J. and P. Tomasik, 2006: Why 1,4-dioxane is a water-structure breaker. Journal of Molecular Liquids, 126, 111-115.

McDougal, J. N. and M. F. Boeniger, 2002: Methods for assessing risks of dermal exposures in the workplace. Critical reviews in toxicology, 32, 291-327.

McGrath, J. A. and J. Uitto, 2010: Anatomy and Organization of Human Skin. Rook's Textbook of Dermatology. Wiley-Blackwell, Oxford, UK.

Michaels, A. S., S. K. Chandrasekaran and S. E. Shaw, 1975: Drug permeation through human skin: Theory and invitro experimental measurement. AIChE journal, 21, 985-996.

Michell, P. B. and K. Atkinson, 1991: The novel use of ion exchange material as an aid to reclaiming derelict mining land. Minerals Eng., 4, 1091-1113.

Mikheev, M. I., P. Gorlinskaya Ye and T. V. Solovyova, 1990: The body distribution and biological action of xenobiotics. J Hyg Epidemiol Microbiol Immunol, 34, 329-336.

Mohr, T. K. G., W. H. DiGuiseppi and J. A. Stickney, 2010: Environmental Investigation and Remediation: 1,4-Dioxane and other Solvent Stabilizers. Book News, Inc., Portland - United States, 34.

Monteiro-Riviere, N. A., 1991: Compartive anatomy, physiology and biochemistry of mammalian skin. In: Hobson, D. W. (ed.0 Dermal and Ocular Toxicology: fundamentals and Methoda. CRC Press, London, UK pp 3 - 71.

Monteiro-Riviere, N. A. and A. O. Inman, 1995: Indirect immunohistochemistry and immunoelectron microscopy distribution of eight epidermal-dermal junction epitopes in the pig and in isolated perfused skin treated with bis (2-chloroethyl) sulfide. Toxicologic pathology, 23, 313-325.

Morsy, H. E. G. and M. Bakr, 2010: Diatomite: Its Characterization, Modifications and Applications. Asian J Mat Sci, 2, 121-136.

Moss, G. P., J. C. Dearden, H. Patel and M. T. Cronin, 2002: Quantitative structure-permeability relationships (QSPRs) for percutaneous absorption. Toxicology *in vitro* : an international journal published in association with BIBRA, 16, 299-317.

Motta, S., M. Monti, S. Sesana, R. Caputo, S. Carelli and R. Ghidoni, 1993: Ceramide composition of the psoriatic scale. Biochimica et biophysica acta, 1182, 147-151.

Murphy, G. F., 1997: Histology of the skin. In D. Elder, R. Elenitsas, C. Jaworsky, & B. Johnson, Jr. (Eds.), Lever's histopathology of the skin. (8th ed.). Philadelphia: Lippincott Williams & Wilkins., 5 -45.

Myers, A. L. and J. M. Prausnitz, 1965: Thermodynamics of mixed gas adsorption. J. Am. Chem. Soc., 11, 235-266.

NCI, 1978: National Cancer Institute : Bioassay of 1,4-dioxane for possible carcinogenicity National Cancer Institute http://ntp.niehs.nih.gov/ntp/htdocs/LT_rpts/tr080.pdf.

Ncibi, M. C., 2008: Applicability of some statistical tools to predict optimum adsorption isotherm after linear and non-linear regression analysis. J Hazard Mater, 153, 207-212.

Nelson, N., 1951: Solvent toxicity with particular reference to certain octyl alcohols and dioxanes Medical Bulletin, 11, 226-238.

NICNAS, 1998: National Industrial Chemicals Notification and Assessment Scheme;1,4-Dioxane Priority Existing Chemical No. 7, Full Public Report,. Commonwealth of Australia, ISBN 0 642 47104 5.

NIOSH, 1977: Criteria for a recommended standard ...: Occupational Exposure to Dioxane. U.S. Department of Health, Education and Welfare, Center for Disease Control, National Institute for Occupational Safety and Health, Washington D.C. DHEW (NIOSH) Publication No.

Norlen, L., 2001: Skin barrier structure and function: the single gel phase model. The Journal of investigative dermatology, 117, 830-836.

Norlen, L., 2003: Molecular skin barrier models and some central problems for the understanding of skin barrier structure and function. Skin pharmacology and applied skin physiology, 16, 203-211.

Norlen, L., I. Nicander, A. Lundsjo, T. Cronholm and B. Forslind, 1998: A new HPLC-based method for the quantitative analysis of inner stratum corneum lipids with special reference to the free fatty acid fraction. Archives of dermatological research, 290, 508-516.

Paschen, S., 1986: Diatomaceous earth extraction, processing and application. Erzmetall, 39, 158-161.

Poet, T. S., R. A. Corley, K. D. Thrall, J. A. Edwards, H. Tanojo, K. K. Weitz, X. Hui, H. I. Maibach and R. C. Wester, 2000: Assessment of the percutaneous absorption of trichloroethylene in rats and humans using MS/MS real-time breath analysis and physiologically based pharmacokinetic modeling. Toxicological sciences : an official journal of the Society of Toxicology, 56, 61-72.

Potts, R. O. and R. H. Guy, 1995: A predictive algorithm for skin permeability: the effects of molecular size and hydrogen bond activity. Pharmaceutical research, 12, 1628-1633.

Ranjit, K. T., G. Medine, P. Jeevanandam, I. N. Martyanov and K. J. Klabunde, 2005: Nanoparticles in Environmental Remediation. In Grassian,V. H. (ed) Environmental Catalysis, 291-420.

Raykar, P. V., M. C. Fung and B. D. Anderson, 1988: The role of protein and lipid domains in the uptake of solutes by human stratum corneum. Pharmaceutical research, 5, 140-150.

Rees, O. J., 2010: Fourier Transform Infrared Spectroscopy: Developments, Techniques, and Applications. Nova Science Publishers, Incorporated, ISBN: 1616688351.

Reid, E. W. and H. E. Hoffman, 1942: 1,4 -Dioxane . Industrial and Engineering Chemistry 21 (7), 695-697.

Riviere, J. E., 2005: Dermal absorption models in toxicology and pharmacology, p. 374 p. Taylor & Francis, Boca Raton.

Roberts, M. S. and Y. Anissimov, 2005: Mathematical models in percutaneous absorption. In: Bronaugh RL & Maibach HI eds. Percutaneous absorption: drugs, cosmetics, mechanisms, methodology, 4th ed. Boca Raton, FL, Taylor & Francis pp 1–44.

Rouquerol, F., J. Rouquerol and K. Sing, 1999: Adsorption by Powders and Porous Solids, Principles, Methodology and Applications. ACADEMIC PRESS, 24-28 Oval Road, London NWl7DX. UK.

Roy, G. M., 1994: Activated Carbon Applications in the Food and Pharmaceutical Industries. CRC Press, ISBN: 978-0-8247-5344-3.

Ruthven, D. M., 1984: Principles of Adsorption and Adsorption Processes. A Wiley-Interscienece Publication.

Sartorelli, P., H. R. Andersen, J. Angerer, J. Corish, H. Drexler, T. Goen, P. Griffin, S. A. Hotchkiss, F. Larese, L. Montomoli, J. Perkins, M. Schmelz, J. van de Sandt and F. Williams, 2000: Percutaneous penetration studies for risk assessment. Environmental toxicology and pharmacology, 8, 133-152.

Sartorelli, P., C. Aprea, A. Cenni, M. T. Novelli, D. Orsi, S. Palmi and G. Matteucci, 1998: Prediction of percutaneous absorption from physicochemical data: a model based on data of *in vitro* experiments. The Annals of occupational hygiene, 42, 267-276.

Scheuplein, R. J., 1967: Mechanism of percutaneous absorption. II. Transient diffusion and the relative importance of various routes of skin penetration. The Journal of investigative dermatology, 48, 79-88.

Scheuplein, R. J. and I. H. Blank, 1971: Permeability of the skin. Physiological reviews, 51, 702-747.

Schrenk, H. H. and W. P. Yant, 1936: Toxicity of dioxan Journal of Industrial Hygiene and Toxicology 18, 448-460

Schwarz, E., 1979: Biochemie der epidermalen keratinisation. In A. Marchionini (Ed.), Handbuch der hautund geschlectskrankheiten (Vol. I). Berlin: Springer-Verlag.

Scott, R. C. and J. D. Ramsey, 1987: Comparison of the *in vivo* and *in vitro* percutaneous absorption of a lipophilic molecule (cypermethrin, a pyrethroid insecticide). The Journal of investigative dermatology, 89, 142-146.

Silverman, L., H. F. Schulte and M. W. First, 1946: Further studies on sensory response to certain industrial solvent vapors. J Ind Hyg Toxicol., 28, 262-266.

Skadsen, J. M., B. L. Rice and D. J. Meyering, 2004: The occurrence and fate of pharmaceuticals, personal care products and endocrine disrupting compounds in a

municipal water use cycle: A case study in the city of Ann Arbor. City of Ann Arbor, Water Utilities and Fleis & VandenBrink Engineering, Inc., http://www.a2gov.org/government/publicservices/water_treatment/Documents/Archive/EndocrineDisruptors.pdf.

Skelly, J. P., V. P. Shan, R. H. Guy, R. C. Wester, G. Flynn and A. Yacobi, 1987: FDA and AAPS report of the workshop on principles and practices of *in vitro* percutaneous penetration studies: relevance to bioavailability and bioequivalence. Pharmaceutical research, 4, 265 - 267.

Smith, B. C., 2011: Fundamentals of Fourier Transform Infrared Spectroscopy, Second Edition. CRC Press, Tylor & Francis Group, LLC. ISBN: 1420069306.

Snoeyink, V. L., 1999: Adsorption of organic compounds In: F.W. Pontius (Ed). water quality & Treatment Handbook, New York : McGraw Hill, pp 781 - 875.

Stickney, J. A., S. L. Sager, J. R. Clarkson, L. A. Smith, B. J. Locey, M. J. Bock, R. Hartung and S. F. Olp, 2003: An updated evaluation of the carcinogenic potential of 1,4-dioxane. Regulatory Toxicology and Pharmacology, 38, 183-195.

Stott, W. T., J. F. Quast and P. G. Watanabe, 1981: Differentiation of the mechanisms of oncogenicity of 1,4-dioxane and 1,3-hexachlorobutadiene in the rat. Toxicol Appl Pharmacol, 60, 287-300.

Sun, D., 2009: Infrared Spectroscopy for Food Quality Analysis and Control. Academic Press, Unitrd State. ISBN: 978-0-12-374136-3.

Suthersan, S. S., 2002: National and Enhanced Remedation System. Boca Raton, FL: Lewis Publisher

Suzuki, M., 1990: Adsorption Engineering. Kodansha, Science, Tokyo.

Swartzendruber, D. C., P. W. Wertz, D. J. Kitko, K. C. Madison and D. T. Downing, 1989: Molecular models of the intercellular lipid lamellae in mammalian stratum corneum. The Journal of investigative dermatology, 92, 251-257.

Thiess, A. M., E. Tress and I. Fleig, 1976 Arbeitsmedizinische Untersuchungsergebnisse von Dioxan-exponierten Mitarbeitern [Industrial-medical investigation results in the case of workers exposed to dioxane] Arbeitsmedizin, Sozialmedizin, Umweltmedizin 11, 35-46.

Thomas, R. G., 1990: Volatilization from water. In: Lyman WJ, Reehl WF, *et al.*, eds. Handbook of chemical property estimation methods: Environmental behavior of organic compounds. Washington, DC: American Chemical Society, 1-34.

TRI, 2013: TRI explorer: Providing access to EPA's toxic release inventory data. Washington, DC. Office of Information Analysis and Access, Offices of Environmental Information, U.S. Environmental Protection Agency. Toxic Release Inventory, http://www.epa.gov/triexplorer.

USEPA, 1992: Dermal exposure assessment: Principles and applications. U.S. Environmental Protection Agency, , Office of Health and Environmental Assessment, Washington D.C.

USEPA, 1993: Final report on ambient concentration summerise for Clean Air ActTitle IIIhazourdous air pollutants. . Research Triangle Parck, North Carolina: USEPA, EPA Contract No. 600/R94/090.

USEPA, 1996: Solvents Study - 4.4 1,4-Dioxane. Annual Solvents Study. EPA -Office of Solid Waste Management. U. S. Environmental Protection Agency. Washington, D.C.

USEPA, 2000: Environmental Protection Agency, preliminary data summary airport deicing operations (Revised). Office of Water (4303) Washington, DC.

USEPA, 2005: U.S. Environmental Protection Agency; Guidelines for carcinogen risk assessment. Washington, DC http://www.epa.gov/raf/publications/pdfs/CANCER_GUIDELINES_FINAL_3-25-05.PDF.

USEPA, 2006: U.S. Environmental Protection Agency;Treatment technologies for 1 4-dioxane: fundamentals and field applications. Washington, DC: American Chemical Society, http://www.epa.gov/tio/download/remed/542r06009.pdf.

USEPA, 2007: Dermal Exposure Assessment: A Summary of EPA Approaches. National Center for Environmental AssessmentOffice of Research and Development U.S. Environmental Protection Agency Washington, DC

USEPA, 2013a: U.S. Environmental Protection Agency; 1,4-Dioxane, Integrated Risk Information System (IRIS). http://www.epa.gov/ncea/iris/subst/0326.htm

USEPA, 2013b: U.S. Environmental Protection Agency;Toxicological Review of 1,4-Dioxane (CAS No. 123-91-1). In Support of Summary Information on the Integrated Risk Information System (IRIS). U.S. Environmental Protection Agency, Washington, DC: American Chemical Society, http://www.epa.gov/iris/toxreviews/0326tr.pdf.

Vallombroso, T. M., 2001: Organic Chemistry Pearls of Wisdom. Boston Medical Publishing Corporation, Boston, MA.

VCCEP, 2007: Voluntary Children's Chemical Evaluation Program, Tiers 1, 2, and 3 Pilot Submission For 1,4-Dioxane. The Sapphire Group, Inc., http://www.tera.org/peer/VCCEP/p-Dioxane/p-Dioxane%20Submission.pdf.

Volodin, A. M., A. F. Bedilo, D. S. Heroux, V. I. Zaikovskii, I. V. Mishakov, V. V. Chesnokov and K. J. Klabunde, 2006: Nanoscale oxides as destructive sorbents for halogenated hydrocarbons. In Blitz, J. Gun'ko, V. (eds) Surface Chemistry in Biomedical and Environmental Science. Springer. New York 403-412.

Walsom, G. D. and B. Tunnicliffe, 2002: 1,4-dioxane -- a little known compound. Changing the investigation and remediation of TCA impacts. Environmental Science & Engineering, http://www.esemag.com/archive/0502/tca.html.

Wertz, P. W., D. C. Swartzendruber, K. C. Madison and D. T. Downing, 1987: Composition and morphology of epidermal cyst lipids. The Journal of investigative dermatology, 89, 419-425.

Wester, R. C. and H. I. Maibach, 1992: Percutaneous absorption of drugs. Clinical pharmacokinetics, 23, 253-266.

WHO, 2005: World Health Organization ; 1,4-Dioxane in Drinking-water, Background document for development of WHO Guidelines for Drinking-water Quality. WHO/SDE/WSH/05.08/120.

WHO, 2008: Guidelines for Drinking-water Qualit[Electronic Resource]: Incorporating 1st and 2nd Addenda, Vol. 1, Recommendations, third ed., http://www.who.int/water_sanitation_health/dwq/fulltext.pdf.

Wolfe, N. L. and P. M. Jeffers, 2000: Hydrolysis. In: Boethling RS, Mackay D, eds. Handbook of property estimation methods for chemicals: Environmental and health sciences. Boca Raton, FL: Lewis Publishers.

Wolff, K. and E. C. Wolff-Schreiner, 1976: Trends in electron microscopy of skin. The Journal of investigative dermatology, 67, 39-57.

Woo, Y. T., J. C. Arcos, M. F. Argus, G. W. Griffin and K. Nishiyama, 1977b: Structural Identification of P Dioxane-2-One as the Major Urinary Metabolite of P Dioxane. Naunyn-Schmiedeberg's Archives of Pharmacology, 299, 283-288.

Woo, Y. T., M. F. Argus and J. C. Arcos, 1977a: Metabolism in-Vivo of Dioxane Effect of Inducers and Inhibitors of Hepatic Mixed Function Oxidases. Biochemical Pharmacology, 26, 1539-1542.

Woo, Y. T., M. F. Argus and J. C. Arcos, 1978: Effect of mixed-function oxidase modifiers on metabolism and toxicity of the oncogen dioxane. Cancer Res, 38, 1621-1625.

Yaqoob, M. and G. M. Bell, 1994: Occupational factors and renal disease. Renal Failure, 16, 425-434.

Young, J. D., W. H. Braun and P. J. Gehring, 1978a: The dose-dependent fate of 1,4-dioxane in rats. J Environ Pathol Toxicol, 2, 263-282.

Young, J. D., W. H. Braun and P. J. Gehring, 1978b: Dose-dependent fate of 1,4-dioxane in rats. J Toxicol Environ Health, 4, 709-726.

Young, J. D., W. H. Braun, P. J. Gehring, B. S. Horvath and R. L. Daniel, 1976: 1,4-Dioxane and beta-hydroxyethoxyacetic acid excretion in urine of humans exposed to dioxane vapors. Toxicol Appl Pharmacol, 38, 643-646.

Young, J. D., W. H. Braun, L. W. Rampy, M. B. Chenoweth and G. E. Blau, 1977: Pharmacokinetics of 1,4-dioxane in humans. J Toxicol Environ Health, 3, 507-520.

Zendzian, R. P., 2000: Use of *in vitro* dermal penetration studies to compare rat and human penetration of chemicals. Presented at the Annual Meeting of the Society for Risk Analysis, Arlington, VA, December 3-6, 2000. http://www.riskworld.com/Abstract/2000/SRAam00/ab0ac403.htm.

Zenker, M., R. Borden and M. Barlaz, 2004: Biodegradation of 1,4-Dioxane Using a Trickling Filter. Journal of Environmental Engineering, 130, 926–931.

Zenker, M. J., R. C. Borden and M. A. Barlaz, 2000: "Cometabolism of Poorly Biodegradable Ethers in Engineered Bioreactors". In: Bioremediation and Phytoremediation of Chlorinated and Recalcitrant Compounds, pg. 421. Proceedings of the Second International Conference on Remediation of Chlorinated and Recalcitrant Compounds. Monterey, California., http://www.battelle.org/BookStore/BookTemplate.aspx?ISBN=1-57477-57098-57475.

Zhang, Z. Z., P. F. Low, H. J. Cushman and C. B. Roth, 1990: Adsorption and heat of adsorption of organic compounds on montmorillonite from aqueous solutions. Soil Sci Soc Am J, 54, 59-66.

CHAPTER II

Chapter 2 - Adsorption of 1,4-Dioxane on Nanoparticles of Metal Oxide, Activated Carbon and Diatomaceous Earth in Vapor and Aqueous Phases

Abstract

Dioxane is a potentially carcinogenic solvent. When spilled or discarded under poorly controlled conditions, it contaminates ground water, rendering the water unusable. It readily evaporates at room temperature and contaminates indoor air. The adsorption process provides an option for removing dioxane from contaminated water and air. In this study, the adsorption efficiencies of activated carbon (AC), metal oxide nanomaterials (TiO_2 and MgO), and diatomaceous earth (DE) were assessed in aqueous and vapor phases using infrared spectroscopy as a quantification tool. In the aqueous phase, the effects of contact time, pH, and type of water on dioxane adsorption were investigated. The contact time for reaching equilibrium and maximum adsorption rate was observed to be < 40 min in both phases. The highest adsorptive capacity of AC, MgO, TiO_2, and DE were seen at the pH values of 7–8, 6–7, 7–8, and 6–8, respectively. Water type had no effect ($P > 0.05$) on the adsorption of dioxane. The adsorption values for 50 mg/L dioxane in water at pH 7 and room temperature were 80.87±3.2 µg/g onto AC, 11.41 ± 2.7 µg/g onto DE, 3.84 ± 1.2 µg/g onto TiO_2, and 3.79 ± 0.84 µg/g onto MgO. The equilibrium adsorption data were analyzed by the Freundlich model of adsorption. The results showed that the equilibrium data for dioxane sorbent systems fitted well for AC and only a relative fit was observed for other adsorbents. In the vapor phase, the adsorption of 40 mg dioxane in 400 ml air at room temperature and 760 mmHg (torr) pressure converted into 66.9± 1.7 µg/g for AC, 19.3 ± 1.4 µg/g for TiO_2, at 8.6 ± 0.91 µg/g for MgO, and 4.7 ± 0.94 µg/g for DE.

Introduction

Several synthetic organic compounds produced by industries are released into the environment. The existence of those chemicals in the environment has the potential to cause adverse effects, which include toxicity, carcinogenicity, mutagenicity, and teratogenicity in animals and humans, toxicity to aquatic life and fishes, and retrogression of the quality of water for human consumption. Therefore, there is a pressing need to regulate the release of hazardous toxic compounds into the environment by developing suitable control technologies that are capable of eliminating hazardous material from water and ambient air so that such materials are stopped from further distribution in the environment.

Dioxane is a synthetic organic compound, which is manufactured and used widely since the 1950s. It is listed as a high production volume chemical with a volume of more than 500 metric tons produced domestically or imported. Nearly 90% of the total volume of dioxane is utilized to stabilize 1,1,1- trichloroethane in vapor degassing of metals (Mohr *et al.*, 2010). Dioxane has attracted increasing attention for its possible presence at thousands sites of chlorinated solvent release, landfills, and in factory effluents. It was estimated that 600,000 to 1,300,000 pounds of dioxane was released into the environment annually between 1988 and 2002 (TRI, 2013). The disposal of chemical solvents containing dioxane and disposal of dioxane itself results in the presence of dioxane in the environment. In many countries such as the United States, Canada, and Japan, dioxane has been detected as a contaminant in the natural environment. Drinking water supplies, superfund sites, and public groundwater were found to contain dioxane in more than permissible quantity (Mohr *et al.*, 2010).

Public concern and growing awareness about dioxane as an environmental contaminant has steadily increased due to its probable carcinogenicity and its implication as a major contributor to groundwater contamination. Thus, the increasing public demand for stricter control of environmental contamination by dioxane has stimulated great interest in developing guidelines for treating dioxane in water, soil, and ambient air. In February 2008, the U.S. Environmental Protection Agency (U.S.EPA) included dioxane in its list of 104 candidate chemicals of concern for national drinking water regulation in the future and classified it as a proposed contaminant for third Unregulated Contaminant Monitoring Rule program (UCMR 3). Nonetheless, a federal water standard has not been established for this chemical yet (USEPA, 2011). Several U.S. EPA regions and states have developed guidelines for treating dioxane; for example, Colorado became the first state to establish an enforceable cleanup standard for dioxane in groundwater and surface water in September 2004. The standard was phased in, stipulating facilities to meet dioxane limits of 6.1 and 3.2μg/L by March 2005 and March 2012 , respectively (USEPA, 2011).

The unique properties of dioxane render it very mobile and persistent in the aquatic environment for a long time. At solvent release sites, it is found to be the fastest moving contaminant and the first to arrive at municipal or domestic supply wells. It is ranked first in terms of mobility of more than 100 organic chemicals (Roy & Griffin, 1985). The hydrophilic nature of dioxane makes it relatively resistant to conventional treatment technologies commonly used for chlorinated solvents. Because of dioxane's low Henry's Law constant, high miscibility in water, and low octanol–water partition coefficient (K_{ow}), volatilization and adsorption methods are not expected to be significant removal processes for eliminating a significant amount of dioxane in aqueous environments (USEPA, 2006). Its heterocyclic structure with two ether

linkages makes dioxane very immune to both abiotic and biologically mediated degradation (Zenker *et al.*, 2003).

Technologies that are effective for removing chlorinated solvents usually do not yield favorable results while treating dioxane because of its unique properities. The conventional water and wastewater treatment processes such as air stripping, adsorption, and precipitation-coagulation are not efficient for removing it from aqueous environment (Zenker *et al.*, 2003). Advanced oxidation treatment processes using ozone, hydrogen peroxide, and ultraviolet light were reasonably successful in removing dioxane considerably, but their operational costs are significantly high (Mohr *et al.*, 2010). It was found that air stripping treatment process can remove 30% of dioxane from contaminated groundwater, and granular activated carbon adsorption column can remove about 67% (Mcguire *et al.*, 1978), whereas advanced oxidation treatment processes (hydrogen peroxide with ozone) can reduce more than 96% dioxane from water (Bowman *et al.*, 2003, GRAC, 2003).

During the past few decades, adsorption acquired prominence as an effective water purification technology employed in the treatment of wastewater (Lazaridis *et al.*, 2003). Adsorption systems are rapidly becoming important treatment processes for producing good quality water with low concentration of dissolved organic and inorganic contaminants (Walker & Weatherley, 1999). Adsorption is defined as an integral to a broad spectrum of physical, chemical, and biological processes and operations in the environmental field. It is extensively employed for purification of water and air by removing contaminants. It has played a major role in air pollution control by its capacity to remove dissolved impurities from solution. Currently, adsorption is viewed as a crucial method for wastewater treatment and water reclamation (Weber, 1972a).

A wide variety of adsorbents are used to assess the effectiveness of dioxane removal from groundwater. The adsorbents include activated tri-base pelletized carbon (contains three types of carbon in a single pellet), surfactant-modified zeolites, zero-valent iron with zeolites, and a proprietary macroporous polymer manufactured by Akzo Nobel (Earth Tech Inc, 2004). The treatability testing revealed that only the activated tri-base carbon showed effective dioxane adsorption, whereas the other adsorbents were ineffective in removing dioxane from water (DiGuiseppi & Whitesides, 2007).

Dioxane could be released into air during its production, its use, and the processing of other chemicals like pesticides and pharmaceuticals. The current levels of dioxane in ambient air are not available in the United States, but they are expected to be less than the levels reported in the 1980s or in earlier periods due to decline in the use of dioxane in recent years (ASTDR, 2012). Historical data (1980s or earlier) suggest that ambient mean concentration of outdoor and indoor levels of dioxane were 0.1–0.4 $\mu g/m^3$ and 3.704 $\mu g/m^3$, respectively. In the United States, dioxane in outdoor and indoor air was measured routinely as part of the volatile organic compound National Ambient Database in the early to mid-1980s (Shah & Singh, 1988).

Usually, dioxane enters ambient air as a vapor, and is degraded in the atmosphere through a photochemical reaction with hydroxyl radicals to yield alkyl radicals (Surprenant, 2002). This reaction starts with the hydrogen atom abstraction followed by the oxygen addition to form a radical of cyclic alkylperoxy (Maurer *et al.*, 1999). This product is further degraded by reaction with nitrate radicals (Grosjean, 1990) and may not undergo direct photolysis (Wolfe & Jeffers, 2000). Dioxane is short-lived in the atmosphere and its half-life is estimated to be 6.69 to 9.6 hr (HSDB, 2007).

Dioxane, like other volatile organic compounds, can be removed from ambient air of industrial facilities and through a host of technologies such as adsorption (Yang *et al.*, 2011), absorption (Ohta *et al.*, 2011), and combustion (Hosseini *et al.*, 2011) to protect the environmental systems. Among these technologies, adsorption technique has been widely used in practical applications because of its easy operation, low operating cost, high capacity, high selectivity, and effective recovery at low partial pressures (Shim *et al.*, 2006). Therefore, adsorption is always selected as the purifying technology for dealing with dioxane in ambient air, because of its high rate of diffusion at low concentration (Kirk-Othmer, 1999). Different types of adsorbents have been used in purifying technology, such as zeolite, alumina, silica, titanium oxide, and activated carbon (Wang *et al.*, 2011). Generally, the activated carbon material is extensively employed as the adsorbent due to its pore structure, advantages of huge surface area, chemical stability, low cost, and easy recycling (Wang *et al.*, 2011).

This study aimed to: (i) investigate the adsorption of dioxane onto four different adsorbents (activated carbon, diatomaceous earth, nanocrystalline titanium dioxide, and nanocrystalline magnesium oxide) in aqueous and vapor phases. (ii) Investigate the effect of pH, contact time, and type of water on dioxane adsorption in the aqueous phase. (iii) Estimate the maximum adsorption capacity of the four adsorbents in aqueous phase, where the adsorption equilibrium data were fitted to adsorption isotherms of Freundlich model.

Materials and Methods

Materials

1,4-Dioxane (99.8%) was purchased from ACROS Organics® (New Jersey, USA). Nanocrystalline magnesium oxide (MgO) and titanium dioxide (TiO_2) were obtained from NanoScale Corporation (Manhattan, KS, USA). Diatomaceous earth (DE) (co-batch #058k0012) and activated carbon (AC) were obtained from Sigma Aldrich (St. Louis, MO, USA).

The properties of adsorbent materials are as described by the manufacturer and as shown in transmission electron microscopy (TEM) images (figure 2.1)

- The properties of nanocrystalline metal oxides are listed in Table 2.1.

Table 2.1: Properties of nanocrystalline metal oxides

Properties	**MgO**	**TiO_2**
Specific Surface Area (BET)	≥ 230 m^2/g	≥ 500 m^2/g
Crystallite Size	≤ 8 nm	amorphous
Average Pore Diameter	50Å	32Å
Total Pore Volume	≥ 0.2 cc/g	≥ 0.4 cc/g
Bulk Density	0.6 cc/g	0.6 cc/g
True Density	3.2 g/cc	3.7 g/cc
Mean Aggregate size, $d_{0.5}$	3.3 μm	5 μm
Moisture Content	≤ 1%	≤ 4%
Metal Content (Based on Metal)	≥ 95%	≥ 99.999%

- Diatomaceous earth (DE) is described as a powder form and free of organic matter impurities.
- Activated carbon (AC)

  Vapor pressure : <0.1 mmHg (20°C)

Form: untreated powder

Autoignition temp. : 842°F

Resistivity: 1375 μΩ-cm (20°C, graphite)

Particle size: 100–400 mesh

Mp: 3550 °C (lit.)

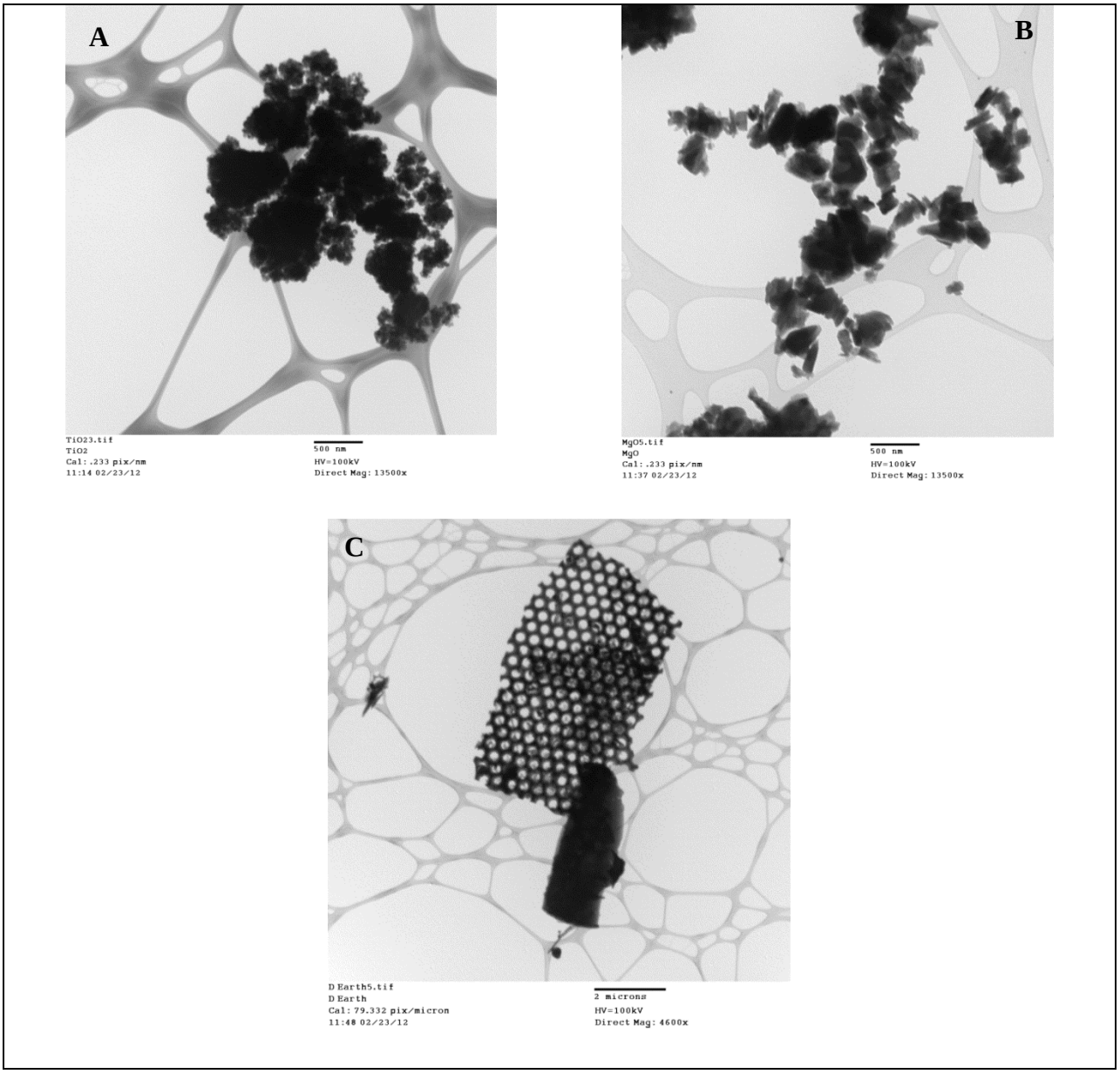

Figure 2.1: TEM image of,(A) nanocrystalline titanium dioxide (B) nanocrystalline magnesium oxide (C) diatomaceous earth

Water sample collection

Surface and ground water samples were collected from Riley County, Kansas. Surface water samples were collected from Big Blue River (N39.2474404, W96.593098). The ground water samples were collected from monitoring network (monitoring well No 20, N39.25887, W96.591446, depth 22 feet) at the Old Chemical West Landfill site at Kansas State University, Manhattan, Kansas. The water was taken from the wells for sampling using disposable bailers, so as to minimize any disturbance of the water column to prevent outgassing or degassing during collection. The collected surface and ground water samples were containerized for transport to the laboratory in 250 ml amber glass bottles. All the bottles were filled, leaving no head space in the bottle. The samples were stored in sealed sample bottles at 4°C.

All surface and ground water samples were tested for water quality properties (Table 2.2). Samples also were checked if they were free of 1,4-dioxane contamination using U.S. EPA Method 522 (EPA/600/R-08/101). In this method, in brief, a water sample was fortified with the isotopically labeled surrogate analyte (SUR), 1,4-dioxane-d_8. Then, the sample was extracted by solid phase extraction (SEP), where a 500 mL sample was passed through an SPE cartridge containing 2 g of coconut charcoal to extract the method analyte and SUR. Thereafter, the compounds are eluted from the solid phase with a small amount (approximately 1.5 mL) of dichloromethane. The extract volume was adjusted and the internal standard and tetrahydrofuran-d_8 were added. Finally, the extract was dried with anhydrous sodium sulfate. Analysis of the extract was performed by GC/MS. The analyte, SUR, and internal standard are separated and identified by comparing the acquired mass spectra and retention times to reference spectra, and retention times for calibration standards acquired under identical GC/MS conditions. The

concentration of the analyte is determined by comparison to its response in calibration standards relative to the internal standard (Munch & Grimmett, 2008).

Table 2.2: Water quality properties

Prosperity	Surface water	Ground water
Sp. conductivity ($\mu s/cm$)	9.17	12.43
Total Dissolved Solids (TDS) *g/l*	4.58	6.21
pH	8.11	7.59
Salinity (*ppt*)	5.12	7.11

Sample Preparation

Sample Preparation for Aqueous Phase

Aqueous solution of dioxane (50 mg/L) was prepared for using it in adsorption measurements. One mL aliquot of the aqueous dioxane solution and various quantities of adsorbents (AC, MgO, TiO_2, and DE) were placed in a microfuge tube and sealed. The tubes were shaken for 1 minute on a vortex mixer at 296 K and then left for 90 min to achieve adsorption equilibrium. The tubes were centrifuged at 13,000 rpm for 10 min in the microcentrifuge to separate the aqueous dioxane from the adsorbent. The volume of adsorbent was varied over a range of 0.02–0.35 g/ml. After shaking and settling, 50 µl of the aqueous dioxane were used for quantifying the equilibrium concentration of dioxane on FT-IR.

For each tube, the amount of dioxane adsorbed was calculated according to the following equation:

$$x/m = v\,(C_0 - C_e)/w$$

where *x/m* is the weight of the adsorbate divided by the weight of the adsorbent (µg/g), *w* is the dose of adsorbent (mg), *v* is the volume of solution (ml), C_0 *and* C_e are pre- and post-adsorption concentration of dioxane, respectively.

To determine the necessary time for adsorption, the IR adsorption spectra of dioxane at time intervals were obtained, and 50 ml of the aqueous dioxane solution was taken in a 50 ml tube (SC475, Environmental Express). A known amount of the adsorbent was added to the tubes. The tubes were placed on a magnetic stirrer and the aqueous dioxane solution adsorbent mixtures were stirred at a constant speed. Peristaltic pump (PermeGear Inc, Hellertown, PA USA-#10090-16) was used to draw aqueous dioxane solution through a filter from the tube and send it (continuous flow) to a cell placed on the crystal aperture of the FT-IR spectroscopy, with the solution flowing over the crystal and returning back to the tube (Figure 2.2). The flow rate of the peristaltic pump was 5 ml per minute.

The infrared (IR) spectrum of each sample was measured using attenuated total reflection Fourier transform infrared spectroscopy (ATR-FTIR) Thermo-Nicolet FT-IR spectrometer, model 6700, and GladiATR vision unit (PIKE Technologies, Inc. WI, USA). OMNIC FT-IR software program is used in the FT-IR system. Absorbance spectra were measured over the wavenumber range of 4000–400 cm^{-1} with a spectral resolution of 4 cm^{-1}. The IR absorption spectra for dioxane in solution were obtained at various times. These spectra were analyzed using the C–O vibration band. The selected peak region for obtaining the integrated absorbance was 1105.2–1160.2 cm^{-1}. Figure 2.3 shows the typical IR spectra of dioxane in solution.

The crystal aperture surface was cleaned with alcohol and dried, and an uncovered crystal

background was run prior to scanning of the sample sets. With continuous flow measuring method, a macro was created by using OMNIC Macros application to measure absorbance spectra every 2 minutes and the data were saved on computer. Macro is defined as a series of software operation, or tasks which are joined together, and when the macro has been created, the series of tasks can be executed automatically and can be repeated in loop for any number of times.

To determine the effect of pH on dioxane adsorption, equilibrium experiments were conducted on AC, MgO, TiO_2, and DE at different pH levels. Aqueous dioxane solutions (concentration 50 mg/L) were prepared at different pH values ranging from 2 to 10. Hydrochloric acid (HCl) and sodium hydroxide (NaOH) were used for adjusting the pH.

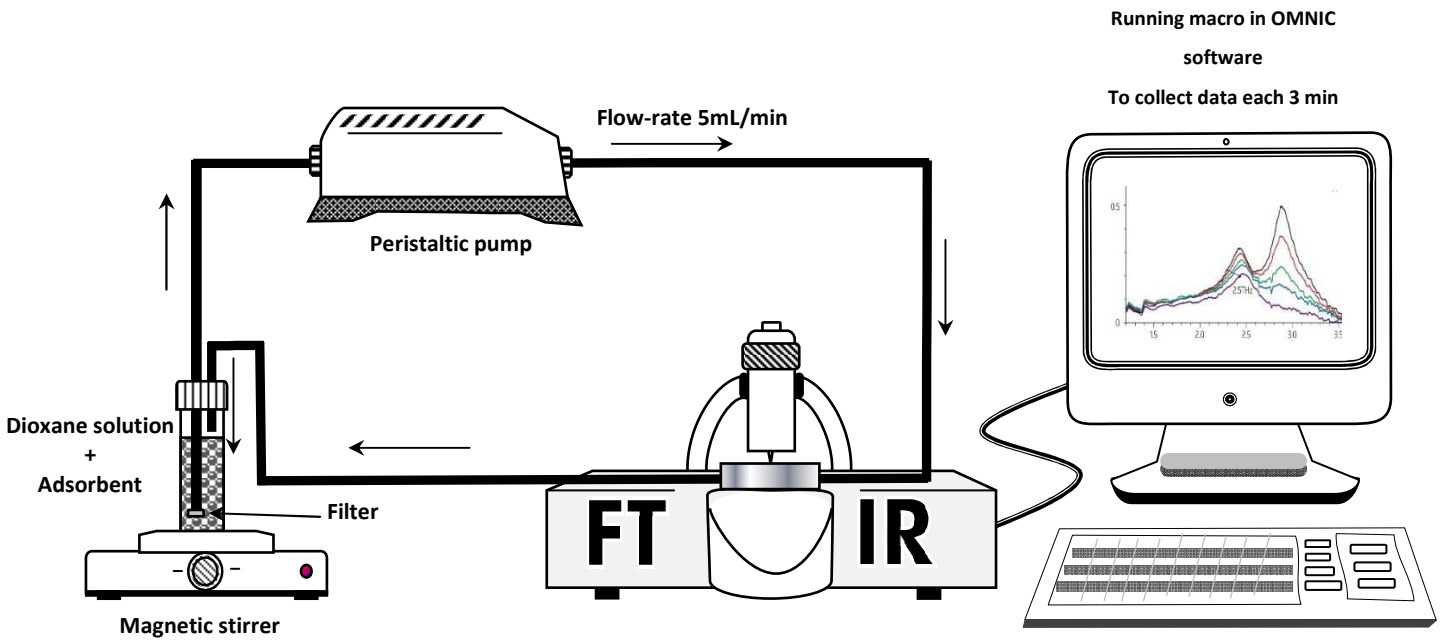

Figure 2.2: Schematic diagram of the necessary time for adsorption

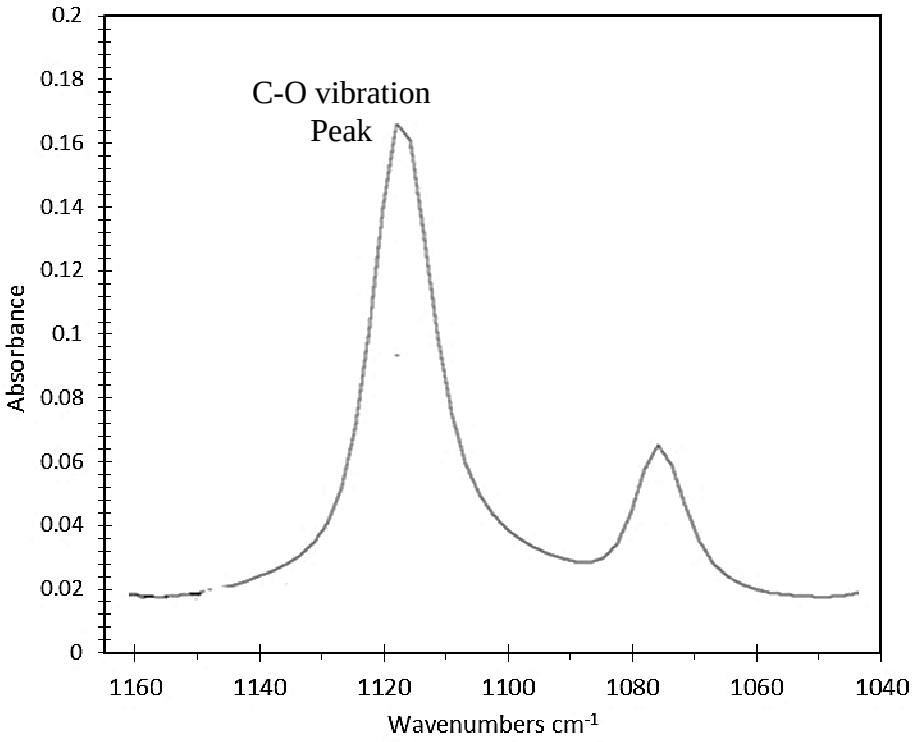

Figure 2.3: Typical IR spectra of dioxane in aqueous solution

Sample Preparation for Vapor Phase

Gas cell (400 ml) for the analysis of gas and vapor phase components using infrared optical spectroscopy was designed out of a glass container, with two zinc selenide (ZnSe) crystal windows to allow light in the mid-infrared range to pass through (Figure 2.5A).

Adsorption of dioxane in vapor phase onto AC, MgO, TiO_2, and DE were measured at 296 K and at a pressure of 760 mmHg (torr). Each adsorbent, measuring 0.2 g, was equally spread on a 24 cm^2 glass slide and placed at the bottom of the cell. The cell was sealed using rubber septum and plastic cover with inner glass faces (Figure 2.5B) and placed on FT-IR

(Figure 2.5C) spectrometer. Fourty mg dioxane were injected using micro-pipette through a small hole on the gas cell's top cover, and the hole was sealed by adhesive tape. Dioxane concentration was 100 µg/ml after it completely evaporated inside the cell. A macro was created by OMNIC Macros application to measure absorbance spectra every 1 minute for 100 minutes using transmission FT-IR mode. The data were saved for analysis.

The IR absorption spectra for dioxane vapors were obtained at various times. These spectra were analyzed using the C–H bending band. The selected peak region for obtaining the integrated absorbance was 1500.2–1420.2 cm^{-1} (Figure 2.4).

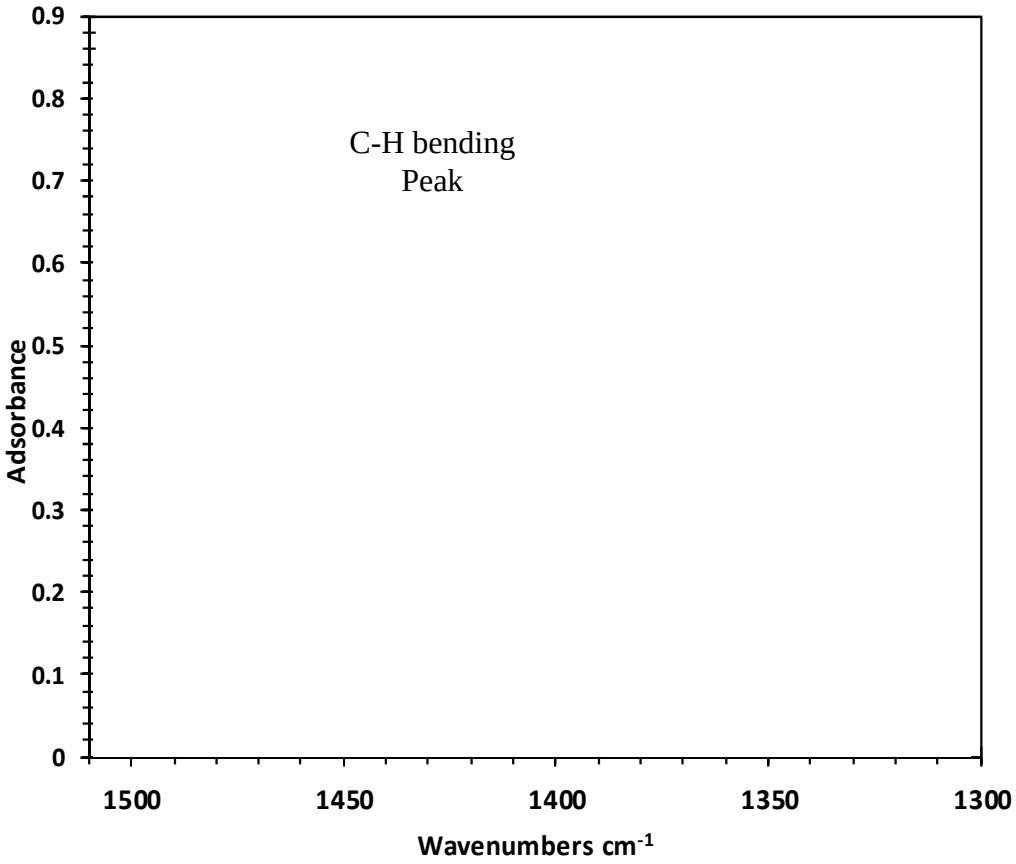

Figure 2.4: Typical IR spectra of dioxane vapor

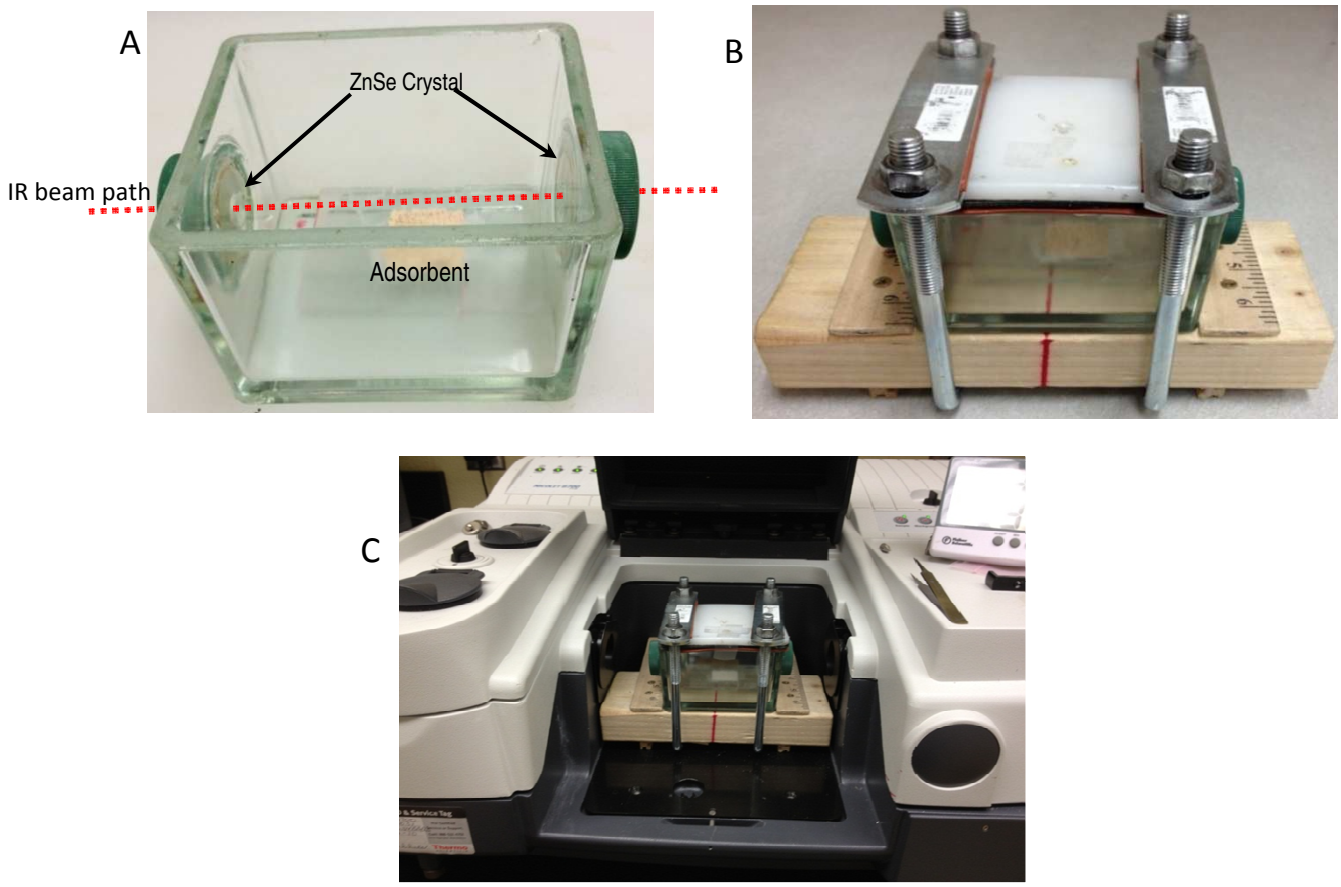

Figure 2.5: Dioxane adsorption measurement on FT-IR in vapor phase.

The amount of dioxane adsorbed was calculated according to the following equation:

$$x/m = v(C_0 - C_e)/w$$

where x/m is the weight of the adsorbate divided by the weight of the adsorbent (µg/g), w is the dose of adsorbent (mg), v is the volume gas cell (ml), C_0 *and* C_e (µg/ml) are pre- and post-adsorption concentrations of dioxane (µg/ml), respectively.

Adsorption Isotherms

The adsorption isotherms of aqueous dioxane solution adsorbed onto AC, MgO, TiO_2, and DE at a temperature of 296 K and a pH value of 7.0 (±0.2) were obtained using batch-type adsorption measurements. Experiments were carried out at equilibrium (at minute 90 of contact) by using a different amount of adsorbent ranging from 20 to 500 mg at a fixed concentration (10 mL; 50 mg/L) of aqueous dioxane. The equilibrium data were analyzed by Freundlich isotherm model equations. The data were used to obtain best-fit estimates of parameters, and the related parameters obtained by calculation from the values of slopes and intercepts of the respective linear plots:

$$\log (x/m) = \log K_f + (1/n) \log C_e$$

where x/m is the weight of the adsorbate divided by weight of the adsorbent (µg/g), K_f and $1/n$ are Freundlich adsorption constants, and C_e is concentration post-adsorption.

Transmission Electron Microscopy (TEM) Analyses

TEM analysis was performed on a Philips CM 100 Transmission Electron Microscope at the Biology Department, Kansas State University, using a 200 mesh Formvar/carbon-coated copper grids for absorbing samples (Ted Pella Inc., CA, USA Lot #:131011-01881, Lacey F/C).

Data Analysis

Data were analyzed statistically using Minitab (version 16.1.1, Minitab Inc., PA, USA, 2010). Analyses of variance (ANOVAs) were used to assess the significance of differences in means between groups. The Tukey's Multiple Comparison Method was used to compare the

means. Data are presented as mean (± standard error) and all statements of significance were based on a 95% confidence ($P < 0.05$).

Results and Discussion

Adsorption in Aqueous Phase

Adsorption Capacity and Effect of Contact Time

The rate of the dioxane adsorption from water was very fast with all the adsorbents. The adsorption of dioxane increases with time and gradually reaches equilibrium. The required contact time for attaining equilibrium and maximum adsorption rate was at the 36^{th}, 26^{th}, 38^{th}, and 34^{th} minute for AC (Figure 2.6), TiO_2 (Figure 2.7), MgO (Figure 2.8), and DE (Figure 2.9), respectively.

The exposure time between the adsorbate and the adsorbent for completing adsorption is one of the most important parameters that has an influence on the performance of adsorption processes. This parameter offers information on the minimum time required for considerable adsorption to take place and the possible diffusion control mechanism between the adsorbates (Al-Anber, 2010). The higher rate of adsorption at the beginning was due to large available surface area of the adsorbent during the initial stage, and with the passage of time, the capacity of the adsorbent gets exhausted (at equilibrium). The remaining unfilled surface sites are difficult to be occupied due to repulsive forces between molecules of the solute on the solid phase and in the bulk liquid phase. The rate of uptake is controlled by the rate at which the

adsorbate is transported from the exterior to the interior sites of the adsorbent particles (Gulipalli *et al.,* 2011, Verma *et al.,* 2006).

The average values of adsorbed dioxane in aqueous solution after reaching equilibrium and at minute 600 were 80.43 ± 0.99, 10.54, 3.41 ± 0.37, and 2.98 ± 0.27 µg/g onto AC, DE, TiO_2, and MgO, respectively. It was observed that the removal curves of all adsorbents were relatively smooth and continuous, and the standard error of adsorption rates on timeline at equilibrium was relatively low. This suggests the possibility of formation of monolayer coverage of dioxane at the interface of the adsorbent.

Effect of pH

We found variation of adsorption capacity of all adsobents at different pH values in our experiments. The adsorption of dioxane on all adsorbents was influenced by the pH of the aqueous solution. The adsorption of dioxane onto AC and DE increased from 71.44 to 85.9 µg/g and 4.08 to 12.91 µg/g, respectively, when the pH of the solution was increased from 5 to 8. The adsorption of dioxane onto MgO and TiO_2 increased from 1.440 to 5.440 µg/g and 1.652 to 6.70 µg/g, respectively, when the pH of the solution was increased from 5 to 7 (Figure 2.11a,b).

Solution pH is additional significant parameter that influences both adsorbate chemistry in solution and surface binding sites of the adsorbent. As seen from the graph, the equilibrium adsorption capacity increases with an increase in pH, reaches a maximum at neutral and slightly basic pH, and then decreases. The lower adsorptive capacity of all adsorbents was observed at low pH (3 to 5). A possible explanation for low adsorption at low pH is the presence of higher concentration and higher mobility of H^+ ions that bond to water molecules to form hydronium ions (H_3O^+), so that the adsorption sites on the surface of the adsorbent are surrounded by H_3O^+,

thereby preventing dioxane from reaching the binding sites of the adsorbents (Onundi *et al.*, 2010). As well as the lower adsorptive capacity of DE, MgO, and TiO_2 onto dioxane at low pH values may be also related to their slight dissolution.

A strong decrease in the dioxane removal efficiency was observed in high pH environments (above pH 9.0). This might be related to the formation of hydroxyl radicals (OH^-), which subsequently compete with the molecules of dioxane for adsorption sites, leading to dioxane's decreased adsorptive capacity (Moussavi & Mahmoudi, 2009)

Effect of Water Type

No significant difference was observed in the adsorption of dioxane (n =5 and $P > 0.05$) between water types and within adsorbent groups. The highest adsorption capacity was found in AC group followed by the DE group. The average x/m of AC group was 79.87 (µg/g), 80.52 (µg/g), and 80.87(µg/g) for ground water, surface water, and DD water, respectively (figure 2.12).

Surface and groundwater contain numerous materials such as particles of soil, suspended sediments, humic material, organic particles, and dissolved matter. This, combined with other factors like pH and residence time, might affect the adsorption of pollutants in water onto adsorbents.

Despite differences in the properties of the three types of water and their quality, the results showed no significant difference in the adsorption of dioxane between them. This observation can be explained by the fact that dioxane has low organic carbon partition coefficient (K_{oc}) and low distribution coefficient (K_d). K_{oc} refers to affinity of the chemical to be adsorbed

onto organic components of the soil or sediment particles. K_d describes the equilibrium concentration ratio of chemicals between soil or suspended sediment particles and water (Suthersan, 2002). Therefore, the existence of suspended organic and inorganic particles in water samples would not affect the adsorption of dioxane onto adsorbents significantly.

The pH of DD water, ground water, and surface water were 7.00, 7.59, and 8.11, respectively. The variation in pH also did not affect the adsorption of dioxane, and the slight basic condition of surface and ground water was not sufficient enough to generate a higher concentration of OH^- radicals that could compete with dioxane molecules for adsorption sites on surfaces.

Adsorption Isotherms

All adsorption isotherms showed a good fit with Freundlich equation. The study found that that AC adsorbed a large amount (x/m = 80.88 µg/g) of dioxane compared to the other adsorbents, with their x/m ranging from 3.79 and 11.41 µg/g.

The Freundlich isotherms derived from the data are shown in figure 2.13, and the extrapolated parameters are summarized in table 2.3.

Adsorption is frequently described through an isotherm. The adsorption isotherm shows how the adsorbed molecules are distributed between the solution and the solid phase as soon as the adsorption attains equilibrium (Nwabanne & Igbokwe, 2008). The adsorption isotherm is useful for representing the capacity of an adsorbent for adsorbing compounds from water and in offering a description of the functional dependence of capacity on the concentration of compounds (Weber, 1972b). Therefore, the adsorptive capacity and also the performance of an

adsorbent are usually predicted from an equilibrium adsorption isotherm (Kumar *et al.*, 2008, Ochonogor & Ejikeme, 2005) .

Activated carbon is extensively employed for the removal of hydrophobic organic chemicals in water. The process of AC adsorption is relatively easy, its performance is reliable, the cost of operation is low, and it can be applied to various scales in a treatment plant (Fukuhara *et al.*, 2011). The amount of dioxane adsorbed onto AC in this study was lower than other hydrophobic organic compounds which have been in other studies (Dobbs & Cohen, 1980). The hydrophilic nature of dioxane may account for its low adsorpability onto AC. The hydrophobicity of a compound increases as the number of carbon atoms increases, and as its solubility in water decreases. The negative charge of oxygen atom forms hydrophilic functional groups such as hydroxyl or ether groups. Therefore, water solubility is increased as the number of these hydrophilic groups increase in the molecule and consequently adsorpability is decreased (Abe *et al.*, 1983). Taking this viewpoint into consideration, dioxane possesses four carbon atoms and two oxygen atoms. Thus, it is substantially influenced by hydrophilicity and weakly influenced by hydrophobicity. Dioxane molecules remain stable in water for the most part. Hence, the affinity between the water and dioxane is relatively strong, which prevents the release of dioxane from water for its adsorption onto the surface of the adsorbent. Generally, the adsorptive capacity of AC is mainly due to London dispersion force, which is part of the van der Waals' force and also dependent on pore size distributions, surface area, and pore diameter (Noll *et al.*, 1992), and therefore adsorption force increases with decreasing pore size (Li *et al.*, 2002).

The results of dioxane adsorption onto AC in this study were consistent with some results of a previous study conducted in 2011. That study was carried out to study dioxane adsorption onto eight different ACs. The ACs were prepared from various sources (coconut, phenol resin, coal,

and sawdust) in different forms (granular, fibrous, and powdered) by direct activation in a rotary kiln, without a carbonization process. The surface area varied from 983 to 1810 m^2/g (Fukuhara *et al.*, 2011). Our results were similar to the result of dioxane adsorbed onto AC prepared from phenol resin with a surface area of 1628 m^2/g.

Because of its high porosity, high surface area properties (80 $m^2/$ g) (Datsko *et al.*, 2011), good hydrophilicity, high chemical inertness, relatively low cost, and environmental friendly nature, DE is extensively employed as a filtering matrix, an adsorbent, and a catalyst carrier to remove many contaminants from water (Wu *et al.*, 2011). Due to its high surface area, DE possesses a high absorptive capacity and can absorb up to 2.5 times its weight of water (Al-Rashdan, 2001). Hence, It has been used for the adsorption of many heavy metals, textile dyes, and other substances from water and wastewaters, either in its natural form or a chemically modified form (Ridha *et al.*, 1998, Khraisheh *et al.*, 2004). It is consists mainly of amorphous silica. It is considered as a mineral of organic origin (fossilized diatom skeleton). Active adsorption sites on DE surface having active hydroxyl groups, which are responsible for adsorption, are thought to be as follows: (i) insulated free silanol groups (–SiOH), (ii) free dual silanol group [$–Si(OH)_2$], and (iii) siloxane group –Si–O–Si bridges with oxygen atoms on the surface (Zhuravlev, 2000). The hydroxyl groups act as the core of molecular adsorption through their specific interaction with adsorbates, which have the capability of creating a hydrogen bond with the hydroxyl groups, or more commonly, of undergoing an interaction as a donor–acceptor. The main forces governing the adsorption of DE are van der Waals force and hydrogen bond. Hydrogen-bonding sites play an important role in DE adsorptive capacity. Two different types of hydrogen bonding sites are related to silanol groups, which act as a proton donor, and to the siloxane group, where the group acts as a proton acceptor. The silanol groups spread over the

surface of the silica are active and have a tendency to react with many polar organic compounds and various functional groups (Zhuravlev, 2000, Caliskan *et al.*, 2011, Grob & Barry, 2004). At a sufficient concentration of silanol groups, the surface becomes hydrophilic. By contrast, the removal of the hydroxyl radicals from these groups result in a decrease in the adsorption and the surface tends to be more hydrophobic in nature (Zhuravlev, 2000).

Although DE has a high porosity and high surface area, it showed low adsorptive capacity toward dioxane in water compared to AC. The relative low adsorption of dioxane onto DE could be explained as follows: Water is a broadly hydrogen bonded system and has ability to form a cage around the solute without sacrificing much of the hydrogen bonding. Therefore, the host water molecules are able to organize themselves into a cage-like structure around the dioxane guest molecules and then can utilize all the four potential hydrogen bonds per dioxane to form a clathrate-like compound (Powell *et al.*, 1995) . The only physical attraction between DE surface and dioxane is van der Waal attractions, which is relatively a weak force on DE surfaces.

Nanocrystalline metal oxides have a high adsorptive capacity toward a wide range of environmental pollutants ranging from acids, chlorinated hydrocarbons, organophosphorus and organosulfur compounds to chemical warfare agents. These compounds also have the capability to destroy various chemical hazards by altering them to much safer by-products in a wide range of temperatures (Koper *et al.*, 2007). The adsorption efficiency of nanocrystalline metal oxides results not only from their high surface area but also due to the high concentration of low arranged sites and structural defects on their surface (Mishakov *et al.*, 2002). A number of different nanoparticles of metal oxides have been shown to be effective toward common water contaminants including halogenated organic compounds and heavy metals. For example, iron nanoparticles were found to be very effective for the transformation and detoxification of a wide

variety of common environmental pollutants, such as chlorinated organic solvents, organochlorine pesticides, chlorinated aliphatics, perchlorate, methyl-*t*-butyl ether and polychlorinated biphenyls, and these materials have also shown some capacity for removing inorganic metal pollutants like chrome, arsenic, and lead (Kent, 2012).

The nanocrystalline MgO has showed a high adsorptive capacity toward some organic compounds in wastewater like textile dyes (i.e., Ponceau S dye, reactive brilliant red X-3B and Congo red) (Hu *et al.*, 2010, Venkatesha *et al.*, 2013, Moussavi & Mahmoudi, 2009), pesticide-like paraoxon and organophosphorus compounds such as dimethyl methyl phosphonate (Koper *et al.*, 2007). Nanoparticle TiO_2 has been effectively used for the remediation of a wide range of organic chemicals like hydrocarbons, chlorinated hydrocarbons such as carbon tetrachloride, chloroform, trichloroethylene, phenols, chlorinated phenols, surfactants, dyes, reductive deposition of heavy metals such as platinum, lead, gold, rhodium, chrome, and others from aqueous solutions to surfaces in addition to destruction of microorganisms like bacteria, viruses, and molds in water (Mills & Hoffmann, 1993). Some nanocrystalline metal oxides such as MgO and TiO_2 have been found to have a high adsorption capacity toward polar organic compounds compared to nonpolar organics (Khaleel *et al.*, 1999). Data on dioxane adsorption in aqueous phase onto nanocrystalline metal oxides, like MgO and TiO_2, are not available.

In this study, the nanoparticle metal oxides of MgO and TiO_2 showed low adsorption capacity toward dioxane in aqueous phase and this may be attributed to their nonpolarity in addition to their hydrophilicity.

Adsorption in Vapor Phase

The adsorption of dioxane by AC, TiO_2, MgO, and DE is examined at different time intervals and the results are shown in figure 2.14. As can be seen from the figure, during the first 40 min of the experiment, the concentration of dioxane adsorbed onto all adsorbents increases with time. The average contact time required for maximum adsorption of dioxane in vapor phase was at 22, 8, 8, and 7 min for AC, TiO_2, MgO, and DE, respectively, whereas the average time required for reaching equilibrium rate of dioxane adsorption in vapor phase was 39, 28, 40, and 18 min for AC, TiO_2, MgO, and DE, respectively. Then there was no significant change of dioxane concentration observed till 100 min.

As shown in figure 2.15, the required contact time for maximum adsorption rate of dioxane onto AC was longer than in other adsorbents, and the results showed no significant difference ($P > 0.5$, n=5) between TiO_2, MgO, and DE. The shorter time was associated with lower adsorptive capacity of the adsorbents. This can be explained through the limitation of interaction sites on the surface of the adsorbent that are occupied and attain saturation state faster than the adsorbent possessing higher adsorptive capacity. The contact time for reaching equilibrium varied between the adsorbents. The longer time was observed for adsorption onto AC and MgO, and it was shorter for TiO_2 and DE. The maximum adsorption time was higher for adsorption on AC compared to that shown on MgO, TiO_2, and DE. The equilibrium is the result of a competition between two contrary mechanisms, represented by the activation energy of adsorption and desorption (Limousin *et al.*, 2007). The time between point of maximum adsorption and first point of equilibrium represents the desorption process. The shorter desorption time was observed in DE and longer in MgO. The duration of desorption may explain the strength of attachment between the dioxane molecule and the adsorbent surface, implying that a stronger attachment

needs a longer time to detach. The short contact time for reaching equilibrium may indicate that the physical adsorption dominates the interaction between dioxane and the adsorbents, because the physical adsorption systems usually reach equilibrium rapidly (Rouquerol *et al.*, 1999).

The results of dioxane adsorption in vapor phase (figure 2.16) showed significant differences between the adsorption means of all adsorbents ($P < 0.001$, n=5), where AC generated the highest rate of adsorption at 66.9 µg/g, followed by TiO_2 at 19.3 µg/g, MgO at 8.6 µg/g, and DE at 4.7 µg/g.

Dioxane, like other volatile organic compounds, easily evaporates at room temperature. Its vapor pressure (40 mmHg at 25°C) under normal conditions allows it to significantly evaporate and enter the atmosphere (Lewis, 2000). Dioxane may be emitted to the indoor or outdoor atmosphere through air effluents at the sites where it is produced, processed, after use, and via unintentional formation (ECB, 2002). As reported to the Toxics Release Inventory by specific types of U.S. industries, U.S. EPA has estimated that 6,522,259 pounds of dioxane were emitted into the atmosphere of the total 19 million pounds released into the environment in the United State between 1988 to 2012 (TRI, 2013). In Japan, a pollutant release and transfer register survey indicates that the total annual release of dioxane into air is greater than that into the aquatic environment. For example, the total annual emission of dioxane into the atmosphere was 160, 184, and 169 tons in 2001, 2002, and 2003, respectively (PRTR, 2003).

Many techniques are used to control the emission of volatile organic compounds. These techniques are basically classified into two different groups: the destruction and the recovery techniques. The destruction techniques include oxidation and bio-filtration, whereas the recovery techniques include absorption, adsorption, condensation, and membrane separation. Adsorption

is the most common process using for removing volatile organic compounds from air (Khan & Ghoshal, 2000).

The phenomenon of adsorption has been employed widely in air pollution control. During adsorption, the molecules of the pollutant in gas phase passing through a bed of solid particles are selectively held there by physical forces, which are weaker and less specific than those of chemical bonds. Adsorption takes place more readily at conditions of lower temperatures and humidity. The adsorptive capacity of the solid (the adsorbent) for the gas molecules tends to increase with the gas phase concentration, molecular weight, diffusivity, polarity, low humidity, and boiling point (Vatavuk, 1999). A wide variety of materials are used as adsorbents to remove the organic pollutants from air like activated carbon, zeolites, activated alumina, synthetic polymers, silica gel, and porous clay minerals. However, all adsorbents have limited capacities and thus require frequent maintenance (Khan & Ghoshal, 2000).

Activated carbon has been used extensively to remove gaseous contaminants from air. It has the potential to remove most hydrocarbons, many aldehydes, and organic acids. The adsorption capacity of AC increased linearly with an increase the molecular weight, dynamic diameter, boiling point, and density of the adsorbate. However, adsorption capacity of AC decreased with an increase in the polarity index and vapor pressure of the adsorbate (Li *et al.*, 2012). Most of the organic compound vapors are adsorbed onto AC through physical adsorption, which is based on the van der Waals force between the adsorbate and AC. In this study, the adsorptive capacity of AC toward dioxane vapor was moderate, and it was lower than that found in other organic volatile compounds such as xylene and toluene (Das *et al.*, 2004). The moderate adsorption of dioxane vapor by AC may be explained through its physical and chemical properties. The polarity index (intensity of adsorbate polarity) of dioxane is 4.8, which indicates that dioxane is

relatively nonpolar. The molecule of AC is nonpolar and therefore the affinity between AC and dioxane is not strong enough.

Li and coworkers reported that the physical adsorption of organic vapor onto AC was similar to gas liquefaction and condensation, which were both closely associated with boiling point. At higher boiling points, liquefaction and condensation take place more easily, which increases the adsorption capacity (Li *et al.*, 2012). Vapor pressure of the adsorbate is the other physical property that can influence the adsorptive capacity of AC. Thus, the adsorptive capacity of AC is affected negatively with increasing vapor pressure (Li, 2010). Boiling point and vapor pressure of dioxane are 101°C and 40 mmHg at 25°C, respectively. They are relatively not high in comparison with the boiling point of other organic compounds, which may also explain the moderate adsorptive capacity of AC toward dioxane vapor.

Many studies have been conducted to investigate the adsorptive capacity of DE or modified DE toward organic compounds in vapor phase. The results have shown a varied range of adsorptive capacities, ranging between very low and high. For example, toluene vapor adsorption onto DE mixed with fly ash was high (Lim *et al.*, 2001). But, xylene vapor adsorption onto DE was moderate (Zaitan & Chafik, 2005). The hydrogen bond with silanol groups on the surface of DE is the most important factor that determines the adsorption of an adsorbate onto DE (Da□browski & Tertykh, 1996). In this study, dioxane vapor adsorption onto DE was low and this may be related to weak hydrogen bonds between the dioxane molecule and the surface of DE. However, data on dioxane adsorption onto DE are not available, and such data can throw light on the adsorption pathway.

Nanocrystalline metal oxides exhibit a wide range of unique properties. One of the unusual properties is their enhanced surface chemical reactivity toward incoming adsorbates (Klabunde *et al.*, 1996). Many studies have reported that nanocrystalline metal oxides such as MgO, CaO, ZnO, TiO_2, Al_2O_3, and Fe_2O_3 have been shown to be highly efficient and active adsorbents toward numerous toxic substances including common air pollutants, chemical warfare agents (i.e., nerve agent, VX, and sulfur mustards), and acid gases (Khaleel *et al.*, 1999, Wagner *et al.*, 2000). In most cases, destructive adsorption occurs on the surface sites of the nanocrystals, so that the adsorbate is chemically broken up and thereby made nontoxic (Volodin *et al.*, 2006).

The reactivity of nanocrystalline MgO and TiO_2 with organic chemicals in gas phase has been examined by many studies. For example, Khaleel *et al.* have investigated nanocrystals of MgO, calcium oxide, and aluminum oxide as adsorbents of typical volatile organic compounds, which are representative of air pollutants. The volatile organic compounds used in that study were acetone, propionaldehyde, benzaldehyde, trimethylacetaldehyde, ammonia, dimethylamine, *N*-nitrosodiethylamine, and methanol. Nanocrystals of MgO have shown remarkably high capacity to chemically adsorb such organic compounds. Additionally, nanocrystalline MgO was found to adsorb acetaldehyde in large quantities in the absence of air. At room temperature and over a short period of time, one mole of MgO adsorbed up to one mole acetaldehyde. The adsorption was very fast and vigorous. The high adsorptive capacity of MgO toward acetaldehyde was attributed to a special reactivity that resulted in a multilayer dissociative adsorption of large amounts of the chemical, and due to the interaction of the carbonyl group with surface sites followed by the aldehydic hydrogen dissociation (Khaleel *et al.*, 1999). Another study was conducted to investigate the potential of nanocrystalline TiO_2 for the destructive adsorption of carbon tetrachloride (CCl_4). It was found that nanocrystalline TiO_2 had

a very high capacity to remove chlorinated hydrocarbons from air. The study suggested that the possible pathway for the destructive adsorption of CCl_4 over nanocrystalline TiO_2 was physical adsorption, where the relatively positive carbon atom interacts with a site of negative oxygen and the relatively negative chlorine atoms interact with positive sites on metal ion to form an intermediate (Liu *et al.*, 2004).

Dioxane is a relatively nonpolar heterocyclic ether molecule, it does not have a permanent dipole moment, and is not usually considered to be polar (Oh *et al.*, 1998). Ether adsorption on metal oxides was believed to be controlled by an interaction through the oxygen lone-pair orbital, and the relative bond strengths were described mainly in terms of inductive depletion of electron density at the oxygen lone-pair (Luth *et al.*, 1977, Walczak & Thiel, 1990). Our study showed that the adsorptive capacity of nanocrystalline TiO_2 and MgO toward dioxane in vapor phase was low (19.3 and 8.6 µg/g, respectively). The strengths of interaction between dioxane and the surface of metal oxide can be explained primarily in terms of physical adsorption and via an interaction controlled by the oxygen lone-pair orbital. Apparently, this interaction is more comparable to a weak dipole–dipole interaction. These results are consistent with a previous study that suggested that nanocrystalline MgO and TiO_2 adsorb nonpolar organic compounds in gas phase in low capacities (Khaleel *et al.*, 1999).

Conclusion

The principal objectives of this study were to (1) study the adsorption of dioxane onto four different adsorbents (activated carbon, diatomaceous earth, and nanocrystalline titanium dioxide and magnesium oxide) in aqueous and vapor phases, (2) determine the effect of pH, contact time, and type of water on dioxane adsorption in aqueous phase, and (3) estimate the maximum adsorption capacity of the four adsorbents in aqueous phase by fitting the adsorption equilibrium data to adsorption isotherms of the Freundlich model. The results of the study could be summed up as follows:

- Generally, the adsorbability of dioxane is qualitatively low in aqueous and vapor phases.
- The highest adsorptive capacity of dioxane in the aqueous phase was found onto AC, followed by DE.
- The nanocrystalline metal oxides showed very low adsorptive capacity toward dioxane in the aqueous phase.
- The study showed that adsorption of dioxane onto all adsorbents reaches maximum at neutral and slightly basic pH solutions.
- The water type was found to have no effect on dioxane adsorption onto AC, TiO_2, MgO, and DE.
- All adsorption isotherms obtained were found to relatively fit a Freundlich equation.
- In vapor phase, the highest adsorptive capacity of dioxane in was found onto AC.
- The nanocrystalline metal oxides showed higher adsorptive capacity in the vapor phase than in the aqueous phase, and TiO_2 exhibited more favorable adsorptive properties than MgO.

- The contact time for reaching equilibrium and maximum adsorption rate was fast (< 40 min) in both phases, indicating that the physical adsorption controls the interaction between dioxane and the adsorbents.

Table 2.3: Freundlich adsorption constants on dioxane onto different adsorbents in aqueous solution

Adsorbent	Freundlich Constants [a]		Correlation coefficient R^2	x/m (µg/g) [b] ±SE n=5
	K_f	1/n		
MgO	-18.659	0.071322	0.547	3.794 ± 0.83
AC	1.225	1.158749	0.981	80.878 ± 3.28
DE	-10.595	0.117578	0.674	11.416 ± 2.92
TiO_2	-26.114	0.051169	0.444	3.842 ± 1.21

[a] Freundlich Constants were determined at dimensions = C_e (mg/L), x/m (µg/g)
[b] x/m amount adsorbed at the equilibrium concentration of 50mg/L

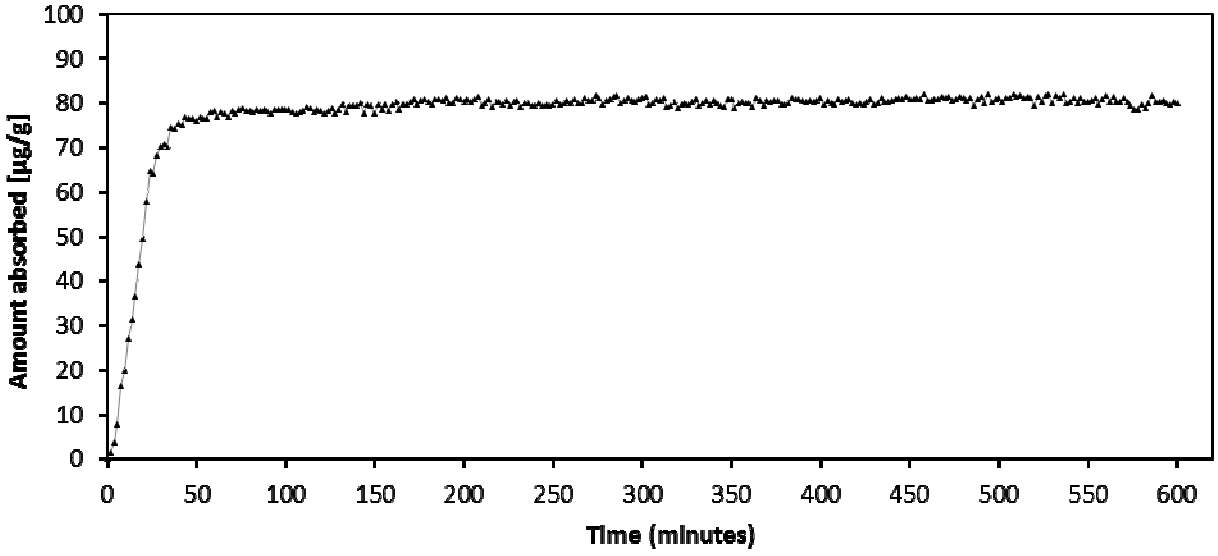

Figure 2.6: Effect of contact time on the dioxane adsorption onto activated carbon in aqueous solution

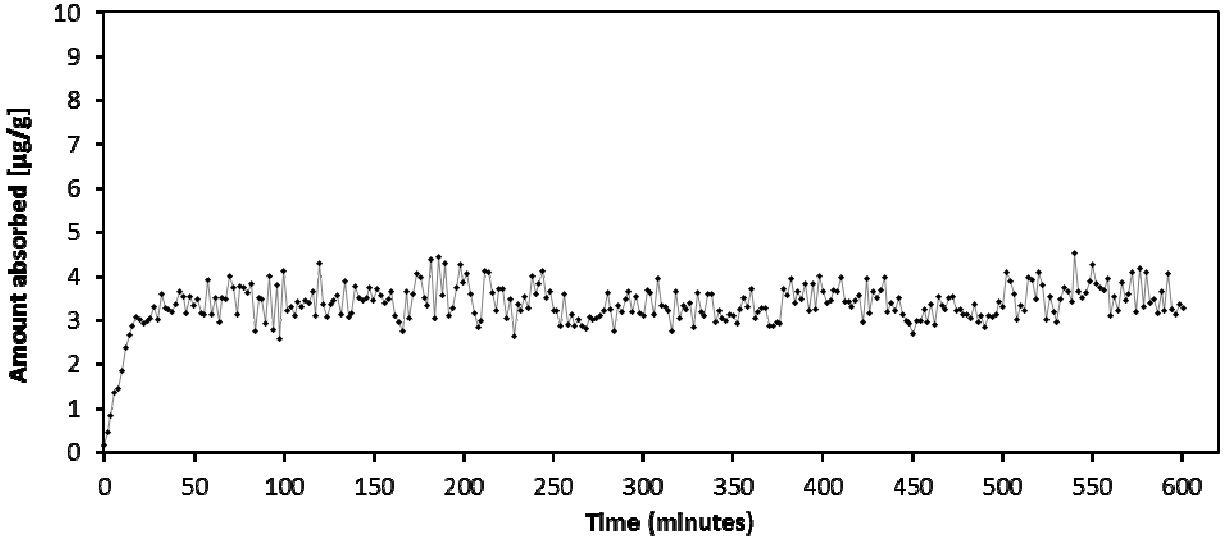

Figure 2.7: Effect of contact time on dioxane adsorption onto titanium dioxide in aqueous solution

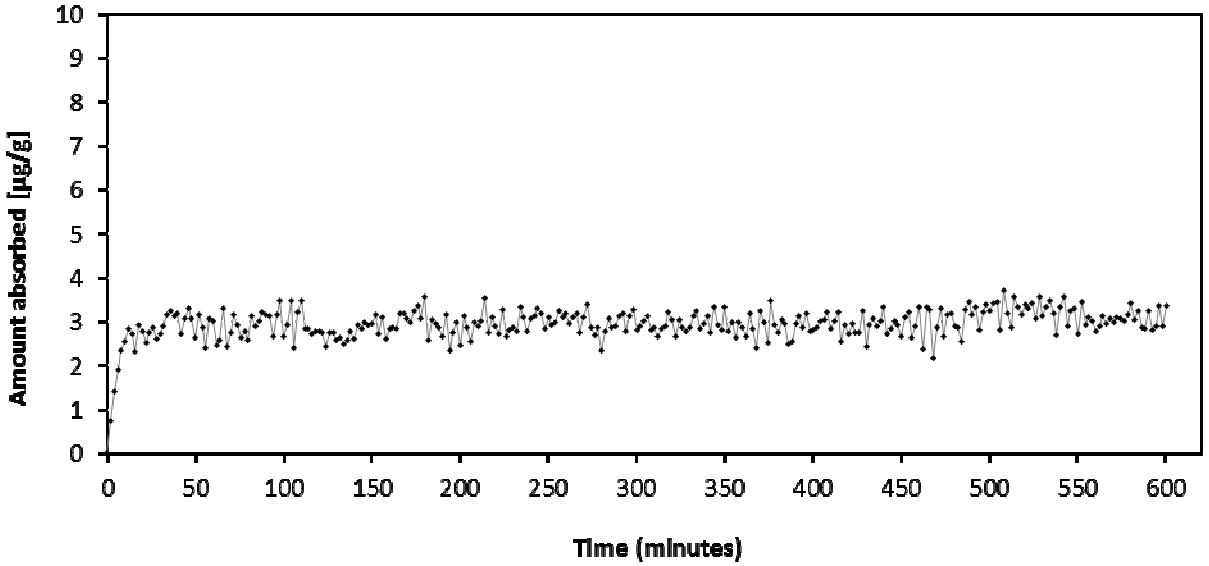

Figure 2.8: Effect of contact time on dioxane adsorption onto magnesium oxide in aqueous solution

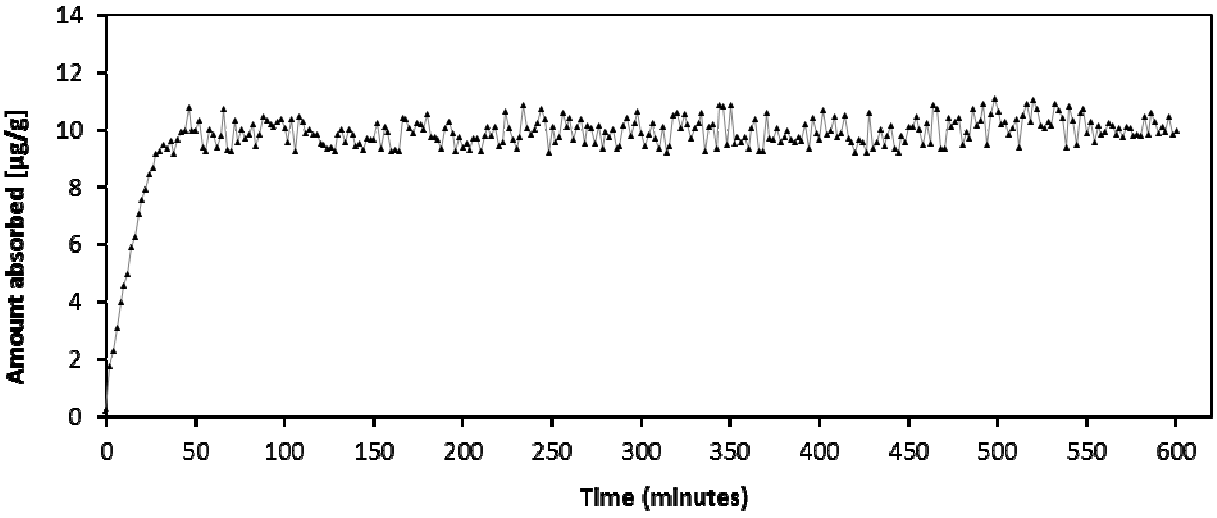

Figure 2.9: Effect of contact time on dioxane adsorption onto diatomaceous earth in aqueous solution

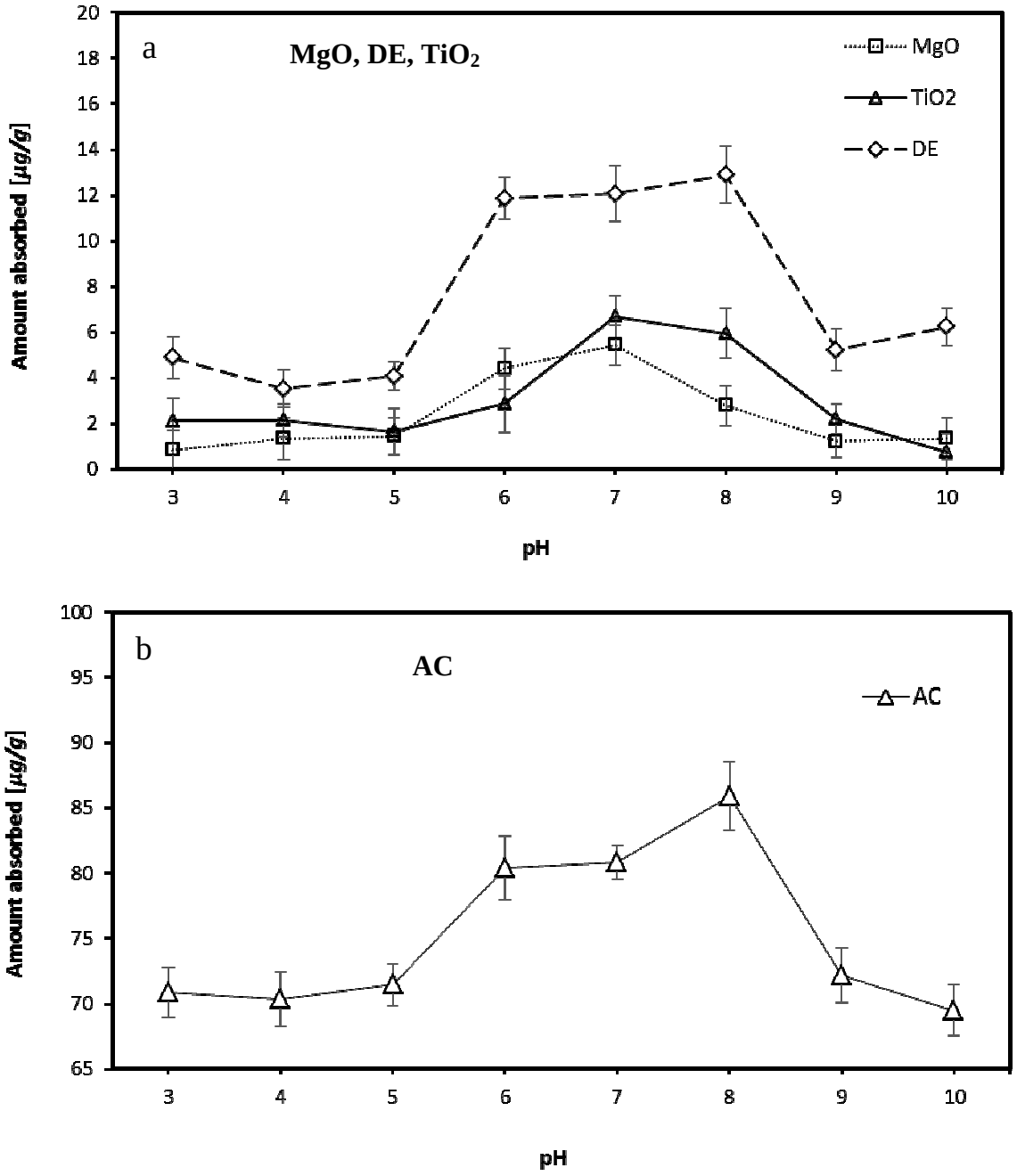

Figure 2.10: Effect of pH on adsorption of dioxane in aqueous solution onto (a) titanium dioxide, magnesium oxide and diatomaceous earth (b) activated carbon (n =5)

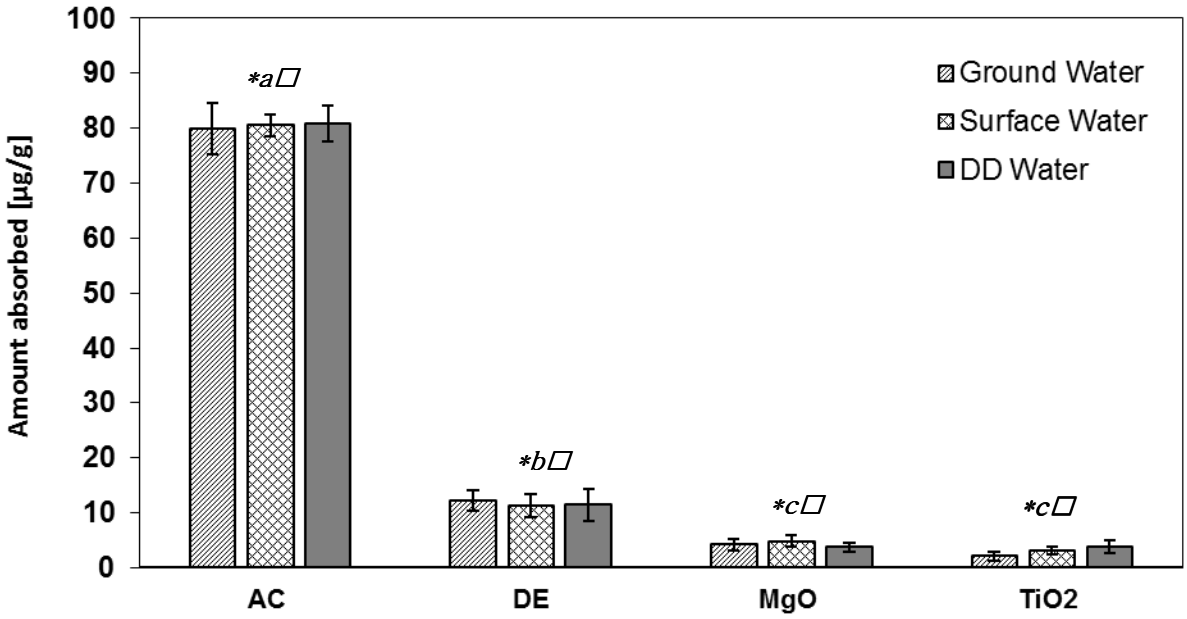

Figure 2.11: Effect of water's types on adsorption of dioxane onto different adsorbents in aqueous solution (n =5)

**With different letters are statistically significant P < 0.05. Bars show standard errors.*

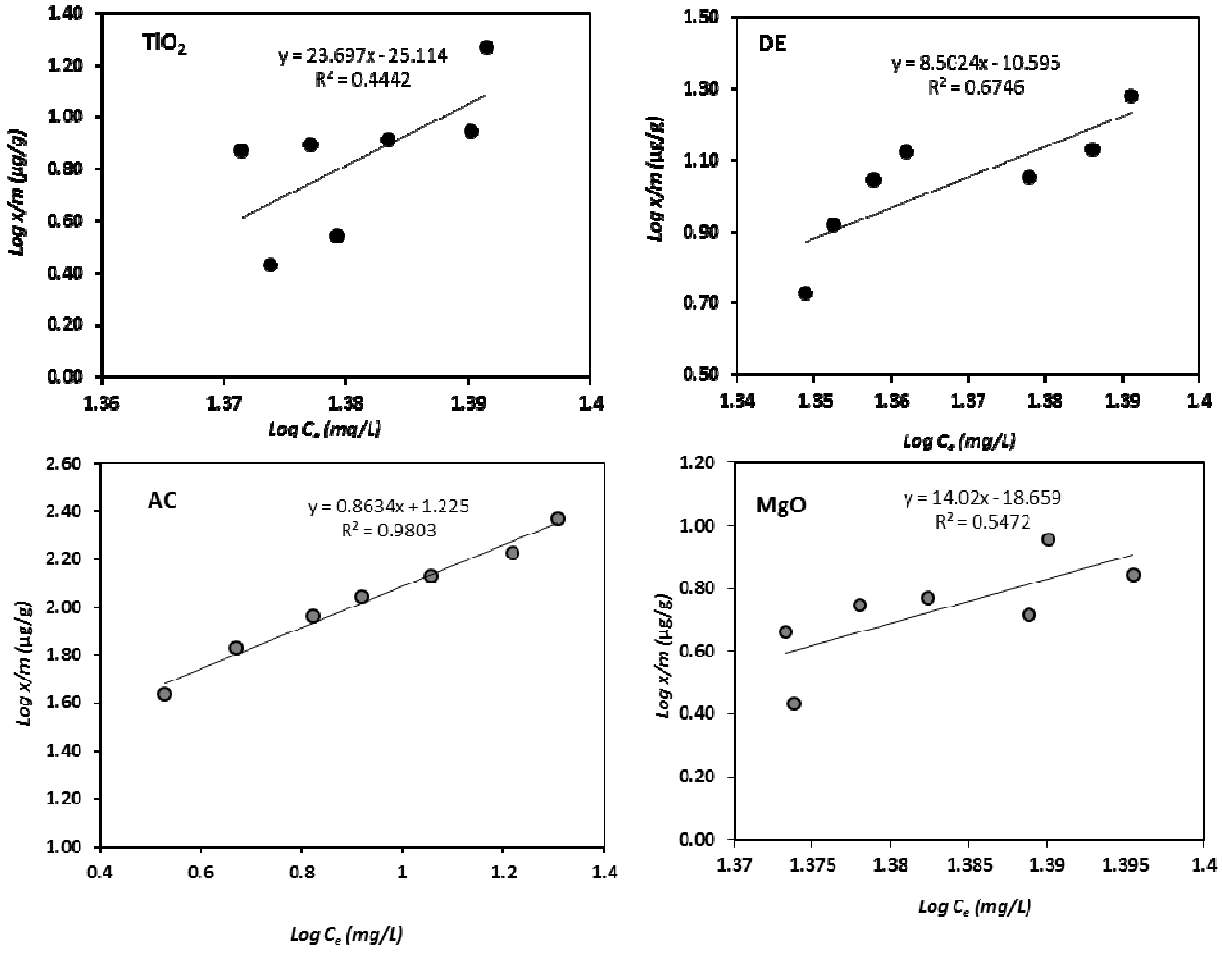

Figure 2.12: Adsorption isotherms of dioxane onto different adsorbents in aqueous solution

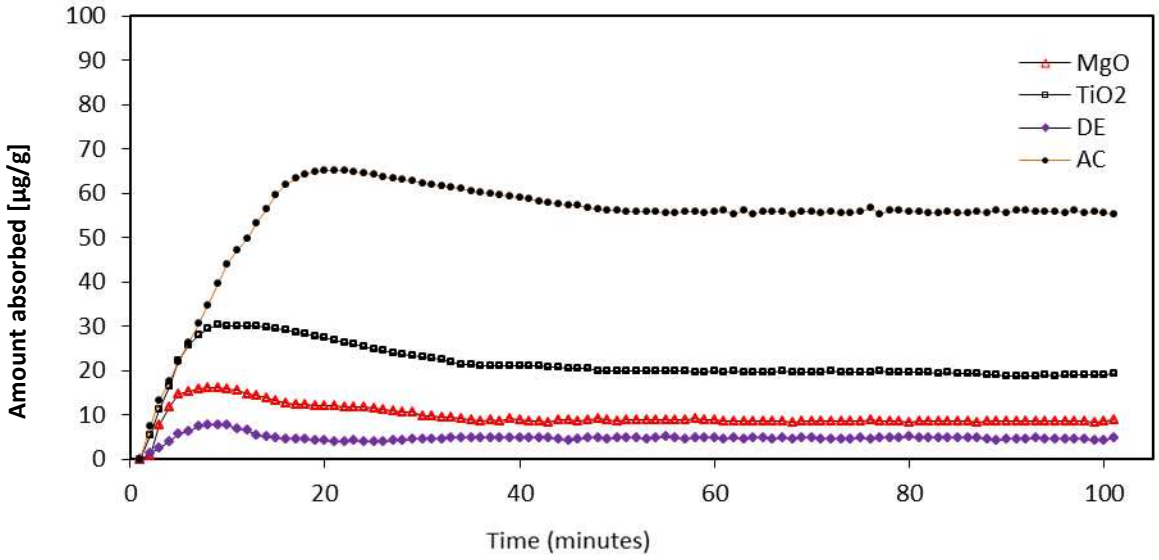

Figure 2.13: Effect of contact time on the dioxane adsorption onto different adsorbents in vapor phase

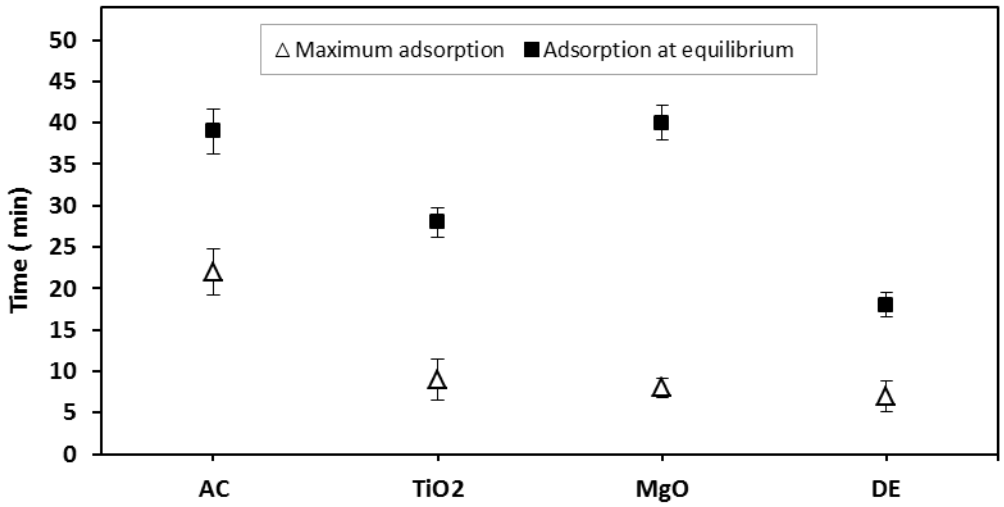

Figure 2.14: Required contact time for reaching equilibrium and maximum adsorption of dioxane (n =5)

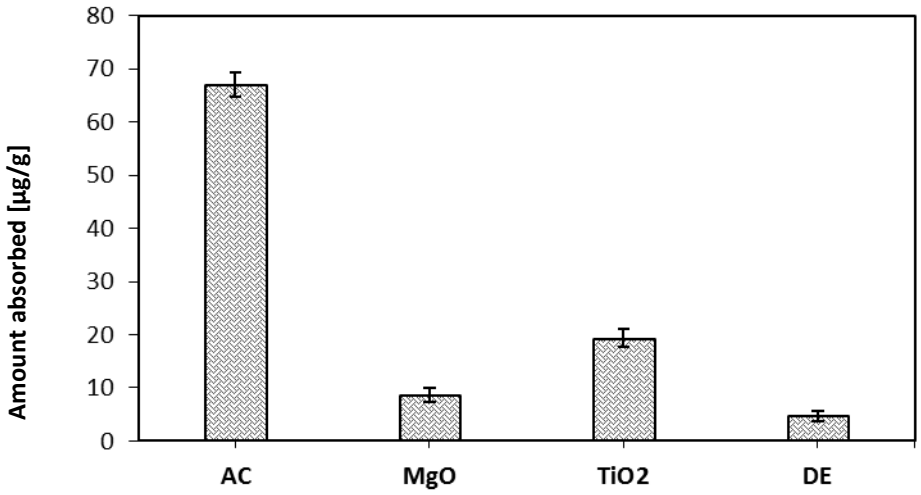

Figure 2.15: Adsorption of dioxane onto different adsorbents in vapor phase (n =5)

References

Al-Anber, M. A., 2010: Removal of high-level Fe3+ from aqueous solution using natural inorganic materials: Bentonite (NB) and quartz (NQ). Desalination, 250, 885–891.

Al-Rashdan, Z., 2001: Investigation of natural Zeolite tuffs on their ability for sewage cleaning purposes. PhD thesis, Oldenburg University, Germany

ASTDR, 2012: Toxicological Profile for 1,4-Dioxane. U.S. Department of Health and Human Services Public Health Service, Agency for Toxic Substances and Disease Registry., http://www.atsdr.cdc.gov/toxprofiles/tp187.pdf.

Bowman, R. H., P. Miller, M. Purchase and R. Schoellerman, 2003: Ozone-peroxide advanced oxidation water treatment system for treatment of chlorinated solvents and 1,4 dioxane. NGWA Conference on MTBE: Assessment, Remediation, and Public Policy. Baltimore, Maryland. .

Caliskan, N., A. R. Kul, S. Alkan, E. G. Sogut and I. Alacabey, 2011: Adsorption of Zinc(II) on diatomite and manganese-oxide-modified diatomite: A kinetic and equilibrium study. Journal of Hazardous Materials, 193, 27-36.

Da□browski, A. and V. A. Tertykh, 1996: Adsorption on new and modified inorganic sorbents, p. xvii, 926 p. Elsevier, Amsterdam ; New York.

Das, D., V. Gaur and N. Verma, 2004: Removal of volatile organic compound by activated carbon fiber. Carbon 42, 2949–2962.

Datsko, T. Y., V. I. Zelentsov and E. E. Dvornikova, 2011: Physicochemical and adsorption-structural properties of diatomite modified with aluminum compounds. Surface Engineering and Applied Electrochemistry, 47, 530-539.

DiGuiseppi, W. and C. Whitesides, 2007: Treatment options for remediation of 1,4-dioxane in groundwater. Environmental Engineer: Applied Research and Practice, 2, 2-6.

Dobbs, R. A. and J. M. Cohen, 1980: Carbon adsorption isotherms for toxic organics. EPA-600-8/80-023, United States Environmental Protection Ageny, Cincinnati, USA.

Earth Tech Inc, 2004: Technology evaluation for treatment of 1,4-dioxane in groundwater. Prepared for the Air Force Center for Environmental Excellence. December 2004.

ECB, 2002: European Union Risk Assessment Report, 1,4-dioxane, CAS No: 123-91-1, EINECS No: 204-661-8. European Chemicals Bureau, Institute for Health and Consumer Protection, 21.

Fukuhara, T., S. Iwasaki, T. Hasegawa, K. Ishihara, M. Fujiwara and I. Abe, 2011: Adsorption of 1,4-Dioxane from Aqueous Solutions onto Various Activated Carbons. J. Water and Environment Technology, 9, 249-258.

GRAC, 2003: Groundwater Resources Association of California. 1,4-Dioxane and other solvent stabilizer compounds in the environment. TThe ninth symposium in GRAC's series on groundwater contaminants. San Jose, California.

Grob, R. L. and E. F. Barry, 2004: Modern practice of gas chromatography.

Grosjean, D., 1990: Atmospheric chemistry of toxic contaminants. 2. Saturated aliphatics: Acetaldehyde, dioxane, ethylene glycol ethers, propylene oxide. Air Waste Mgmt Assoc, 40, 1522-1531.

Gulipalli, C. S., B. Prasad and K. L. Wasewar, 2011: Batch study, equilibirum and kinetics of adsorption of selenium using Rice Husk Ash (RHA) Journal of Engineering Science and Technology 6, 586 - 605.

Hosseini, S. A., S. M. Sadeghi and A. L. Kafi, 2011: Synthesis, characterization, and catalytic activity of nanocrystalline La (1-x)Eu(x)FeO(3) during the combustion of toluene. Chinese Journal of Catalysis, 32, 1465−1468.

HSDB, 2007: Hazardous Substances Data Bank. 1,4-Dioxane National Library of Medicine, National Toxicology Program, Hazardous Substances Data Bank. Bethesda, Maryland

Hu, J. C., Z. Song, L. F. Chen, H. J. Yang, J. L. Li and R. Richards, 2010: Adsorption Properties of MgO(111) Nanoplates for the Dye Pollutants from Wastewater. Journal of Chemical and Engineering Data, 55, 3742-3748.

Kent, J. A., 2012: Handbook of industrial chemistry and biotechnology. Springer, New York.

Khaleel, A., P. N. Kapoor and K. J. Klabunde, 1999: Nanocrystalline metal oxides as new adsorbents for air purification. Nanostructured Materials, 11, 459-468.

Khan, F. I. and A. K. Ghoshal, 2000: Removal of Volatile Organic Compounds from polluted air. Journal of loss prevention in the process industries, 13, 527-545.

Khraisheh, M. A. M., Y. S. Al-Degs and W. A. M. Mcminn, 2004: Remediation of wastewater containing heavy metals using raw and modified diatomite. Chem. Eng. J., 99, 177-184.

Kirk-Othmer, J., 1999: Concise encyclopedia of chemical technology. 4th ed., John Wiley & Sons, New York, USA, p. 1724.

Klabunde, K. J., J. Stark, O. Koper, C. Mohs, D. G. Park, S. Decker, Y. Jiang, I. Lagadic and D. J. Zhang, 1996: Nanocrystals as stoichiometric reagents with unique surface chemistry. Journal of Physical Chemistry, 100, 12142-12153.

Koper, O. B., S. Rajagopalan, S. Winecki and K. J. Klabunde, 2007: Nanoparticle Metal Oxides for Chlorocarbon and Organophosphonate Remediation. In G. E. Fryxell and G. Cao (Ed), Environmental Applications of Nanomaterials: Synthesis, Sorbents and Sensors (pp 3-24). World Scientific, London : Imperial College Press. ISBN: 9781860946622.

Kumar, V. K., K. Porkodi and F. Rocha, 2008: Comparison of various error functions predicting the optimum isotherm by linear and non-linear regression analysis for the sorption of basic red 9 by activated carbon. J. of Hazardous Material, 150, 158-165.

Lazaridis, N. K., T. D. Karapantsios and D. Georgantas, 2003: Kinetic analysis for the removal of a reactive dye from aqueous solution onto hydrotalcite by adsorption. Water Res, 37, 3023-3033.

Lewis, R. S., 2000: Sax's Dangerous Properties of Industrial Materials John Wiley & Sons, Inc. New York, NY

Li, B. Z., 2010: Effect of structure and properties of simple aromatic compounds on adsorption behavior of activated carbon. J. Fuel Chem. Technol., 38, 252-256.

Li, L., P. A. Quinlivan and D. R. U. Knappe, 2002: Effects of activated carbon surface chemistry and pore structure on the adsorption of organic contaminants from aqueous solution. Carbon, 40, 2085 - 2100.

Li, L. Q., Z. Sun, H. L. Li and T. C. Keener, 2012: Effects of activated carbon surface properties on the adsorption of volatile organic compounds. Journal of the Air & Waste Management Association, 62, 1196-1202.

Lim, J. S., S. J. Park, J. K. Koo and H. Park, 2001: Evaluation of porous ceramic as microbial carrier of biofilter to remove toluene vapor. Environ Technol, 22, 47-56.

Limousin, G., J. P. Gaudet, L. Charlet, S. Szenknect, V. Barthès and M. Krimissa, 2007: Sorption isotherms: A review on physical bases, modeling and measurement. Applied Geochemistry, 22, 249-275.

Liu, G., J. Wang, Y. Zhu and X. Zhang, 2004: Destructive adsorption of carbon tetrachloride on nanometer titanium dioxide. Physical Chemistry Chemical Physics, 6, 985-991.

Luth, H., G. W. Rubloff and W. D. Grobman, 1977: Chemisorption and decomposition reactions of oxygen-containing organic molecules on clean Pd surfaces studied by UV photoemission. Surface Science, 63, 325-338.

Maurer, T., H. Hass, I. Barnes and K. H. Becker, 1999: Kinetic and Product Study of the Atmosphere Photooxidation of 1,4-Dioxane and its Main Reaction Product Ethylene Glycol Diformate. Journal Physics Chemistry A, 103, 5032-5039.

Mcguire, M. J., I. H. Suffet and J. V. Radziul, 1978: Assessment of Unit Processes for Removal of Trace Organic-Compounds from Drinking-Water. Journal American Water Works Association, 70, 565-572.

Mills, G. and M. R. Hoffmann, 1993: Photocatalytic degradation of pentachlorophenol on titanium dioxide particles: identification of intermediates and mechanism of reaction. Environ. Sci. Technol. , 27, 1681-1689.

Mishakov, I. V., A. F. Bedilo, R. M. Richards, V. V. Chesnokov, A. M. Volodin, V. I. Zaikovskii, R. A. Buyanov and K. J. Klabunde, 2002: Nanocrystalline MgO as a dehydrohalogenation catalyst. Journal of Catalysis, 206, 40-48.

Mohr, T. K. G., W. H. DiGuiseppi and J. A. Stickney, 2010: Environmental Investigation and Remediation: 1,4-Dioxane and other Solvent Stabilizers. Book News, Inc., Portland - United States, 34.

Moussavi, G. and M. Mahmoudi, 2009: Removal of azo and anthraquinone reactive dyes from industrial wastewaters using MgO nanoparticles. Journal of Hazardous Materials, 168, 806-812.

Munch, J. W. and P. E. Grimmett, 2008: Method 522 Determination of 1,4-Dioxane in Drinking Water by Solid Phase Extraction (SPE) and Gas Chromatography/ Mass Spectrometry (GC/MS) With Selected Ion Monitoring (SIM). National Exposure Research Laboratory Office Of Research And Development U. S. Environmental Protection Agency Cincinnati, Ohio EPA/600/R-08/101 http://www.epa.gov/microbes/documents/Method%20522_final%20520for%20520OGWDW%22009_20522_20508.pdf.

Noll, K. E., V. Gounaris and W. S. Hou, 1992: Adsorption technology for air and water pollution control. Lewis Publishers, Inc., Chelsea, MI, USA.

Nwabanne, J. T. and P. K. Igbokwe, 2008: Kinetics and equilibrium modeling of nickel adsorption by cassava peel. J. of Engineering and Applied Sciences, 3, 829-834.

Ochonogor, A. E. and P. M. Ejikeme, 2005: Adsorption potentials of cinnarium schweinfurthi nut shell activated carbon. J. Chemical Society of Nigeria, 30, 91-94.

Oh, E., D. E. Wurster, S. Majuru and J. C. Wang, 1998: Use of Fourier transform infrared (FT-IR) spectroscopy to follow the adsorption of heptane and 1,4-dioxane vapors on a zinc oxide surface. Journal of pharmaceutical sciences, 87, 1124-1129.

Ohta, M., V. M. Boddu and M. Uchimiya, 2011: Thermal response and recyclability of poly (stearylacrylate-co-ethylene glycol dimethacrylate) gel as a VOCs absorbent. Polymere Bulletin, 67, 915−926.

Onundi, Y. B., A. A. Mamun, M. F. Al Khatib and Y. M. Ahmed, 2010: Adsorption of copper, nickel and lead ions from synthetic semiconductor industrial wastewater by palm shell activated carbon. Int. J. Environ. Sci. Tech., 7, 751-758.

Powell, R. M., R. W. Puls, S. K. Hightower and D. A. Sabatini, 1995: Coupled iron corrosion and chromate reduction: mechanisms for subsurface remediation. Environ. Sci. Technol., 29, 1913- 1922.

PRTR, 2003: Pollutant Release and Transfer Register. Ministry of of Economy, Trade and Industry and Ministry of Environment. Japan

Ridha, A., H. Aderdour, H. Zineddine, M. Z. Benabdallah, M. El Morabit and A. Nadiri, 1998: Aqueous silver (I) adsorption on a low density Moroccan silicate. Annales De Chimie-Science Des Materiaux, 23, 161-164.

Rouquerol, F., J. Rouquerol and K. Sing, 1999: Adsorption by Powders and Porous Solids, Principles, Methodology and Applications. ACADEMIC PRESS, 24-28 Oval Road, London NWl7DX. UK.

Roy, W. R. and R. A. Griffin, 1985: Mobility of Organic-Solvents in Water-Saturated Soil Materials. Environmental Geology and Water Sciences, 7, 241-247.

Shah, J. J. and H. B. Singh, 1988: Distribution of Volatile Organic-Chemicals in Outdoor and Indoor Air - a National Vocs Data-Base. Environmental Science & Technology, 22, 1381-1388.

Shim, W. G., H. Moon and J. W. Lee, 2006: Performance evaluation of washcoated MCM-48 monolith for adsorption of volatile organic compounds and water vapors. Micropor. Mesopor. Mater., 94, 15–28.

Surprenant, K. S., 2002: 1,4 Dioxane. In Ullmann's Encyclopedia of Industrial Chemistry (6th ed.). Weinheim, Germany: Wiley-VCH Verlag, 309-314 http://dx.doi.org/310.1093/toxsci/kfm1251.

Suthersan, S. S., 2002: National and Enhanced Remedation System. Boca Raton, FL: Lewis Publisher

TRI, 2013: TRI explorer: Providing access to EPA's toxic release inventory data. Washington, DC. Office of Information Analysis and Access, Offices of Environmental Information, U.S. Environmental Protection Agency. Toxic Release Inventory, http://www.epa.gov/triexplorer.

USEPA, 2006: U.S. Environmental Protection Agency;Treatment technologies for 1 4-dioxane: fundamentals and field applications. Washington, DC: American Chemical Society, http://www.epa.gov/tio/download/remed/542r06009.pdf.

USEPA, 2011: U.S. Environmental Protection Agency; 1,4- Dioxane in Drinking water treatabilty database. http://iaspub.epa.gov/tdb/pages/contaminant/contaminantOverview.do?contaminantId=10860.

Vatavuk, W. M., 1999: VOC controls, VOC Recapture Controls. EPA/452/B-02-001. (U.S. EPA, OAQPS, Research Triangle Park, NC). http://www.epa.gov/ttn/catc/dir1/cs3-1ch1.pdf.

Venkatesha, T. G., Y. A. Nayaka and B. K. Chethana, 2013: Adsorption of Ponceau S from aqueous solution by MgO nanoparticles. Applied Surface Science, 276, 620-627.

Verma, A., S. Chakraborty and J. K. Basu, 2006: Adsorption study of hexavalent chromium using tamarind hull based adsorptions. Sep. Purify. Technol., 50, 336-341.

Volodin, A. M., A. F. Bedilo, D. S. Heroux, V. I. Zaikovskii, I. V. Mishakov, V. V. Chesnokov and K. J. Klabunde, 2006: Nanoscale oxides as destructive sorbents for halogenated hydrocarbons. In Blitz, J. Gun'ko, V. (eds) Surface Chemistry in Biomedical and Environmental Science. Springer. New York 403-412.

Wagner, G. W., O. B. Koper, E. Lucas, S. Decker and K. J. Klabunde, 2000: Reactions of VX, GD, and HD with nanosize CaO: Autocatalytic dehydrohalogenation of HD. The journal of physical chemistry. B, 104, 5118-5123.

Walczak, M. M. and P. A. Thiel, 1990: Cyclic ethers adsorbed on Ru(001). Surface Science, 238, 180-186.

Walker, G. M. and L. R. Weatherley, 1999: Kinetic of acid dye adsorption on GAC. Water Res, 33, 1895–1899.

Wang, D., M. Elisabeth, P. Robert and Y. S. Lin, 2011: Adsorption of organic compounds in vapor, liquid, and aqueous solution phases on hydrophobic aerogels. Industrial and Engineering Chemistry Research, 50, 12177−12185.

Weber, W. J., 1972a: Physicochemical processes for water quality control. Wiley-Interscience. ISBM: 9780471924357.

Weber, W. J., 1972b: Physicochemical Processes: For Water Quality Control. Wiley, John & Sons, Incorporated. SBN-13: 9780471924357.

Wolfe, N. L. and P. M. Jeffers, 2000: Hydrolysis. In: Boethling RS, Mackay D, eds. Handbook of property estimation methods for chemicals: Environmental and health sciences. Boca Raton, FL: Lewis Publishers.

Wu, C. D., X. J. Xu, J. L. Liang, Q. Wang, Q. Dong and W. L. Liang, 2011: Enhanced coagulation for treating slightly polluted algae-containing surface water combining polyaluminum chloride (PAC) with diatomite. Desalination, 279, 140-145.

Yang, K., Q. Sun, F. Xue and D. Lin, 2011: Adsorption of volatile organic compounds by metal-organic frameworks MIL-101: influence of molecular size and shape. J Hazard Mater, 195, 124-131.

Zaitan, H. and T. Chafik, 2005: FT-IR determination of adsorption characteristics for volatile organic compounds removal on diatomite mineral compared to commercial silica. Comptes Rendus Chimie, 8, 1701-1708.

Zenker, M. J., R. C. Borden and M. A. Barlaz, 2003: Occurrence and treatment of 1,4-dioxane in aqueous environments. Environmental Engineering Science, 20, 423-432.

Zhuravlev, L. T., 2000: The surface chemistry of amorphous silica. Zhuravlev model. Colloids and Surfaces a-Physicochemical and Engineering Aspects, 173, 1-38.

CHAPTER III

Chapter 3 - Developing a New FT-IR-based Real-Time Detection Method for Flow-Through Diffusion Cell studies for Assessing *in vitro* Transdermal Permeation

Abstract

The skin serves as an important portal for entry of chemicals into the body. Skin absorption data are required for toxicological risk assessment and pharmaceutical availability of topical medicaments. *In vitro* techniques are usually used to evaluate skin absorption. A new flow-through diffusion method was developed by modifying the Bronaugh flow-through diffusion cell with flow capacity in both the donor and receptor compartment and using ATR–FT-IR as an analytical technique. The current method performance for *in vitro* transdermal permeation was evaluated by (1) comparing permeation flux in a flow-through donor chamber and a static donor chamber, (2) evaluating the effect of the receptor fluid flow rate on dermal permeation flux, (3) evaluating the effect of the donor fluid flow rate on dermal permeation flux, and (4) comparing permeation flux data obtained by flow-through cell with automated sampling system (ASS) with data from modified flow-through system (MFTS). The experiment was performed using dioxane permeating through human stratum corneum at room temperature. The results showed that the highest dioxane flux obtained at a slower receptor fluid flow rate, and the lowest flux obtained at the highest rate (R2 =0.935). The variability of the flux at steady state was increased as the receptor fluid flow rate increased ($R^2 = 0.977$), where the coefficient of variation was 1.13 ± 0.23 % at 1 mL/hr and 6.01 ± 0.57 % at 40 mL/hr. No significant difference ($P = 0.73$) was found between dioxane flux obtained by ASS and by MFTS. But the results showed a significant

difference ($P < 0.001$) in variability of dioxane flux over time between the two systems, with MFTS showing a lesser coefficient of variation (1.12 ± 0.19 %). The cumulative amount of dioxane in MFTS and ASS was linear with time, and the lag time was significantly different ($P <0.02$) between MFTS and ASS with values of 2.19 ± 0.25 and 2.58 ± 0.33hr, respectively. The donor fluid flow rate showed no effect ($P > 0.05$) on the dioxane steady state flux. This model may present an alternative *in vitro* model for evaluating dermal absorption with the added advantages of providing 'real time' quantitative high density permeation data, control of steady donor concentrations over time, simplicity of use, and the low cost of test samples.

Introduction

In toxicological risk assessment, skin absorption data are required for a wide range of chemical compounds to evaluate the internal doses following a dermal exposure to these compounds and to provide exposure assessors with an understanding of safety limits. Moreover, there has been a growing interest in dermal administration of drugs for both local (topical application) and systemic (transdermal delivery) therapy. Skin absorption can be measured by *in vivo* or *in vitro* methods with humans and animals. *In vivo* studies frequently present many challenges, such as cost, country-specific legislation, ethical considerations, and others. *In vitro* methods can provide a valid alternative to the *in vivo* methods for many significant aspects of skin exposure. *In vitro* methods also offer an economical and practical alternative for low-cost testing of a large number of formulations, saving time and effort, and overcoming legal and ethical considerations. However, *in vitro* dermal absorption studies should be carried out under conditions mimicking those in the real world if reliable and accurate data is to be obtained (USEPA, 2007).

In vitro dermal absorption studies often use the principle of diffusion, where a penetrant solution is applied to one side of the skin and its diffusion flow measured on the other side. Usually, the method for evaluating penetrant permeability *in vitro* uses a rate limiting membrane (commonly, skin) that separates two chambers. The outer surface of the skin faces the donor chamber and the inner surface faces the receptor (or acceptor) chamber. The receptor chamber is filled with a proper physiological receptor fluid, the penetrant is added into the donor chamber on the outer surface of the skin, and its rate of accumulation in the receptor chamber receptor fluid is used to measure the dermal absorption kinetic. The penetrant remains on the skin for a given time under specific environments (such as temperature, pH, and osmolarity).

Receptor chamber samples are taken at periodic intervals to measure the amount of penetrant permeating over time (Kielhorn *et al.*, 2006, Chilcott & Price, 2008, Permegear, 2014, Hanson, 2014).

There are two basic approaches to assess skin permeation *in vitro*: the static (non-flowing) cell and the flow-through cell. The most extensively used static design for investigating *in vitro* dermal absorption is the Franz diffusion cell. This cell has a static receptor fluid reservoir with a side-arm sampling port (Franz, 1975). The use of the Franz-type diffusion cell to conduct dermal experiments has rapidly become widespread despite some of its inconveniences and limitations. The flow-through diffusion cell is a modification of the previous static design for mimicking *in vivo* conditions. It is characterized by continuously changed receptor fluid to maintain sink conditions during the course of the experiment. The flow is driven by a pump and the cell has a much smaller receptor chamber to allow easy removal of contents with moderate flow of receptor fluid (Bronaugh & Stewart, 1984). Flow-through type diffusion cells have been used to assess chemical flux through skin and other membranes of interest. These cells have the advantage that the experimental apparatus can be automated, permitting quick collection of dermal absorption data (Sclafani *et al.*, 1993).

Sampling from a diffusion cell to measure permeates in dermal absorption experiments is an important factor in terms of time intervals between samples, frequency, and volume for determining accurate dermal absorption data. However, manual sampling is often tedious, time consuming, and sometimes requires complicated sampling schedules that pose challenges for the investigator (Cordoba-Diaz *et al.*, 2000). In a static cell system, the volume of receptor fluid is the same for all the diffusion cells; thus, the quantity of permeate that is found in the receptor fluid can simply be measured for that specific volume. The samples must be obtained rapidly and

consecutively from all receptor chambers (at consistent time intervals). Automated sampling, usually used with a flow-through diffusion cell, facilitates more consistent time-interval sampling from all the cells. However, there may be trivial differences in the volume of receptor fluid driven through each diffusion cell into the collection vials because of tubing component diameters or clamping pressures in the pump. Shortening of collection time intervals from a small receptor chamber with an automated sampling system results in a small sample volume, which is insufficient for analysis (Sclafani *et al.*, 1993, Talreja *et al.*, 2001).

Permeating substances from the dermal absorption are measured using radiolabeled or non-radiolabeled material (Kielhorn *et al.*, 2006). Liquid scintillation counting is the most common method for quantifying the concentration of permeates in receptor fluid. In this method, the target molecules (the permeate) are radiolabelled with beta-emitting radioactive isotopes (H^3, C^{14}, S^{35}, and P^{32}) and beta radiation is measured by the scintillation counters. C^{14} and H^3 are the two most commonly used isotopes, but C^{14} is preferred for organic compound molecules. The advantages of using a radiolabelled substance are that it is easy to monitor the distribution of the substance in the experimental system, simple to quantify (by liquid scintillation counting) mass balance measurements, and usable in combination with micro-autoradiography to more determine the distribution of the test substance within the dermal layers. However, there are many disadvantages associated with radiolabelled substances. They are expensive to synthesize, only available in small amounts, difficult to distinguish parent molecule and metabolite, in addition to safety considerations (Chilcott & Price, 2008). Non-radiolabeled materials can also be used in dermal absorption studies and detected with techniques such as HPLC, ELISA, LC-MS, GC-MS, and fluorescence. These techniques can be adapted to many permeates, and can be used to perform multiple analyses. Their disadvantage is that very small amounts of permeate can remain undetected or

under-detected due to the large volume of receptor fluid in static cells or the large volume collected from flow-through diffusion cells (Cordoba-Diaz *et al.*, 2000).

Over the years there have been many proposed diffusion cell modifications since the earliest design by Hans Ussing in 1949, which he developed to measure ion transport through frog skin held between two half-static chambers (Ussing, 1949). Most modifications have been designed to evaluate the *in vitro* permeability of a diversity tissues, and have contained mammalian skin (Treherne, 1956), buccal mucosa (Bergman *et al.*, 1969, Squier *et al.*, 1997), mucosal corneal membrane (Schoenwald & Huang, 1983), and gastrointestinal mucosal membrane (Grass & Sweetana, 1988).

One of the disadvantages of the side-by-side diffusion cell arrangement was the need to immerse both sides of the membrane in an aqueous condition, resulting in hydration of the normally dry skin external surface. For this reason, Franz proposed a vertical diffusion cell design (Franz, 1975). The Franz diffusion cell permits the external skin surface to remain dry and also facilitates direct application.

Another disadvantage of the static diffusion cell is accumulation of the permeating substance in the receptor compartment between samplings, which results in decreased flux across the membrane. This limitation led to the continuous-flow system. The first use of a continuous-flow system was describe by Ainsworth (Ainsworth, 1960). The continuous-flow system allows constant removal of permeating compound from the receptor chamber, thus maintaining a concentration gradient through the membrane that mimics *in vivo* conditions. Bronaugh and coworkers (Bronaugh & Stewart, 1985) introduced further refinements to the flow-through

system that permitted system automation if used with a fraction collector or similar sampling device.

Many other specially modified versions of diffusion cells have been proposed and validated against the classical apparatus. For example, the enhancer cell, which was a modified version of the USP type II dissolution apparatus, has served as a diffusion cell and has been used to compare the permeation characteristics of hydrocortisone (Kumar *et al.,* 1993), and also the modified automatic sampling system (Akazawa *et al.*, 1989, Martin *et al.*, 1989).

The purpose of the present study was to evaluate the performance of a new modified flow-through diffusion cell method for *in vitro* transdermal permeation, which has flow-through capacity in both the donor and receptor chambers with real time quantifying of the concentration of permeating compound in receptor fluid. The method performance was evaluated by comparing permeation flux in flow through the donor chamber with a static donor chamber, evaluating the effect of the receptor fluid flow rate on dermal permeation flux, evaluating the effect of donor fluid flow rate on dermal permeation flux, and comparing permeation flux data obtaining by a flow-through cell with automated sampling system (ASS) with data from the modified flow-through system (MFTS). The experiment was performed using the 1,4 dioxane permeating through human stratum corneum at room temperature.

Material and Methods

Chemicals

The 1,4 dioxane 99.8% was purchased from ACROS Organics (New Jersey, USA). The receptor fluid chemicals were: sodium chloride (NaCl) Lot No. 045779, potassium chloride (KCl) Lot No. 076729, sodium bicarbonate ($NaHCO_3$) Lot No. 073814, magnesium sulfate ($MgSO_4.7H_2O$) Lot No. 060337, potassium phosphate (KH_2PO_4) Lot No. 056327, dextrose Lot No. 054971, and bovine serum albumin (fraction V; cold alcohol precipitated) Lot No. 095503. They were obtained from Fisher Scientific (Pittsburgh, PA, USA). Calcium chloride (CaCl) Lot No. A0214153001 was obtained from Acrose Organic (New Jersey, USA). Levofloxacin Lot No. 0001425507 was obtained from Sigma Aldrich Chemical Co (St. Louis MO, USA). Heparin Lot No. 045058 was purchased from Baxter (Illinois, USA).

Receptor Fluid Preparation

The receptor fluid was designed to mimic a blood plasma environment, and consisted of 13.78 g NaCl, 0.71 g KCl, 0.56 g CaCl2, 0.32 g KH_2PO_4, 0.58 g $MgSO_4.7H_2O$, 5.50 g $NaHCO_3$, 2.40 g dextrose, 90.0 g bovine serum albumin, 4 mg levofloxacin, and 10 mL heparin, to which distilled water was added to attain a total volume of 2 L of fluid. The fluid was left on magnetic stirrer for several hours until all components had dissolved. The fluid was decanted into 1L bottles, was labeled, and placed in a freezer until it was used.

Skin Preparation

Human skin was donated under conditions of informed consent as set forth in the "Federal Policy for the Protection of Human Subjects," 45 CFR 46.116-117, and with approval by the Institutional Review Board for Kansas State University (proposal number 4206).

Human skin from the abdominal region was obtained from white-skinned females who had undergone tummy tuck surgery (Manhattan Surgical Hospital, Manhattan, KS). The skin was dermatomed (Padgett Model S Dermatome, Integra LifeSciences Corp., Plainsboro, NJ, USA) to 0.5 mm thickness and stored at −20°C until use during the next two months. Thereafter, dermatomed skins were thawed at room temperature for 30 min and cut into disks. Skin disks were mounted in the flow-through diffusion cell system with exposed skin surface areas of 1 cm^2.

Flow-Through Diffusion System Modification

The flow-through diffusion cell system (PermeGear Inc., Hellertown, PA, USA) was used as modified. This cell is made from plastic Kel-F (a 3M product) or Neoflon. It has a clamping system to securely clamp tissue or membranes. Clamping is achieved with a stainless steel spring that applies pressure preset by the user to the upper surface of the donor compartment for leak proof clamping. The diffusion cell has a contact area of 1 cm^2 and consists of two compartments a static donor compartment and a flow-through receptor compartment. This flow-through diffusion cell was modified to provide flow-through capacity in both the donor and receptor compartments, and was connected to the test cell, which was mounted on the FT-IR spectroscope where the effluent from the receptor compartment flowed over the crystal aperture. The test cell is made from Plexiglas and has a chamber (diameter = 5.2 mm, depth = 4.71 mm,

volume = 100 µL) to be placed directly on the crystal aperture. A schematic representation of the modified flow-through diffusion system is shown in figure 3.1.

The human skin disk was mounted on the diffusion cell. Thereafter, tubing was attached to the inlet port of the receptor compartment which was perfused with receptor solution, and to the donor compartment inlet port, which was supplied with donor solution using high-precision multi-channel pumps for analytical applications (ISMATEC, IPC-N 16, ISM 938, Switzerland). Both the donor and receptor solutions were perfused at a 2 ml/hour flow rate. The donor compartment was filled with 3 ml of the donor solution for permeability studies. This ensured that the skin was exposed to donor solution at the beginning of the permeability study. The concentration of the dioxane in the donor solution was 50 mg/ml. The skin was exposed to the test formulations over a period of 10 hours at room temperature.

To determine the proper flow rate for flow-through cell experiments, dioxane water was applied to the surface of the skin in a water vehicle and the steady-state dermal absorption rate of the dioxane was measured at different receptor fluid flow rates (1, 5, 10, 20, 40 ml/hour). To compare permeation flux data obtaining by MFTS and the automated sampler system (ASS), the PermeGear Model (Hellertown, PA, USA) was used. From 5 diffusion cells, perfusate was collected in receptor vials after the application of the formulations to the skin at 20-minute intervals for the first hour and at one-hour intervals thereafter for a 10-hour period. Hence, each perfusate sample represents the collective flow-through over the preceding hour. The permeating dioxane concentration in the collected samples was measured by FT-IR.

Analytical Procedure

To determine the dioxane permeating through the skin, IR adsorption spectra at time intervals were obtained. The attenuated total reflectance IR spectrum of effluent from the receptor compartment was measured using attenuated total reflection Fourier transform infrared spectroscopy (ATR-FTIR) with a Thermo-Nicolet FT-IR spectrometer, model 6700, and a GladiATR vision unit (PIKE Technologies, Inc. WI, USA). The OMNIC FT-IR software program was used in the FT-IR system. Absorbance spectra were measured over the wave number range of 4000–400 cm^{-1} with a spectral resolution of 4 cm^{-1}. The IR absorption spectra for dioxane in solution were obtained at various times. These spectra were analyzed using the C–O vibration band. The selected peak region for obtaining the integrated absorbance was 1105.2–1160.2 cm^{-1}. The crystal aperture surface was cleaned with alcohol and dried, and an uncovered crystal background was run prior to scanning of the sample sets. With the continuous flow measuring method, a macro was created by using the OMNIC Macros application to measure absorbance spectra every 3 minutes, with the data saved on the computer.

Data analysis

Data were analyzed by calculating both flux ($mg/cm^2/hr$) and cumulative penetration (mg/cm^2). The steady state flux (J_{ss}) was calculated according to the following equation:

$$\boldsymbol{J_{ss}} = \Delta Q/A^* \Delta t$$

where (ΔQ) is the amount of compound permeating the skin during time (Δt) and (A) is the diffusional area (1 cm^2). The amount of dioxane passing through the test cell chamber over each time interval was calculated by multiplying the measured concentration by the volume of

receptor solution inside test cell chamber (100 µL) over the time interval. The lag time for dioxane was estimated by extrapolating the linear part of the permeability curve and assigning its intercept on the time axis. This was assigned to confirm that the duration of the permeability experiment was long enough to offer an accurate evaluation of the steady state flux, as the length of the experiment must typically be three times the duration of the lag time (Shah, 1993).

Minitab (version 16.1.1, Minitab Inc., PA, USA - 2010) Analyses of variance (ANOVA) was used to assess the significance of differences in means between groups. Tukey's Multiple Comparison Method was used to compare the means. Pearson's correlation was used to measure the strength of a linear association between the coefficient of variation and flux with the flow rate of receptor fluid. All data obtained are presented as mean (± SD), unless otherwise stated. All statements of significant differences were based on a 95% confidence level ($P < 0.05$). A statistical measure of the dispersion of data points series of flux over time interval was evaluated by the coefficient of variation (%), as follows:

$$\text{Coefficient of variation (\%)} = (\text{standard deviation} / \text{mean}) * 100$$

Lag time of dioxane in MFTS and ASS was calculated from linear extrapolation of the steady-state portion of the penetration profile back to the x-axis.

Results and Discussion

Effect of Receptor Fluid Flow Rate on Permeability through Skin

Primarily, the experiments were conducted to ascertain the suitable receptor fluid flow rates for flow-through cell study. The receptor fluid flow rates of 1, 5, 10, 20, and 40 mL/hr were used, and the experiment was repeated 5 times. The results showed a significant difference ($P < 0.001$) in the permeated amount of dioxane through the skin at steady state absorption between the flow rates. The higher permeated amount was determined at a slower flow rate (1mL/hr), and as flow rate increased, the permeating dioxane decreased (Table 3.1). The result showed a strong correlation ($R^2 = 0.935$) between the flow rate of receptor fluid and the flux of the dioxane through the skin (Figure 3.2).

To evaluate the effects of flow rate on the variability of flux at steady state absorption through human skin, the results showed that the variability of flux increased as the flow rate increased. The variability at the slower rate (1 mL/hr) was 1.13 ± 0.23% coefficient of variation and 6.01 ± 0.57% at the faster rate (Table 3.1). The absorption profiles (Figure 3. 3) show that almost identical variability was found at the 1 and 5 mL/hr rates, whereas the results presented a significant difference ($P < 0.001$) between the variability at the 5, 10, 20, and 40 mL/hr rates. Linear regression analysis showed a strong correlation ($R^2 = 0.977$) between the variability and flow rate (Figure 3.4). The 2 mL/hr flow rate was used in subsequent experiments.

The flow rate of receptor fluid in flow-through diffusion cells is important to ensure that removal of perfusate is sufficiently rapid as to avoid stasis and alterations in the diffusion gradient through the skin. The required optimum flow rate for good mixing and for removing permeated compound is influenced by different factors like the solubility in receptor fluid, the

volume of the receptor chamber, and the contact area of the skin (Bronaugh, 2004). A number of studies have shown that the flow rate can affect *in vitro* dermal absorption. For example, Crutcher and Maibach reported that the permeating amount of testosterone and testosterone propionate across guinea pig skin varied with the flow rates used in their system. Where flow rates of 0.5, 1, 2, and 4 mL/hr and 4.52 cm^2 contact area of skin were used for 24 hrs, the experimental results showed increasing perfusate in receptor fluid as flow rate increased (Crutcher & Maibach, 1969). This variability may be attributed to the relative contact area of exposed skin or the low water solubility of the permeating compound. In another study, three flow rates (1, 5, and 40 mL/hr) were used to determine the suitable flow rate for flow-through cell *in vitro* experiments using tritiated water permeating across rat skin. This study showed almost identical permeation at the 5 and 40 mL/hr rates, and the absorption at the lower rate (1 mL/ hr) was not significantly different, but the variability was much greater (Bronaugh & Stewart, 1985). The findings of the current study were not consistent with previous studies regarding the impact of flow rate on the compound permeation across the skin in steady state absorption, as our study found a strong negative correlation between them. This difference could be related to the high density data sets (many data points per unit of time at steady state absorption), which reduce the standard errors of the means of permeated amounts over time points, or may be related to the solubility of the permeated compound in receptor fluid.

The rate at which receptor fluid flows through a receptor chamber can significantly impact dermal absorption. Ideally, the flow rate used must be appropriately rapid so that it does not affect dermal absorption rates and must be regularly calibrated (Chilcott & Price, 2008). In most studies, receptor fluid flow rates mostly range from 1 to 6 mL/ hr (Crutcher & Maibach, 1969, Bronaugh & Stewart, 1984, Bronaugh & Stewart, 1985, Sclafani *et al.*, 1993, Squier *et al.*,

1997). Our findings showed that the range from1 to 5 mL/hr was the appropriate flow rate to be used in a flow-through diffusion system because this range exhibited the maximum flux and low variability at steady state dermal absorption. Thus, our results are compatible with those of earlier studies.

Flux Evaluation by MFTS and ASS

To compare the permeation flux data obtained by ASS and data from MFTS, permeation flux of dioxane at steady state was evaluated in both systems. The results showed no significant difference ($P = 0.73$) between dioxane permeation flux obtaining by ASS and MFTS. But the results presented a significant difference ($P < 0.001$) in variability of dioxane flux over time between the two systems, where MFTS showed a lesser coefficient of variation (Table 3.2, Figure 3.5).

Transdermal permeation experiments are tiresome because they require around-the-clock monitoring of the dermal absorption profile. In the absence of an automated system, manual sampling of the receptor solution is used to generate flux data. In this case, regular samples are obtained over the first 8 to 12 hours during the day, and then mostly at final time points taken the following day, which generates inconsistent data (Chilcott & Price, 2008). Considering this fact, it is obvious that the use of automation system in this type of experiment is highly advised to facilitate obtaining accurate and consistent data, in addition to save labor and costs (Cordoba-Diaz *et al.*, 2000). To achieve this goal, many modified automatic sampling systems have been developed over the years (Akazawa *et al.*, 1989, Martin *et al.*, 1989, Hanson, 2014, Permegear, 2014). The frequent monitoring in short intervals of a permeate transport across skin in a diffusion cell offers an accurate measurement of the dermal absorption process, which can mimic the physiological situation, especially with respect to the dynamics associated with blood flow,

and avoids the change of perfusate concentrations in receptor fluid over time due to the evaporation or decomposition (Martin *et al.*, 1989). Therefore, shortening the interval time for measuring perfusate concentration would provide high density data that can minimize variation in results and offer more accuracy of interpretation. The outcomes obtained from MFTS demonstrate an obvious outperforming to collect high density, consistent permeability data from a membrane over relatively long periods of time compared to ASS data collection. The result of current study showed that the lag time of permeating dioxane was less in present system than that in ASS. Additionally, the coefficient of variation of steady state flux means was smaller in MFTS, and that was due to the obtained high density data in comparison to the obtained ASS data.

The cumulative amount of dioxane in MFTS and ASS was linear with time, following an appropriate lag phase (Figure 3.6). The lag time of dioxane was significantly different ($P < 0.02$) between MFTS and ASS with values of 2.19 ± 0.25 and 2.58 ± 0.33hr, respectively. The lesser lag time obtained with the present method may not be detectable earlier using ASS because of its lesser capability to sample frequently compared to the present method, suggesting an advantage of MFTS over ASS. The aim of evaluating the lag time in both systems was to confirm that the duration of the experiment was sufficient for accurate assessment of steady state flux. Typically, to achieve a constant steady state flux through the membrane, the duration of the permeability experiment must be at least three times the duration of the permeate lag time (Shah, 1993, Cordoba-Diaz *et al.*, 2000). In both systems the duration of the permeability experiment exceeded three times the duration of the lag time of the dioxane, indicating that the flux values obtained were accurate. The lag time was 2.19 and 2.58 hr in MFTS and ASS, respectively,

which suggested that the experimental duration should have been at least 7.75 hr for accurate assessment of steady state flux.

Effect of Donor Fluid Flow Rate on Permeability through Skin

The donor fluid flow rate of 0 (static donor chamber), 2, 5, 10, 20, and 40 mL/hour were used for the experiment (n = 5). The results exhibited no significant effect ($P > 0.05$) of the donor fluid flow rates on the amount of permeated dioxane through the skin at steady state absorption. The steady state flux of dioxane ranged between 12.157 ± 0.907 and 12.805 ± 1.125 µg/cm^2/hr (Figure 3.7). No linear relationship ($R^2 = 0.332$) was found between donor fluid flow rate and permeating of dioxane through human skin (Figure 3.8).The cumulative amount of dioxane in all donor fluid flow was linear with time, following a suitable lag phase (Figure 3.9). The flux between the flow rates was not significantly different ($P > 0.05$).

Use of a flow-through diffusion cell provided an alternative approach to using a static diffusion cell for assessing *in vitro* dermal absorption. Where the receptor solution flows underneath the membrane at a certain rate to provide suitable sink conditions and mimic *in vivo* blood circulation. This model provides significant advantages by allowing for replenishment of the receptor fluid to maintain sink conditions and the possibility of automatic sampling (Bronaugh & Stewart, 1984, Bosman *et al.*, 1996). However, in the flow through systems, the donor compartment remained static. One of the main restrictions of this model is that the concentration of compound in the donor compartment can considerably decline over time of the dermal absorption experiment, consequently decreasing the thermodynamic activity of the perfusate, leading to flux that is not at a steady state (Lestari *et al.*, 2009). To overcome this restriction of static donor compartments, some studies have suggested using a flow-through

diffusion cell with flow-through capacity in both receptor and donor compartments that can preserve steady concentrations in the donor compartment and sink conditions in the receptor compartment to attain accurate evaluation of steady state perfusate flux (Squier *et al.,* 1997, Lestari *et al.,* 2009).

Studies of the effect of donor flow on the permeability of compounds through a membrane are limited. However, Lestaria and a coworker developed a flow-through diffusion cell with a flow-through donor chamber for assessing the permeability of compounds across the buccal mucosa (Lestari *et al.,* 2009). This flow-through diffusion cell was compared to a modified model of Ussing's chambers (Nicolazzo *et al.,* 2003), which has a static donor compartment, however, this study found no significant difference between the two models in the flux of compounds through the mucosal membrane. The findings of the current study were consistent with Lestari's findings, in that our results showed no significant difference in dioxane flux through skin between the static donor chamber and the flow-through donor chamber even at different flow rates. Although the current results showed no effect of the donor flow chamber on the compound permeability through the skin, further studies with different compounds, vehicles and experimental durations may show different outcomes.

Advantages and Disadvantages

The objective in designing the current method was to develop an automated alternative for static diffusion cells and conventional automated flow-through methods. Therefore, experiments could be run for a long time without requiring the investigator to be present. MFTS allows replenishment of fluid in the donor and receptor compartments, which maintains sink conditions in the receptor compartment and secures constant concentration of the compound in the donor

fluid during the experiment. The main advantage of the current method is that it can provide in 'real time' quantitative high density data over time about permeation, which means a more accurate fitting of the permeation profile. Using FT-IR, which is fast and easy, requiring little or no sample preparation as an analytical technique in MFTS substantially reduces the total cost of test samples when compared to the cost of conventional techniques like liquid scintillation counting, HPLC, and GCMS.

Although MFTS has many advantages, there also are limitations that may detract from its usefulness. MFTS does not allow running multiple samples at the same time with one FT-IR instrument. This limitation poses a challenge in long duration studies involving a large number of samples. Difficulties in obtaining a representative FT-IR background and perfusate containing a mixture of substances can affect the detection of the target compound. The temperature of an *in vitro* system should be controlled to maintain the target temperature and reduce variation in experimental environments (Tojo, 1987). With Franz diffusion cells, temperature control of receptor solution is maintained with a water jacket (Franz, 1975), whereas in Bronaugh diffusion cells, heated water from a water bath is pumped through the block of cells to maintain a physiological temperature (Bronaugh & Stewart, 1985). Current experiments with MTFS were conducted to focus on design and were not temperature controlled. In future studies, diffusion cells and the donor and receptor fluid sink will be placed in a temperature-controlled cabinet to ensure adequate temperature control.

Conclusion

A new flow through diffusion method was developed by modifying the Bronaugh flow-through diffusion cell with flow capacity in both the donor and receptor compartments and using ATR – FT-IR as the analytical technique. The current method performance for *in vitro* transdermal permeation was evaluated by comparing permeation flux in the flow-through donor chamber with a static donor chamber, evaluating the effect of the receptor fluid flow rate on dermal permeation flux, evaluating the effect of the donor fluid flow rate on dermal permeation flux, and comparing permeation flux data obtained by ASS with that obtained by MFTS. It was concluded that:

- The suitable receptor fluid flow rate was ranged from 1 to 5 mL/hr, which rate can offer the highest flux and lowest variability at steady state.

- The results presented no effect of the donor flow chamber on skin permeability; however, further studies with different compounds, vehicles, and experiment durations may show different findings.

- The current method can provide 'real time' quantitative high density permeation data over time, which provides a more accurate fitting of the permeation profile.

- This method is easy to use, requires no sample preparation, and is low cost for conducting transdermal absorption *in vitro* studies.

- This *in vitro* model is an alternative for evaluating dermal absorption, and has the added advantages of better maintenance of sink conditions, and control of steady donor concentrations over time.

- In spite of some limitations, the present flow-through diffusion method provides significant advantages over conventional automated methods, especially in terms of time, effort, and acquisition of permeating data.

Table 3.1: Effect of receptor fluid flow rate on permeating amount of dioxane through human skin and steady state flux variation (n =5)

Flow rate (mL/hr)	Flux (µg/cm^2/hr)	Coefficient of variation (%)
1	12.674 ± 0.286	1.13 ± 0.23
5	12.172 ± 0.271	1.11 ±0.19
10	11.107 ± 0.545	2.45 ± 0.31
20	8.740 ± 0.648	3.73 ± 0.39
40	7.3495 ± 0.883	6.01 ± 0.57

Table 3.2: Effect of system type on permeating amount of dioxane through human skin and steady state flux variation (n =5)

System	Flux (µg/cm^2/hr)	Coefficient of variation (%)
MFTS	12.295 ± 0.274	1.12 ± 0.19
ASS	12.150 ± 0.879	3.82 ± 0.75

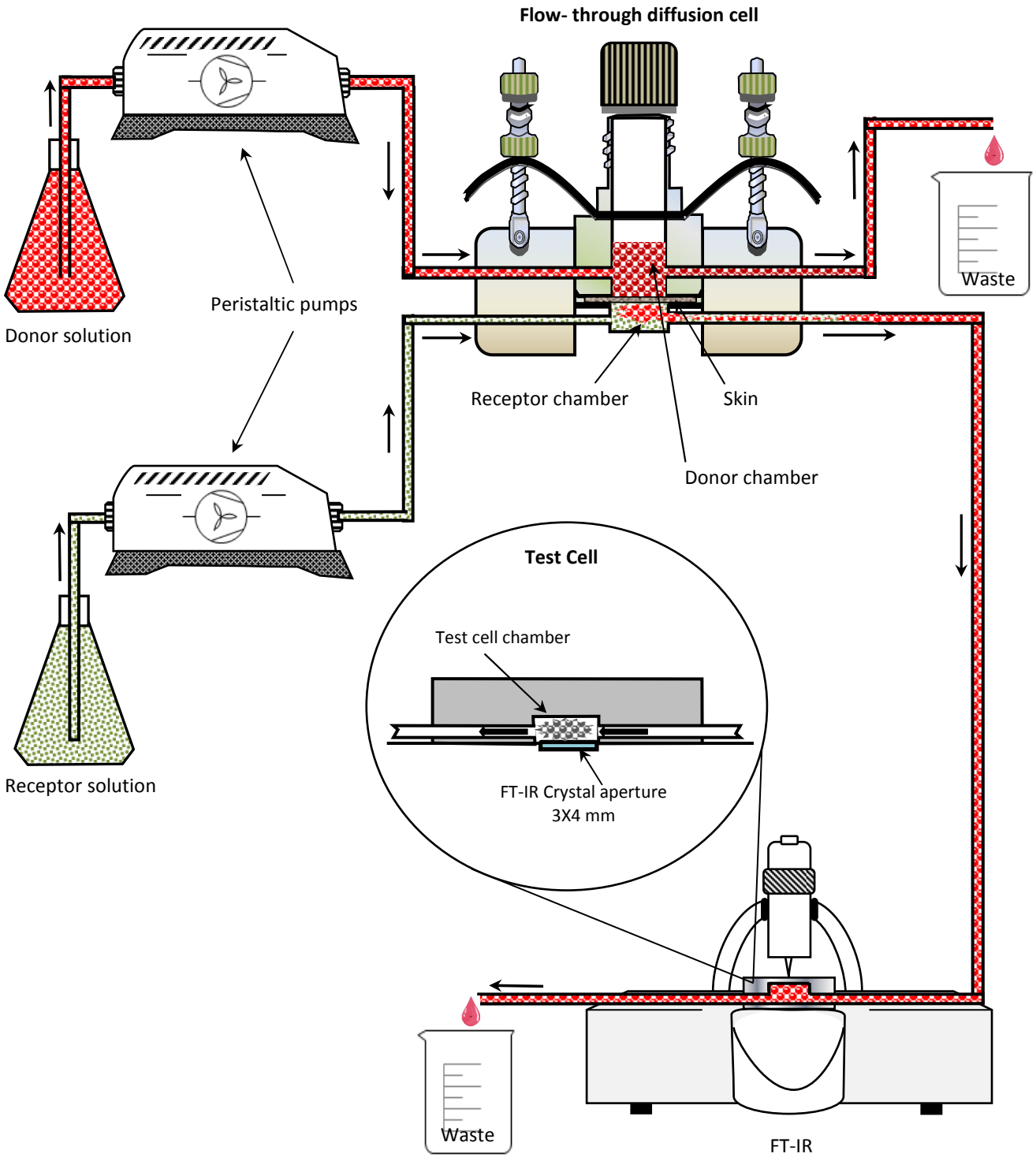

Figure 3.1: Schematic diagram of the modified flow through diffusion system

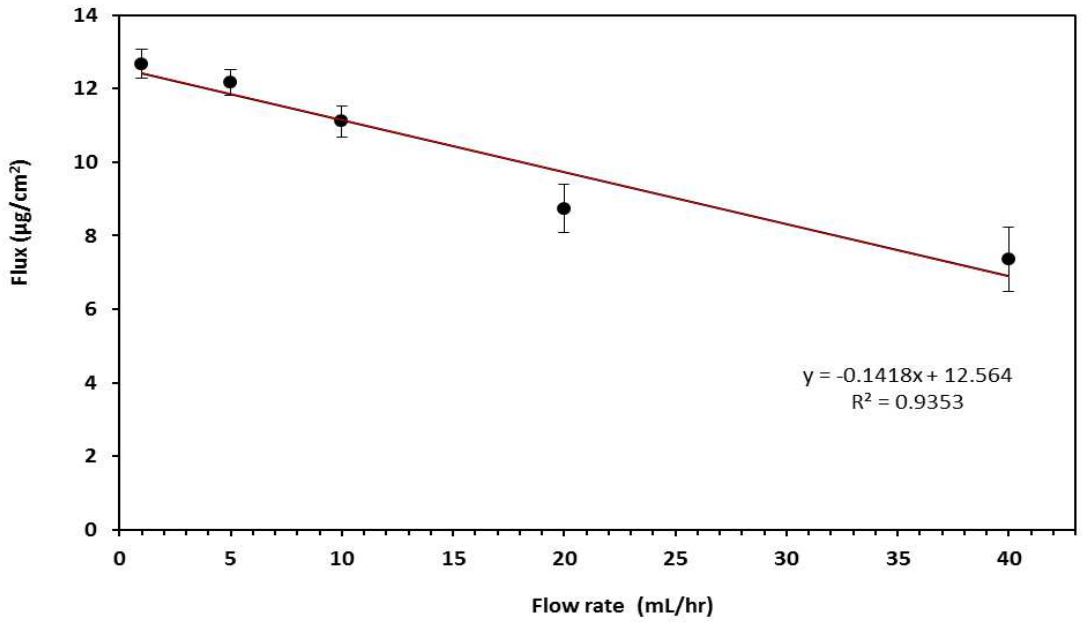

Figure 3.2: Dioxane steady state flux through human skin against receptor fluid flow rate. The linear regression line, regression equation and R^2 value is displayed (n =5)

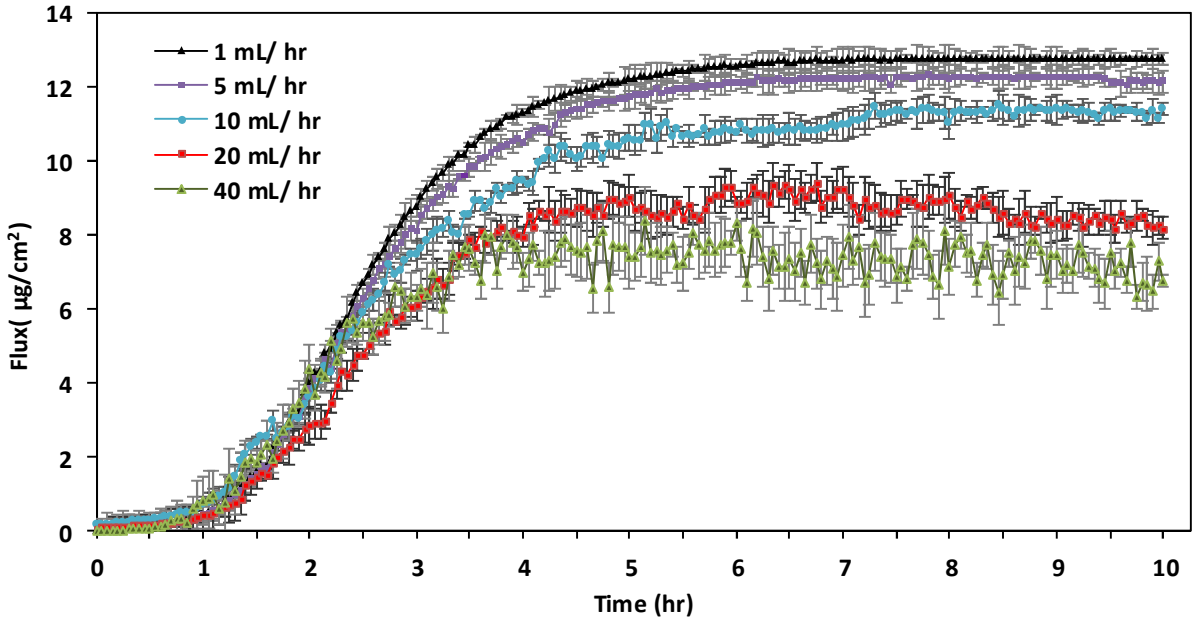

Figure 3.3: Effect of receptor fluid flow rate on permeability of dioxane through human skin (n =5)

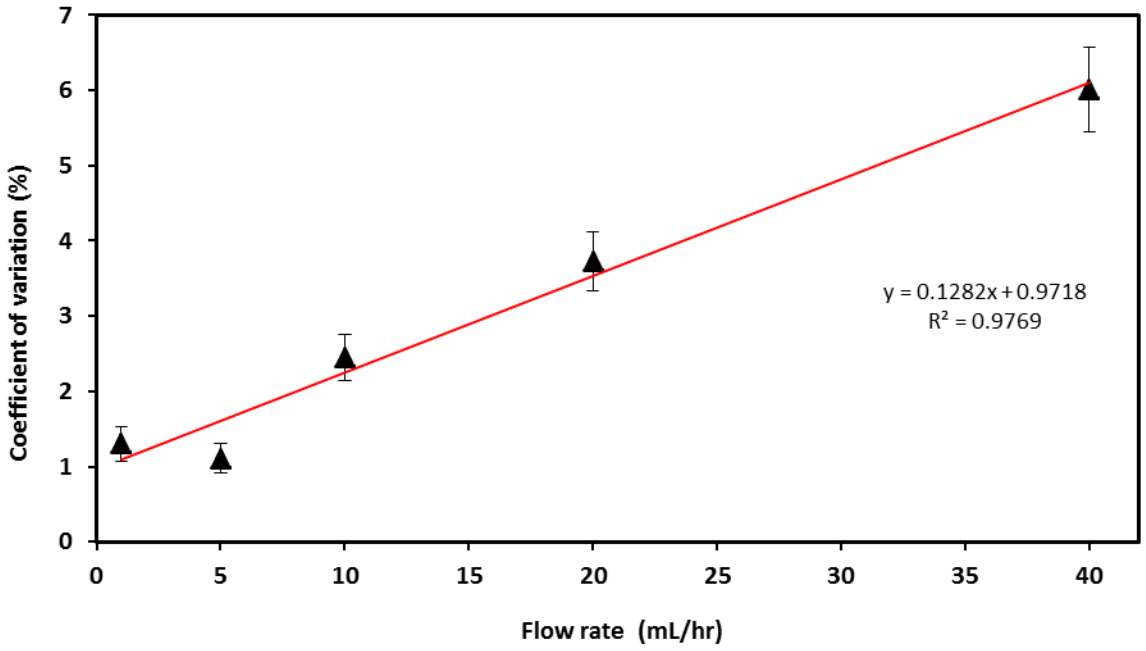

Figure 3.4: Variability in dioxane steady state flux through human skin against receptor fluid flow rate. The linear regression line, regression equation and R^2 value is displayed (n =5)

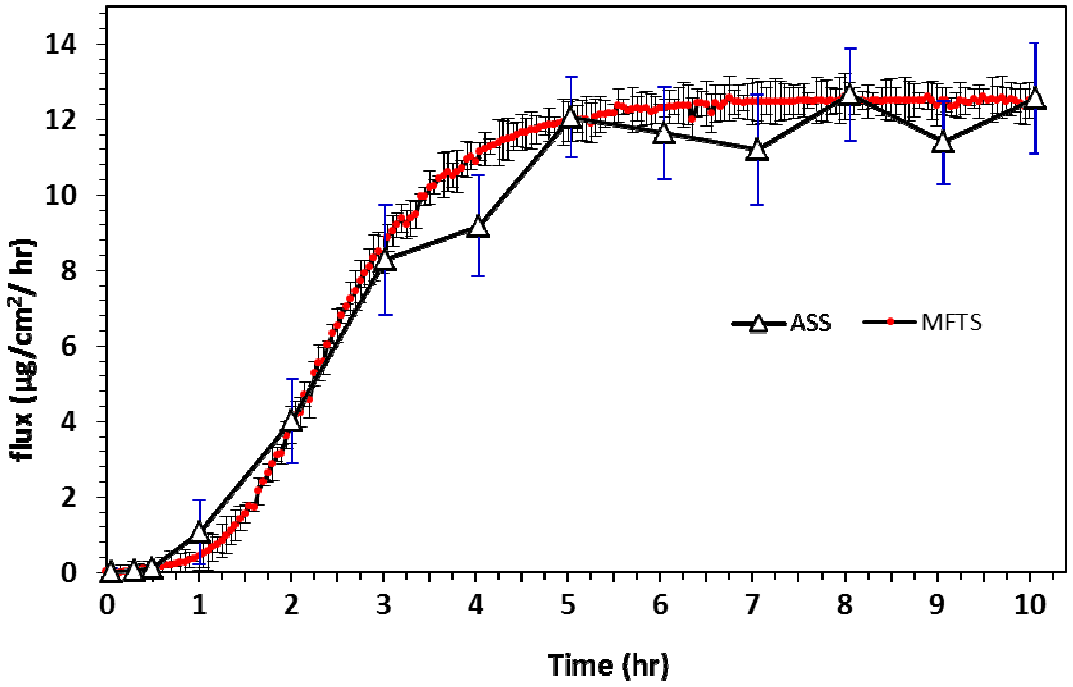

Figure 3.5: Effect of system type on the absorption of dioxane across human (n =5)

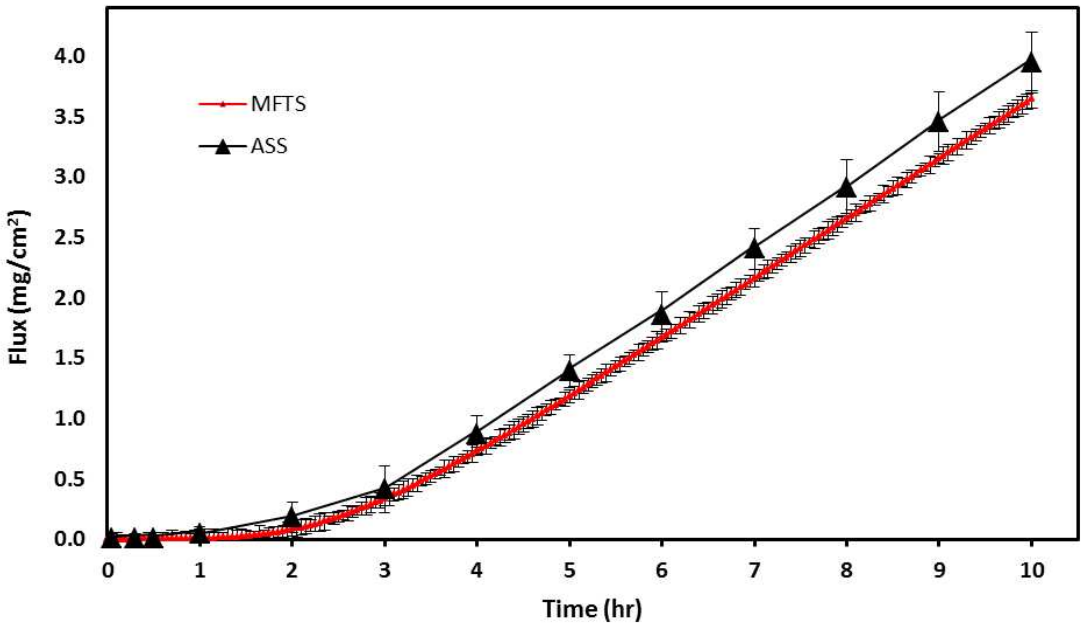

Figure 3.6: Accumulation of dioxane across human skin evaluated in the modified flow-through system and flow-through cell with automated sampling system (n =5)

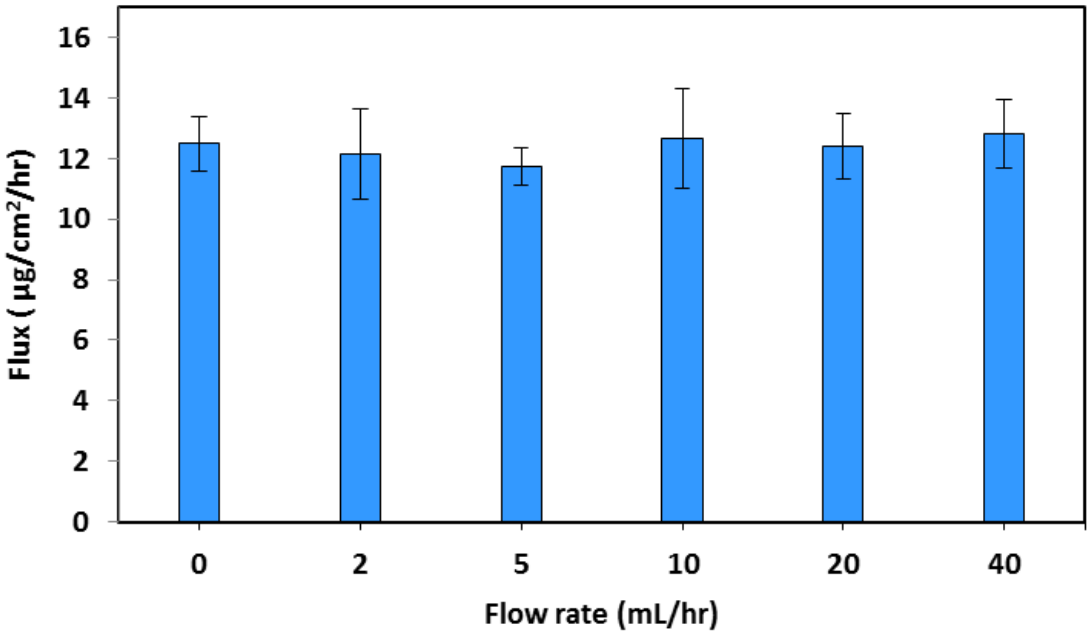

Figure 3.7: Effect of donor fluid flow rate on permeating of dioxane through human skin (n =5)

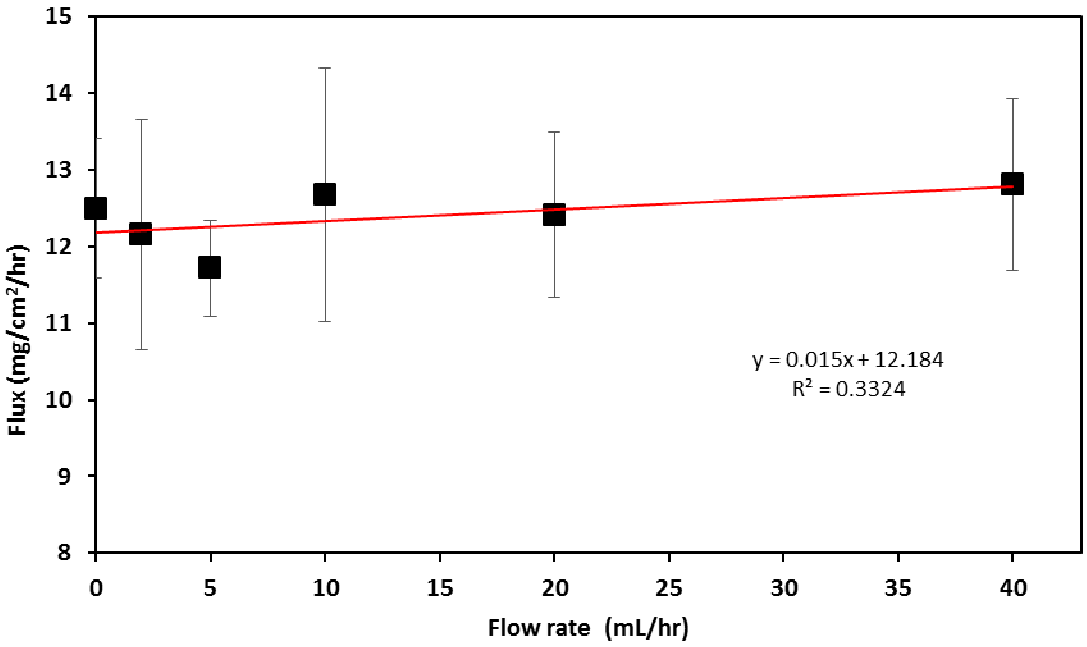

Figure 3.8: Dioxane steady state flux through human skin against Donor fluid flow rate. The linear regression line, regression equation and R^2 value is displayed (n =5)

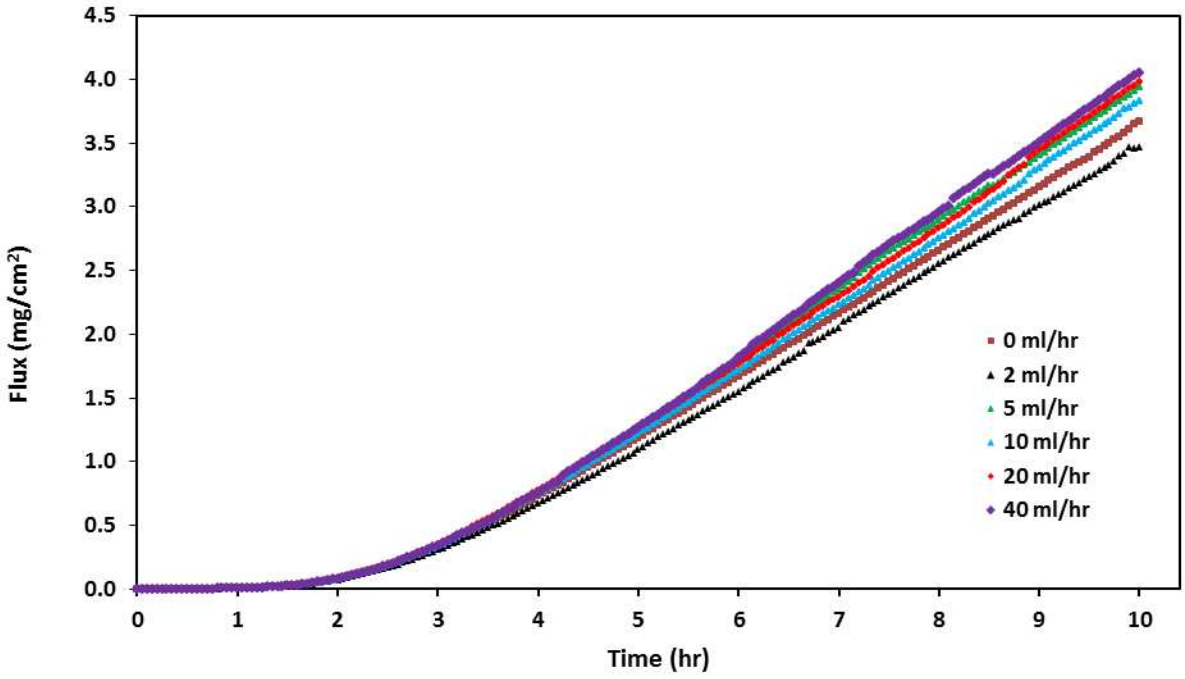

Figure 3.9: Effect of donor fluid flow rate on cumulative amount of dioxane permeated through human skin

References

Ainsworth, M. J., 1960: Methods for measuring percutaneous absorption J. Soc. Cosmetic Chemists, 11, 69–78.

Akazawa, M., T. Itoh, K. Masaki, B. T. Nghiem, N. Tsuzuki, R. Konishi and T. Higuchi, 1989: An automated method for continuously monitoring diffusion cells in skin penetration studies. International Journal of Pharmaceutics, 50, 53-60.

Bergman, S., D. Kane, I. A. Siegel and S. Ciancio, 1969: *In vitro* and in situ transfer of local anaesthetics across the oral mucosa. Arch. Oral. Biol. , 14, 35-43.

Bosman, I. J., A. L. Lawant, S. R. Avegaart, K. Ensing and R. A. de Zeeuw, 1996: Novel diffusion cell for *in vitro* transdermal permeation, compatible with automated dynamic sampling. Journal of pharmaceutical and biomedical analysis, 14, 1015-1023.

Bronaugh, R. L., 2004: Methods for *in vitro* percutaneous absorption. In: Zhai, H. and Maibach, H. I. eds. Dermatotoxicology, 6th ed. New York, CRC Press, . pp 520–526.

Bronaugh, R. L. and R. F. Stewart, 1984: Methods for *in vitro* percutaneous absorption studies III: hydrophobic compounds. Journal of pharmaceutical sciences, 73, 1255-1258.

Bronaugh, R. L. and R. F. Stewart, 1985: Methods for *in vitro* percutaneous absorption studies IV: The flow-through diffusion cell. Journal of pharmaceutical sciences, 74, 64-67.

Chilcott, R. and S. Price, 2008: Principles and Practice of Skin Toxicology. John Wiley & Sons.

Cordoba-Diaz, M., M. Nova, B. Elorza, D. Cordoba-Diaz, J. R. Chantres and M. Cordoba-Borrego, 2000: Validation protocol of an automated in-line flow-through diffusion equipment for *in vitro* permeation studies. Journal of controlled release : official journal of the Controlled Release Society, 69, 357-367.

Crutcher, W. and H. I. Maibach, 1969: The effect of perfusion rate on *in vitro* percutaneous penetration. The Journal of investigative dermatology, 53, 264-269.

Franz, T. J., 1975: Percutaneous absorption on the relevance of *in vitro* data. The Journal of investigative dermatology, 64, 190-195.

Grass, G. M. and S. A. Sweetana, 1988: *In vitro* measurement of gastrointestinal tissue permeability using a new diffusion cell. Pharmaceutical research, 5, 372-376.

Hanson, 2014: http://www.hansonresearch.com/ (accessed 28.03.2014).

Kielhorn, J., S. Melching-Kollmuss, I. Mangelsdorf and W. H. Organization, 2006: Environmental Health Criteria 235: Dermal Absorption. World Health Organization.

Kumar, P., P. Sanghvi and C. C. Collins, 1993: Comparison of Diffusion Studies of Hydrocortisone Between the Franz Cell and the Enhancer Cell. Drug Development and Industrial Pharmacy, 19, 1573-1585.

Lestari, M. L., J. A. Nicolazzo and B. C. Finnin, 2009: A novel flow through diffusion cell for assessing drug transport across the buccal mucosa *in vitro*. Journal of pharmaceutical sciences, 98, 4577-4588.

Martin, B., O. Watts, B. Shroot and J. C. Jamoulle, 1989: A new diffusion cell — an automated method for measuring the pharmaceutical availability of topical dosage forms. International Journal of Pharmaceutics, 49, 63-68.

Nicolazzo, J. A., B. L. Reed and B. C. Finnin, 2003: The effect of various *in vitro* conditions on the permeability characteristics of the buccal mucosa. Journal of pharmaceutical sciences, 92, 2399-2410.

Permegear, 2014: http://www.permegear.com/ilc14.htm (accessed 28.03.2014).

Schoenwald, R. D. and H. S. Huang, 1983: Corneal penetration behavior of beta-blocking agents I: Physiochemical factors. Journal of pharmaceutical sciences, 72, 1266-1272.

Sclafani, J., J. Nightingale, P. Liu and T. Kurihara-Bergstrom, 1993: Flow-through system effects on *in vitro* analysis of transdermal systems. Pharmaceutical research, 10, 1521-1526.

Shah, J. C., 1993: Analysis of permeation data: evaluation of the lag time method. International Journal of Pharmaceutics, 90, 161-169.

Squier, C. A., M. Kremer and P. W. Wertz, 1997: Continuous flow mucosal cells for measuring the in-vitro permeability of small tissue samples. Journal of pharmaceutical sciences, 86, 82-84.

Talreja, P., N. K. Kleene, W. L. Pickens, T. F. Wang and G. B. Kasting, 2001: Visualization of the lipid barrier and measurement of lipid pathlength in human stratum corneum. AAPS pharmSci, 3, E13.

Tojo, K., 1987: Design and calibration of *in vitro* permeation apparatus. In: Transdermal Controlled Systemic Medications (Chien YW, Ed), Marcel Dekker, New York,. pp 127 - 158.

Treherne, J. E., 1956: The permeability of skin to some non-electrolytes. J. Physiol, 133, 171-180.

USEPA, 2007: Dermal Exposure Assessment: A Summary of EPA Approaches. National Center for Environmental AssessmentOffice of Research and Development U.S. Environmental Protection Agency Washington, DC

Ussing, H. H., 1949: The active ion transport through the isolated frog skin in the light of tracer studies. Acta physiologica Scandinavica, 17, 1-37.

CHAPTER IV

Chapter 4 - *In vitro* Evaluation of Transdermal Absorption of 1,4 Dioxane in Human Skin and The Effects on Absorption of Sodium Lauryl Sulphate , Ethanol, Propylene glycol, and Ethyl acetate

Abstract

Skin contact with dioxane is a potential hazard encountered in environmental, accidental spill, and occupational contamination scenarios. An *in vitro* dermal absorption study was carried out to investigate the absorption of dioxane across human skin. The effect of the surfactant sodium lauryl sulphate (SLS) and solvent system water, ethanol (EtOH), propylene glycol (PG), and ethyl acetate (EA) on the permeation profile of dioxane was also studied. Fourier transform-infrared (FT-IR) spectroscopic studies were done to investigate the effect of solvents on the biophysical properties of the stratum corneum (SC) to understand the mechanism of permeation alteration of dioxane by the solvent systems used. The absorption parameters of dioxane were 1.16 ± 0.22 hr, 5.7 X 10^{-4} ± (0.62) cm/hr, 0.286 ± 0.035 mg/cm^2/hr, 4.8 X 10^{-5} (± 0.32) cm^2/hr, and 1.99 ± 0.086 mg for lag time, permeability(K_p), steady-state flux, diffusivity, and total amount absorbed over 8 hr, respectively. The flux and K_p of dioxane were found to increase as the concentration increased up to 50% PG in water, and there was no significant increase in flux at 70% PG ($P < 0.05$). With further increases of PG concentration to 100% dioxane flux, K_p showed no significant decrease. EtOH was found to increase flux and K_p with an increasing of concentration, which was greatest with 70% ($P < 0.05$). At 100% of EtOH, flux declined. There was no significant difference between dioxane flux at 30%, 50%, or 100% of EtOH ($P > 0.05$). EA and SLS were found to increase the permeation of dioxane across the skin. The FT-IR spectra

of SC treated with EA and PG showed no significant effect on symmetrical or asymmetrical vibration of the CH_2 peak shift nor on the broadening near 2850 and 2920 cm^{-1}. FT-IR spectra of SC pre-treated with EtOH revealed that there was boarding of peaks near 2920cm^{-1} with increasing EtOH concentrations. Lipid extract precipitates were detected only from SC treated with solvent EtOH. The FT-IR spectra of the extract precipitates revealed that they were mostly composed of part SC lipid.

Introduction

Chemical transport through human skin can play a significant role in human exposure to potentially toxic substances confronted in environmental contamination, occupational, and unintentional spill scenarios. Dermal absorption can be an important factor for systemic toxicity, and determination of absorbed effective amount is integral to human risk assessments. The rate of dermal absorption ranges widely between different compounds, and its evaluation depends on sufficient description and understanding of the processes that affect the barrier properties of the membrane. The stratum corneum (SC) is a formidable barrier to exogenous substance absorption and water loss via skin in mammalians. It is found between 15 and 20 tightly packed, flattened, and keratin-enriched cell (corneocyte) layers embedded in an intercellular lipid matrix. The SC is composed of a heterogeneous structure containing 20-40% water, 20% lipids, and 40% keratinized protein (Poet & McDougal, 2002). Partitioning into SC is dependent on the lipophilicity of the chemicals. More lipophilic chemicals tend to partition into the lipid matrix, whereas more hydrophilic chemicals tend to partition into the corneocytes. Generally, the dermal absorption of the more lipophilic chemicals occurs more readily, whereas hydrophilic chemicals are absorbed only very slowly (USEPA, 1992, Wester & Maibach, 2000, Modamio *et al.*, 2000).

1,4-dioxane (dioxane) is a synthetic organic compound that is extensively used as an industrial solvent or solvent stabilizer or is produced as a by-product of the ethoxylation process (Zenker *et al.*, 2003). This compound is considered to be carcinogen in test animals, is classified as a Group B2 (probable human carcinogen) by the U.S.EPA, and as a group 2B (possible human carcinogen) by the International Agency for Research on Cancer. Other harmful effects of

dioxane in animal studies include liver and kidney damage in animals chronically exposed to it by inhalation, ingestion, or dermal contact (Mohr *et al.*, 2010).

The main routes of human exposure to dioxane are ingestion, inhalation, and dermal contact. Exposure by ingestion mostly occurs through contaminated drinking water, whereas exposure by inhalation or dermal contact to dioxane can occur from direct contact with the compound in a workplace, or with products containing its residues (a common source of exposure by the general population). The National Occupational Exposure surveys have indicated that 86,489 workers involved in handling, transporting, and processing dioxane, including 30,542 women, potentially were exposed directly to dioxane compound between 1981 and 1983 (NIOSH, 1984). According to the Consumer Product Safety Commission, consumers may be exposed to residual levels of dioxane produced during the manufacture of cosmetic detergents, shampoos, surfactants, and many pharmaceuticals that contain ethoxylated ingredients (CPSC, 2014). Polyethoxylated surfactants are usually used in the formulation of cosmetics, products for dish washing, and detergents. During the production of polyethoxylated detergents by the reaction of ethylene oxide with fatty alcohols, some of ethylene oxide is polymerized to form dioxane that can contaminate these products (Rastogi, 1990). The Environmental Working Group analyzed the ingredients of 15,000 personal care and cosmetic products reporting that 22% of these products may be contaminated with dioxane (EWG, 2007).

There is strong evidence that dermal exposure to dioxane may cause significant skin absorption, which may result in adverse health effects. Dermal exposure may occur from using contaminated water during showering or bathing or from using consumer cosmetics, detergents, or shampoos containing ethoxylated surfactants (ASTDR, 2012), in addition to occupational exposure during their production or use as a solvent (IARC, 1999). Data on toxic effects in

humans following dermal exposure to dioxane are very limited. Historically, Wirth and Klimmer reported that the application of 0.05 ml dioxane to human skin three times within one day caused dryness but no signs of inflammation(Wirth & Klimmer, 1937). In a lethal occupational case, Johnstone described the probability that dioxane dermal exposure had contributed to the liver and kidney toxicity that the researchers observed (Johnstone, 1959a). Generally, prolonged and repeated contact with dioxane can cause skin irritation and eczema in humans (Sonneck, 1964, Gingell *et al.*, 1994). In laboratory animals, dermal exposure to dioxane can cause skin irritation, liver and kidney damage, and neoplastic lesions (Fairley *et al.*, 1934, Kano *et al.*, 2009, ASTDR, 2012).

In environmental or occuptional dermal exposure, skin may be exposed to dioxane as a single compound or in complex mixtures. Mostly, the mechanism of dermal absorpion for a single compound has been investigated and risk assessment profiles focus on the behavior of single compounds (Bronaugh & Maibach, 1999). The dermal absorption profile of a compound in a mixture may be altered due to chemical interactions. The interactions can occur through different mechanisms such as altering physical–chemical properties, chemical–chemical binding on the surface of the skin, altering permeability through the lipid pathway, or altered partitioning into the SC (Raykar *et al.*, 1988, KAI *et al.*, 1990, Rosado *et al.*, 2003). Hence, there is a need to understand how dioxane is absorbed through human skin not only as a single chemical but also in the presence of other environmental chemicals, like solvents and surfactants, that are known to impact chemical permeability in human skin.

In addition to the role of ethoxylated surfactants as a source of dioxane impurity in many personal products and detergents, they have effects on the permeability characteristics of many biological membranes containing skin. They can modify the intercellular lipids or change their

organization in SC above the level of the critical micelle concentration (CMC) (Florence *et al.*, 1994, Lopez *et al.*, 2000, Shokri *et al.*, 2001). Surfactants can also bind extensively to SC intracellular keratin and alter dermal absorption by inducing inflammation and swelling of the epidermis (Faucher & Goddard, 1978, Black, 1993). Surfactants can also enhance the dermal penetration of some compounds which present in their formulation. Hence, they have been used to improve the permeation rates of many pharmaceticals (Chowhan & Pritchard, 1978, Aungst *et al.*, 1986). However, they can also decrease the quantity of the compound available for permeation fluid (Baynes *et al.*, 2002, van der Merwe & Riviere, 2005b) through the formation of micelles in the donor fluid that can affect the thermodynamic activity of the diffusing chemicals (Shokri *et al.*, 2001).

Solvents and dioxane may combine under different conditions and in different environments. Propylene glycol (PG), ethanol (EtOH), and ethyl acetate (EA) are solvents widely used by industries and may present with dioxane in contaminated environments such as chemical waste landfills and industrial wastewater effluent. Effects of these solvents on dermal absorption across a variety of chemicals have been described in many studies (Friend *et al.*, 1991, Friend, 1991, Megrab *et al.*, 1995, Panchagnula *et al.*, 2001, Baynes *et al.*, 2002). EtOH is a common short chain alcohol employed in transdermal products and topical preparations as a co-solvent and penetration enhancer. The suggested ways in which ethanol alters the barrier function of the skin have been reported to include changes in SC hydration, lipid fluidization, altered keratinized protein, lipid extraction, and its effects on lipid ordering (Berner *et al.*, 1989b, Liu *et al.*, 1991, Bommannan *et al.*, 1991, Watkinson *et al.*, 2009). PG has been used since 1932 either as a co-solvent for poorly soluble substances or to enhance chemical dermal absorption in topical preparations. However, its mechanism of action in enhancing chemical transdermal

permeation is not clearly understood (Barrett *et al.*, 1965, Ostrenga *et al.*, 1971, Hoelgaard & Møllgaard, 1985, Bouwstra *et al.*, 1989, Nicolazzo *et al.*, 2005). EA is an alkyl ester solvent used in glues, nail polish removers, decaffeinating tea and coffee, and cigarettes. Friends and co-workers have found that EA has the ability to increase transdermal penetration of some compounds. The mechanism of action of EA for altering skin permeability is not well understood (Friend, 1991, Friend *et al.*, 1991).

Studying dermal absorption of dioxane as a single chemical or from solvents and surfactant mixtures offers an opportunity to understand its risk assessment profile in possible scenarios. This study therefore investigated the dermal absorption profile of dioxane as a single chemical in human skin and examined the effects of different concentrations of sodium lauryl sulphate (SLS), EtOH, PG, and EA on permeability in dermatomed human skin.

Material and Methods

Chemicals

1,4 dioxane 99.8% was purchased from ACROS Organics (New Jersey, USA). Ethyl acetate and sodium lauryl sulfate were obtained from Fisher Scientific (Fair Lawn, New Jersey, USA). Propylene glycol and ethanol were purchased from Sigma Aldrich (St. Louis, MO, USA). The receptor fluid chemicals were: sodium chloride (NaCl) Lot No. 045779, potassium chloride (KCl) Lot No. 076729, sodium bicarbonate (NaHCO3) Lot No. 073814, magnesium sulfate (MgSO4.7H2O) Lot No. 060337, potassium phosphate (KH2PO4) Lot No. 056327, dextrose Lot No. 054971, and bovine serum albumin (fraction V; cold alcohol precipitated) Lot No. 095503 and were obtained from Fisher Scientific (Pittsburgh, PA, USA). Calcium chloride (CaCl) Lot No. A0214153001 was obtained from Acrose Organic (New Jersey, USA). Levofloxacin Lot No. 0001425507 was obtained from Sigma Aldrich Chemical Co. (St. Louis, MO, USA). Heparin Lot No. 045058 was purchased from Baxter (Illinois, USA).

Receptor Fluid Preparation

The receptor fluid was designed to mimic a blood plasma environment. It consisted of 13.78 g NaCl, 0.71 g KCl, 0.56 g CaCl2, 0.32 g KH_2PO_4, 0.58 g $MgSO_4.7H_2O$, 5.50 g $NaHCO_3$, 2.40 g dextrose, 90.0 g bovine serum albumin, 4 mg levofloxacin, and 10 mL heparin, to which distilled water was added to attain a total volume of 2 L of fluid. The fluid was left on a magnetic for several hours until all components were dissolved and then decanted into 1L bottles, labeled, and placed in a freezer until used.

Skin Preparation

Human skin was donated under conditions of informed consent as set forth in the Federal Policy for the Protection of Human Subjects, 45 CFR 46.116-117, and with approval of the Institutional Review Board for Kansas State University (proposal number 4206).

Human skin of the abdominal region was obtained from white-skinned females who had undergone tummy tuck surgery (Manhattan Surgical Hospital, Manhattan, KS). The skin was dermatomed (Padgett Model S dermatome, Integra LifeSciences Corp., Plainsboro, NJ, USA) to 0.5 mm thickness and stored at −20°C until used (within no more 2 months). Thereafter, dermatomed skins were thawed at room temperature for 30 min and cut into disks. Skin disks were mounted in a flow-through diffusion cell system with exposed skin surface areas of 1 cm^2.

Permeability

The modified flow-through diffusion cell system, which is described in chapter 3, was used to determine the permeability of dioxane through the skin. A human skin disk was mounted on the diffusion cell with an exposed surface of $1cm^2$. 50 mg/ml of dioxane in solution was applied to the SC side in an occluded donor chamber. The solutions used were:

- Pure water
- Aqueous solution of 10%, 30%, 50%, 70%, and 100% EtOH, PG, and EA (v/v)
- Aqueous SLS of 1%, 2%, 5%, 7%. and 10% (w/w)

The receptor solutions were perfused at a 2 ml/hour flow rate with infinite sink conditions and a concentration gradient across the skin maintained. The skin was exposed to the test formulations over periods of 8 and 15 hours at room temperature.

To determine the amount of dioxane permeating through the skin, the IR adsorption spectra at time intervals were obtained. The attenuated total reflectance IR spectrum of effluent from the receptor compartment was measured using attenuated total reflection Fourier transform infrared spectroscopy (ATR-FTIR) with a Thermo-Nicolet FT-IR spectrometer, model 6700, and GladiATR vision unit (PIKE Technologies, Inc. WI, USA). The OMNIC FT-IR software program is used in the FT-IR system. Absorbance spectra were measured over the wave number range of 4000–400 cm^{-1} with a spectral resolution of 4 cm^{-1}. The IR absorption spectra for dioxane in solution were obtained at various times. These spectra were analyzed using the C–O vibration band. The selected peak region for obtaining the integrated absorbance was 1105.2–1160.2 cm^{-1}. The crystal aperture surface was cleaned with alcohol and dried, and an uncovered crystal background was run prior to scanning of the sample sets. Using the continuous flow measuring method, a macro was created with the OMNIC Macros application to measure absorbance every 6 minutes.

FT-IR Analysis of SC

Human SC sheets were dried at room temperature for 24 hours and thereafter in a desiccator for 24 hours. The dried SC sheets were used for lipid order evaluation. FT-IR analysis of SC was based on the procedures used in previous studies described by (Panchagnula *et al.*, 2001) and (Levang *et al.*, 1999). Circular SC samples (24 mm diameter) were scissored from the dried sheets for each experiment (n = 5). The samples were immersed for 12 hours in 5 ml of solvent with and without 50mg/ml dioxane in capped 20 ml vials. The solvents used were: (i) pure water; (ii) aqueous SLS (2 mg / ml); and (iii) an aqueous solution of 0% (control), 10%, 30%, 50%, 70%, and 100% of EtOH, PG, and EA. The treated samples were washed with water

and gently blotted on Kimwipe^{TM}. They were then mounted in a demountable FT-IR liquid cell and scanned with FT-IR (Thermo-Nicolet FT-IR spectrometer, model 6700) to obtain transmission spectra in the range of 3000 – 1000 cm^{-1}. Thereafter, the samples were dried in a desiccator for 24 hours at room temperature and scanned again with FT-IR. The transmission spectra were compared with the respective scans before treatment.

Dried SC was prepared as mentioned above for lipid extraction. SC samples (n = 5) weighting 60-80 mg were placed for 24 hours in capped vials with 5 ml of water, 50% (v/v) of aqueous EtOH, aqueous PG, aqueous EA, and 100% of EtOH, PG, and EA. Then, each SC sample was removed from the vials, blotted on Kimwipe^{TM}, placed in a desiccator for 48 hours for drying, and weighed once more. The solvents were evaporated by nitrogen gas using a Temp-Block module heater (Lab-Line Instruments Inc, Melrose Park, IL, USA) at 50°C and the precipitated lipid was re-dissolved in 0.5 ml carbon tetrachloride. A drop of the re-dissolved precipitate solution was spread on a KBr crystal (KBr RCT POL., International crystal labs, Garfield, NJ, USA). The spread drop was left to evaporate at room temperature. Then, the FT-IR transmission spectra were recorded in the range of 3000 – 1000 cm^{-1} (van der Merwe & Riviere, 2005a).

FT-IR peaks near 2850 and 2920 cm^{-1} were used to indicate symmetric and asymmetric absorbance, respectively, associated with methylene group (H-C-H) stretching. Peaks around 2960 cm^{-1} indicated absorbance due to asymmetric vibration associated with the CH3 group (Potts & Francoeur, 1993)

Data Analysis

Data were analyzed by calculating both flux (mg/cm^2/h) and cumulative penetration (mg/cm^2). The steady state flux (J_{ss}) was calculated using the following equation:

$$\boldsymbol{J_{ss}} = \Delta Q / A^* \Delta t$$

Where (ΔQ) is the amount of compound permeating the skin during time (Δt) and (A) is the diffusional area (1 cm^2). The amount of dioxane passing through the test cell chamber over each time interval was calculated multiplying the measured concentration by the volume of receptor solution inside test cell chamber (100 µL) over the time interval. The lag time for dioxane was estimated by extrapolating the linear part of the permeability curve and assigning its intercept on the time axis. This was assigned to confirm that the duration of the permeability experiment was long enough to offer an accurate evaluation of the steady state flux, as the length of the experiment must typically be three times the duration of the lag time (Shah, 1993). Absorption was defined as the total quantity (mg) of dioxane detected in the perfusate (receptor fluid) for the entire 8 hr perfusion period.

Permeability coefficient values (cm/hr) were calculated using the following equation:

$$\boldsymbol{K_p} = J_{ss} / C_d$$

Where (K_p) is the permeability coefficient, J_{ss} is steady state flux (mg/cm^2/h), and C_d (mg /ml) is the concentration in the donor chamber. Diffusivity (cm^2/h) was calculated using the following equation:

$$D = X^2 / 6\tau$$

Where D is the diffusion coefficient, X is skin thickness (500 μm), and τ is the lag time.

Statistical analysis of permeability constant, steady state flux (J_{ss}), diffusion coefficient (K_p), and absorption data were performed using analyses of variance (ANOVAs) to assess the significance of differences in means between groups. The Tukey's Multiple Comparison Method was used to compare the means. All data obtained are presented as mean (± SEM), unless otherwise stated. All statements of significance difference were based on a 95% confidence ($P < 0.05$) level. All analyses were carried out using Minitab for Windows software (version 16.1.1, Minitab Inc., PA, USA - 2010)

Results and Discussion

Dioxane Dermal Permeation Profile

The dermal absorption of dioxane in human skin was determined after application of an aqueous solution of dioxane (50 mg/ml). The transdermal flux of dioxane is plotted versus time in figure 1. The maximum dioxane flux was attained after 4 hours of permeation and continued at a steady level for the duration of the experiment (15 hr).

Plots of the cumulative penetration of dioxane (Figure 2) showed that the lag time was 1.16 ± 0.22 hr. The mean K_p value (± SEM) at room temperature for skin to dioxane was 5.7 X 10^{-4} ± (0.62) cm/hr. The steady state flux (J_{ss}) of dioxane through human SC was 0.286 ± 0.035 mg/cm^2/hr. Diffusivity of dioxane in human SC was 4.8 X 10^{-5} (± 0.32) cm^2/hr. The cumulative amount of dioxane absorbed through human SC over 8 hr was 1.99 ± 0.086 mg.

Although dermal absorption of dioxane has been considered as a possible exposure route in several cases of human fatalities following short-term exposure, data on the absorption of dioxane in humans following dermal exposure are limited and insufficient to create a comprehensive understanding about its behavior in skin. In an *in vitro* a study with excised human skin to investigate the ability of radiolabeled dioxane (^{14}C-1,4-dioxane) to permeate, it was found that there were significant differences in dioxane ability to penetrate the skin under occluded and non-occluded conditions. Where the dioxane penetration was ten times greater under occluded conditions (3.2%) than under unoccluded conditions (0.30%) for 3.5 hr, these differences were attributed to the evaporation of dioxane after application to the skin surface (Bronaugh, 1982b). Therefore, conducting an *in vitro* dermal absorption of dioxane experiment

in occluded conditions controlling the alteration of the compound dose in the donor chamber would offer consistent permeation data.

The results of dermal absorption parameters for dioxane obtained from empirical studies or derived from previous formulae have been varied and inconsistent. The Bronaugh study (Bronaugh, 1982b) showed that the transdermal fluxes of dioxane from water in human skin were very low (0.36 ± 0.03 μg /cm^2/hr). In another study also done with excised human skin, the results showed that the flux was very high (1263.8 ± 448 μg /cm^2/hr) in a 4-hr experiment. In this study the total penetrated amount of dioxane was also very high ranging from 3.629- 4.481 mg/cm^2/4 hr (Dennerlein *et al.*, 2013), whereas the National Industrial Chemicals Notification and Assessment Scheme (NICNAS) used the Potts and Guy formula (Potts & Guy, 1992) to calculate the dioxane flux value to be approximately 0.3 mg/cm^2/hr (NICNAS, 1998). The flux value (0.286 ± 0.035 mg/cm^2/hr) in our study was similar to that calculated by NICNAS. K_p is an empirically measured parameter describing the total barrier property of a membrane. It can be calculated under *in vitro* empirical conditions or estimated from *in vivo* data by fitting suitable variables into pharmacokinetic models. Where data are insufficient, K_p can be evaluated from suitable physical property-permeability relationships (USEPA, 1992). Dioxane K_p of 4.3 x 10^{-4} cm/hr was measured in water for the occluded test system, and this value was classified as intermediate, below the average speed of penetration (Bronaugh, 1982b). This value is close to that estimated for dioxane using the formula of Flynn (Flynn, 1990) or Potts and Guy (Potts & Guy, 1992). The estimated K_p value was 3.4 x 10^{-4} cm/hr according to Flynn's formula (VCCEP, 2007b), while it was 3.0 x 10^{-4} cm/hr according to the equation of Potts and Guy (NICNAS, 1998). The K_p value of the current study (5.7 X 10^{-4} ± 0.62 cm/hr) was within the range of

intermediate (below average) speed penetration, which result was consistent with both previously measured and estimated values.

Lag time is the time taken to attain steady-state conditions under infinite dose conditions. Lag time of dioxane dermal absorption has been reported in only a few studies. Dennerlein and coworkers reported that on excised fresh and frozen stored human skin, the lag time of dioxane ranged between 0.74 and 0.85 hr (Dennerlein *et al.*, 2013), whereas the value of 0.3 hr was predicted by U.S. EPA based on the Potts and Guy formula (USEPA, 1992). The lag time of dioxane dermal absorption in the current study was a little different from that in the Dennerlein *et al.* study. Since the lag time is derived from a curve of the cumulative absorbed amount and time, it is the intercept of the tangent of the linear part of the absorption profile with the x-axis (USEPA, 1992). The linear part of the cumulative absorbed dose in the Dennerlein *et al.* graph was created from 4 points, while the linear part in our graph was created from 64 points. This may explain the tendency of the line to slope and its intercept with x-axis.

Effect of Solvents on Dioxane Dermal Absorption

The effect of solvent systems on the *in vitro* dermal absorption of dioxane across human SC is shown in table 4.1. The flux of dioxane in PG combinations was found to increase up to 50% PG in water. There was no significant increase in flux at 70% PG ($P < 0.05$), and further increases of PG concentration to 100% dioxane flux showed no significant decrease. The flux of dioxane in 10% and 100% PG was not significantly different ($P > 0.05$) from 0% PG (control). Dioxane absorption over the entire 8-hr perfusion in PG combinations showed a significant increase ($P < 0.05$) in 30% and up to 100% PG from the control. The lag time of dioxane in PG

concentrations was found to be not significantly different ($P > 0.05$) from that of the control in 10%, 30%, and 50%, and with further increases of PG to 100%, there was a significant increase ($P < 0.05$) from that of the control in lag time of dioxane (Table 4.1, Group A).

The flux of dioxane in EtOH concentrations presented a significant increase from that of the control and was greatest with 70% ($P < 0.05$). At 100% of EtOH, flux declined, and there was no significant difference between dioxane flux at 30%, 50%, or 100% of EtOH ($P > 0.05$). Dioxane absorption over the entire 8-hr perfusion in EtOH combinations was found to increase significantly ($P < 0.05$) with the EtOH concentration increasing up to 70% and declining at 100% of EtOH. No significant difference was found between EtOH combinations in dioxane lag time (Table 4.1, Group B).

The flux of dioxane in the EA group showed a significant difference ($P < 0.05$) with the control and with flux of EA concentrations at > 30%. Dioxane absorption over the entire 8-hr perfusion in the EA group showed a significant increase at 30% EA concentration and above; there was no significant difference between dioxane flux at 50%, 70%, and 100% of EA ($P > 0.05$). The dioxane lag time of the EA group was found to be different ($P < 0.05$) from the control at 30% EA concentration and higher (Table 4.1, Group C).

Although studies of skin absorption of compounds from water are usually used to assess risk from dermal exposure, chemical mixtures studies of dermal exposure are also important to predict risk in many exposure scenarios, and investigations of the effects of solvents on processes that influence skin absorption can provide appropriate data for risk assessment profiles. Data on the effects of solvents on dioxane dermal absorption are not available. Most organic solvents have been reported in the literature to be a skin penetration enhancer for wide

range of chemicals. In the current study, the results showed that the PG solvent enhanced dioxane permeation across the human SC at a >30% concentration. The mechanism of action of PG in promoting chemical penetration through skin is not clearly understood. Its action has been described in most of the literature as based on PG co-solvency action, where thermodynamic activity is considered as the primary driving force (Barry, 1983), and also on its possible carrier effect (as a carrier-solvent), where PG partitions into the skin and thereafter induce the mobility of the chemical into and through the skin (Hoelgaard & Møllgaard, 1985). Ostrenga and coworkers observed in a study of steroid permeability in human skin that treating skin with 100% PG resulted in losing the elasticity of the skin and attributed this influence to dehydration (Ostrenga *et al.,* 1971). Others studied the effects of PG on dermal permeation using differential thermal analysis. In their findings, they showed that PG treatment decreased the hydration of skin (Bouwstra *et al.*, 1989). The increase in dioxane permeation with an increasing concentration of PG in water may be related to variations in the dehydration of SC at various concentrations of PG. However, the influence of change in the thermodynamic activity as a result of change in the co-solvent concentration cannot be disregarded. The decrease of SC weight after treatment with different concentrations of PG in water up to 15% may support this speculation. Maximum lag time was observed with PG at 70% concentration. This may be related to an increase in the tortuosity of skin by dehydration of SC, which results in increased diffusional path length (Ostrenga *et al.*, 1971).

The effect of EtOH on dermal absorption has been investigated extensively and various mechanisms have been suggested to describe its action on skin. In a human *in vivo* study, Bommannan and coworkers found that EtOH promotes skin permeability by removing measurable quantities of the lipid barrier material from the SC. This lipid extraction may

decrease the skin barrier function resulting in increased membrane permeability, which may explain the influence of EtOH as a dermal penetration enhancer (Bommannan *et al.*, 1991). In another study, the researchers remarked that the permeation enhancement may result not only from lipid extraction but also from skin proteins in the presence of aqueous EtOH (Goates & Knutson, 1994). Accordingly, the mechanism of EtOH as a dermal permeation enhancer was described as a so-called "pull" or "drag" effect in which permeation of chemical molecules is increased due to a reduction in the membrane barrier property of SC by EtOH. Kadir and workers attributed the enhancing effect of EtOH on skin penetration to the increase in thermodynamic activity due to evaporation, which is known as the "push effect" (Kadir *et al.*, 1987). Other studies attribute the effect of EtOH on skin permeation to its ability as a pure solvent or aqueous solution to modify the barrier function of the skin by a number of mechanisms such as lipid extraction and the effects of lipid ordering (Kurihara-Bergstrom *et al.*, 1990, Bommannan *et al.*, 1991, Goates & Knutson, 1994), and also its effect on keratin (Berner *et al.*, 1989a, Kurihara-Bergstrom *et al.*, 1990). The EtOH concentration dependent effect has been reported in many studies, and it has been postulated that, at low concentration of EtOH (less than 33%), it effects only the lipoidal pathway due to increased lipid fluidity especially near the polar interface, whereas higher concentrations effect the lipoidal and polar pathways (Berner *et al.*, 1989a, Ghanem *et al.*, 1992). Results from the current study showed that dioxane flux, $K_{p,}$ and absorption amount were increased at a concentration >30% EtOH ($P < 0.05$). Dioxane has amphiphilic properties, allowing complete miscibility in both water and organic solvents. Its flux with 100% EtOH was found to be less than that of 70% EtOH ($P < 0.05$). This may be attributed to stabilization of the gel phase of the lipid bilayer at 100% of EtOH resulting in rigidization of the lipid bilayer (Rowe, 1983).

Very limited studies have investigated the effect of EA on skin penetration. Its mechanism of action is not clearly understood. In a study of rabbit skin to evaluate the dermal permeation of levonorgestrel with EA and EtOH as transdermal enhancers, the findings showed that the use of the molecule in transdermal patches was associated with irritation and erythema (Friend *et al.*, 1991). Catz and Friend investigated the effect of various co-solvents on EA enhanced percutaneous absorption of levonorgestrel using excised hairless mouse skin finding that the pure EA or a mixture of EA with EtOH increased the dermal steady-state flux and the diffusivity of levonorgestrel relative to the water (Catz & Friend, 1990). The findings of our study showed a significant increase of dioxane dermal permeation with EA in water at a concentration over 30%. The FT-IR spectra of the treated SC with EA showed no change in peak symmetrical or asymmetrical vibration of CH_2. Therefore, explaining the mechanism of EA effect on dioxane dermal permeation is difficult. The lag time was found to increase with an increasing PG concentration, which may be due to skin dehydration that will also increase the tortuosity of skin and thereafter the results for the increased diffusional path length (Ostrenga *et al.*, 1971)

In the FT-IR studies on SC, it was found that there was no significant effect of EA and PG on the symmetrical or asymmetrical vibration of the CH_2 peak shift or broadening near 2850 and 2920 cm^{-1} at the concentrations studied and also of the CH_3 peak around 2960 cm^{-1} (Figures 3 and 4). The FT-IR spectra of SC in the EtOH group revealed that there was boarding of peaks near 2920cm^{-1} with increasing EtOH concentrations (Figure 5). The treatment of SC with water and solvents for 24 hr showed that there was no significant change in mass after treatment with water, but there was an increasing loss of SC mass after treatment with 50% and 100% of solvent (Figure 6). Lipid extract precipitates were detected only from SC treated with solvent EtOH. The

FT-IR spectra of the extract precipitates revealed that they were mostly composed of the SC lipid part (Figure 7).

The biophysical changes in the lipid bilayer of SC after treatment with solvents can be investigated with FT-IR spectroscopy. The SC has low water content and its lipids are ordered into bilayers. The lipid bilayers exist either in a gel state (ordered) or a fluidized state. FT-IR spectra of lipid bilayers demonstrate typical IR absorbance patterns in the 3000–2800 cm^{-1} region that are associated with H–C–H vibrational modes (Parker, 1983). Alteration of the lipid bilayer structures results in changes of the absorption spectra of IR that are passed through or reflected off the SC (Moore *et al.*, 1997). Of particular interest in this context are the IR absorbance regions around 2850 and 2920 cm^{-1} relevant to symmetric and asymmetric methylene groups H-C-H stretching successively (Potts & Francoeur, 1993). CH_2 symmetric and asymmetric stretching bands are sensitive to lipid alkyl chain conformation in addition to torsional and librational mobility reflecting the changes in the trans to gauche ratio in acyl chains (Mautone *et al.*, 1987). Shifts to a higher wave number of peaks around 2854 cm^{-1} and 2925 cm^{-1} point out a reduced order in a lipid membrane due to deviations in the mobility of lipid acyl chains (Vaddi *et al.*, 2002). On the other hand, increased broadening of peaks at 2850 and 2920 Cm^{-1} is an indication of increased translational movement or mobility of lipid acyl chains (Naik & Guy, 1997). Wide variability between SC samples was observed in the current study, and this is due to inconsistency in SC thickness and variability in lipid combination. But the pattern of solvent-caused changes was symmetric when single samples were matched before and after treatment. In the FT-IR spectra of SC treated with EtOH, it was found that there was broadening of peaks at 2920 cm^{-1} region with increasing concentration of EtOH. This indicates that EtOH reduces the lipid order due to increasing rotational freedom of lipid acyl chains leading to an

increase in the fluidity of the lipid bilayer. And this may be explained by lipid extraction with EtOH treatment, where lipid extraction results in altered IR absorbance due to C–H_2 groups in the 3000–2800 cm^{-1} region. Lipid extraction could also change the lipid composition and solvation properties of the SC lipids.

Effect of SLS on Dioxane Dermal Absorption

The permeation parameters of various SLS concentrations on the *in vitro* skin absorption of dioxane in human SC are shown in Table 4.2. The flux of dioxane was found to increase with the concentration increasing up to 5% SLS in water. There was no significant increase in flux at 7% SLS ($P < 0.05$), and with further increases of SLS concentration to 10% dioxane, the flux showed no significant decrease. In SLS combinations, dioxane absorption over the entire 8-hr perfusion, K_p and diffusivity showed a significant increase ($P < 0.05$) in 1% and up to 10% SLS from the control. The lag time of dioxane in SLS concentrations was found to be not significantly different ($P > 0.05$) from control. Figure 4.8 shows the permeation profiles of dioxane in the presence of various concentrations of SLS through human SC.

Dioxane is produced as a by-product during the sulfonation reaction with alcohol ethoxylates, a process used to produce surfactants in a wide range of soaps and detergents. Therefore, dioxane may be formed as a by-product of reactions based on condensing ethylene oxide or ethylene glycol during the production of ethoxylated SLS from SLS to reduce its abrasiveness and enhance its foaming properties. Ethoxylated SLS is a component of anionic surfactant in detergents, shampoos, toothpastes, bath gels, bubble baths, and industrial degreasants (Mohr *et al.*, 2010). It is likely that there is human skin exposure to dioxane with surfactants such as ethoxylated SLS whenever consumers use products like shampoo, detergents,

soaps, dishwashing liquids, and other cosmetic products. Therefore, mixture-studies of dioxane with surfactants are of interest in the field of risk assessment because they provide reliable data relating to common dermal exposure scenarios.

It is well known that anionic surfactants such as SLS or ethoxylated SLS have effects on the permeability characteristics of many biological membranes, including skin (Florence *et al.*, 1994, Lopez *et al.*, 2000). It has been reported that SLS can penetrate the skin and interact strongly resulting in large changes in its barrier properties (Walters, 1989, Lee *et al.*, 1994) including both the keratin and lipid components (Reiger & Rhein, 1997). SLS interaction with keratin occurs between the anionic head groups and the cationic sites of the proteins, which induces strong hydrophobic interactions between SLS molecules and the protein that may result in protein denaturation (Somasundaran & Hubbard, 2006). Out of skin, SLS can promote the dissolution of the proteins leading to release of sulfhydryl groups from the sclera proteins and then react upon various enzymes of skin and eventually denature the skin (Gloxhuber & Kunstler, 1992). SLS has also an ability to cause variations in the structural organization of lipid bilayers when it is used above the critical micellar concentration (Ribaud *et al.*, 1994). It has been found that SLS increases penetration into the skin by increasing the fluidity of epidermal lipids (Somasundaran & Hubbard, 2006). The effect of SLS on the dermal permeation has been found to depend on the lipophilicity of the compound. Nielsen studied the effect of SLS on *in vitro* dermal permeation of a number of pesticides varying in lipophilicity across skin that was treated with two concentrations of SLS (0.1% and 0.3%) for three hr. The findings of this study indicated that the dermal permeation of more hydrophilic penetrants was effected more. The lipophilic compounds with log $K_{o/w} > 3$ exhibited a slight increase in their permeation through the SLS pretreated skin, while for less lipophilic compounds (log $K_{o/w}$ of 0.7 and 1.7), the

permeation increased twofold (Nielsen, 2005). This study's findings were in agreement with a previous study conducted by Borras-Blasco and coworkers in 1997. It is noteworthy that the Borras-Blasco *et al.* study investigated the effect of SLS on *in vitro* dermal absorption across rat skin of a number of compounds with lipophilicity values ranging from log $K_{o/w}$ = -0.95 to 4.42. They reported that the SLS surfactant was able to enhance the permeation rates of compounds that possess lipophilicity values less than the optimum lipophilicity value (log $K_{o/w} < 3$), but do not affect compounds with log $K_{o/w} > 3$ (Borrás-Blasco *et al.*, 1997). Dioxane has a log $K_{o/w}$ value of about -0.27, and the effect of SLS observed in the current study was similar to that reported for other hydrophilic compounds in other studies (Borrás-Blasco *et al.*, 1997, Nokhodchi *et al.*, 2003, Nielsen, 2005, Jakasa *et al.*, 2006). This may be explained by fact that for compounds with a lipophilicity value less than log $K_{o/w} = 3$ like dioxane, the compound may be controlled by diffusion through the lipid bilayers, which is rate controlling. When SLS disorders the lipid bilayers, the diffusion coefficient increases, and consequently the flux increases, as was observed in our study. The enhancing effect of SLS on dioxane dermal permeation may also be attributed to other mechanisms, where SLS could involve the hydrophobic interaction of the SLS alkyl chain with the skin structure that leaves the end sulphate group of SLS exposed, forming more sites in the skin, which permits an increase in dermal hydration (Gibson & Teall, 1983, Rhein *et al.*, 1986).

Conclusion

This study investigated the dermal absorption profile of dioxane in human skin and demonstrated the effect of solvents and surfactants on processes that control the rate of skin permeation. The investigation of dermal absorption post exposure to dioxane as a single penetrant or in chemical mixtures provides appropriate data for risk assessment profiles and helps to predict risk in many exposure scenarios. These dermal absorption studies demonstrated that:

- The dermal absorption of aqueous mixtures of dioxane *in vitro* in human skin is significantly greater than previously reported (Bronaugh, 1982b), and that its transport can be affected by the composition of the mixture components.
- The presence of a surfactant like SLS in chemical mixtures enhances the dermal absorption of dioxane.
- The presence of solvents in chemical mixtures can increase the dermal absorption of dioxane at a concentration > 30% in water. EtOH was found to have the greatest ability to increase the dermal permeation of dioxane in comparison to that of PG and EA.
- EtOH can extract lipids from SC and alter its properties, which may influence rates of penetration through the skin.

Table 4.1: Dioxane skin permeation parameters in presence of various solvents concentrations in water (% v/v)

Solvent conc. in water	Lag time (hr)	Flux ($mg/cm^2/hr$)	Absorption (mg)	Permeability (cm/hr)	Diffusivity (Cm^2/hr)
Group A					
EtOH 0%	1.16 ± 0.22 [a]	0.286 ± 0.035[a]	1.99 ± 0.086 [a]	5.7 X 10^{-4} ± (0.62)	4.3 X 10^{-5} ± (0.71)
EtOH 10%	1.15 ± 0.25 [a]	0.374 ± 0.048[b]	2.45 ± 0.192 [b]	7.5 X 10^{-4} ± (0.83)	4.8 X 10^{-5} ± (0.83)
EtOH 30%	1.05 ± 0.28 [a]	0.533± 0.069[c]	2.72 ± 0.218 [c]	10.6 X 10^{-4} ± (0.89)	4.4 X 10^{-5} ± (0.66)
EtOH 50%	0.92 ± 0.21 [a]	0.756 ± 0.112[c]	3.78 ± 0.256 [d]	15.1 X 10^{-4} ± (1.22)	3.8 X 10^{-5} ± (0.65)
EtOH 70%	0.79 ± 0.19 [a]	0.992 ± 0.101[d]	4.52 ± 0.133[e]	19.8 X 10^{-4} ± (1.69)	3.3 X 10^{-5} ± (0.48)
EtOH 100%	1.18 ± 0.33 [a]	0.781 ± 0.181[c]	4.06 ± 0.111 [d]	15.6 X 10^{-4} ± (1.56)	4.9 X 10^{-5} ± (0.91)
Group B					
PG 0%	1.16 ± 0.22 [a]	0.286 ± 0.035 [a]	1.99 ± 0.086 [a]	5.7 X 10^{-4} ± (0.62)	4.3 X 10^{-5} ± (0.71)
PG 10%	1.22 ± 0.38 [a]	0.211 ± 0.076 [a]	2.16 ± 0.161 [a]	4.2 X 10^{-4} ± (0.71)	5.1 X 10^{-5} ± (1.13)
PG 30%	1.35 ± 0.44 [ab]	0.385 ± 0.042[b]	2.59 ± 0.203 [b]	7.7 X 10^{-4} ± (0.44)	5.6 X 10^{-5} ± (0.95)
PG 50%	1.71 ± 0.38 [ab]	0.478 ± 0.059 [c]	2.92 ± 0.289 [b]	9.6 X 10^{-4} ± (0.92)	7.1 X 10^{-5} ± (0.88)
PG 70%	2.06 ± 0.47[b]	0.493± 0.039[c]	3.31 ± 0.153 [c]	9.8 X 10^{-4} ± (1.13)	8.6 X 10^{-5} ± (1.52)
PG 100%	1.93 ± 0.51[b]	0.396± 0.042[b]	2.85 ± 0.181 [b]	7.9 X 10^{-4} ± (0.36)	8.0 X 10^{-5} ± (1.18)
Group C					
EA 0%	1.16 ± 0.22 [a]	0.286 ± 0.035 [a]	1.99 ± 0.086[a]	5.7 X 10^{-4} ± (0.62)	4.3 X 10^{-5} ± (0.71)
EA 10%	1.52 ± 0.36 [ab]	0.312 ± 0.039 [a]	1.88 ± 0.093[a]	6.2 X 10^{-4} ± (0.49)	6.3 X 10^{-5} ± (1.32)
EA 30%	1.69 ± 0.18[b]	0.393± 0.061 [b]	2.26 ± 0.131[b]	7.9X 10^{-4} ± (0.73)	7.0 X 10^{-5} ± (0.56)
EA 50%	2.62 ± 0.43[c]	0.431 ± 0.076 [b]	2.67 ± 0.109[c]	8.6 X 10^{-4} ± (1.51)	10.9 X 10^{-5} ± (0.87)
EA 70%	2.56 ± 0.52[c]	0.422 ± 0.089 [b]	2.79 ± 0.239[c]	8.4 X 10^{-4} ± (1.38)	10.7 X 10^{-5} ± (0.32)
EA 100%	2.18 ± 0.61[c]	0.416 ± 0.095 [b]	2.65 ± 0.211[c]	8.3 X 10^{-4} ± (1.21)	9.1 X 10^{-5} ± (1.18)

Within column different superscript letters are statistically significant $P < 0.05$. (n =5)

Table 4.2: Dioxane skin permeation parameters in presence of various sodium lauryl sulphate concentrations in water (% w/w)

SLS conc.	Lag time (hr)	Flux (mg/cm^2/hr)	Absorption (mg)	Permeability (cm/hr)	Diffusivity (Cm^2/hr)
0%	1.16 ± 0.22^a	0.286 ± 0.035^a	1.99 ± 0.086^a	5.7 X 10^{-4} ± (0.62)	4.3 X 10^{-5} ± (0.71)
1%	1.37 ± 0.33^a	0.393 ± 0.048^b	2.85 ± 0.182^b	7.8 X 10^{-4} ± (0.75)	5.7 X 10^{-5} ± (0.82)
2%	1.55 ± 0.38^a	0.426 ± 0.029^b	3.34 ± 0.121^c	8.5 X 10^{-4} ± (0.49)	6.4 X 10^{-5} ± (0.94)
5%	1.34 ± 0.25^a	0.619 ± 0.041^c	3.95 ± 0.132^d	12.4 X 10^{-4} ± (0.81)	5.5 X 10^{-5} ± (0.93)
7%	1.51 ± 0.41^a	0.551 ± 0.065^c	3.82 ± 0.119^d	11.0 X 10^{-4} ± (0.74)	6.2 X 10^{-5} ± (1.28)
10%	1.42 ± 0.53^a	0.533 ± 0.052^c	3.12 ± 0.108^c	10.7 X 10^{-4} ± (0.59)	5.9 X 10^{-5} ± (0.89)

Within column different superscript letters are statistically significant P < 0.05. (n =5)

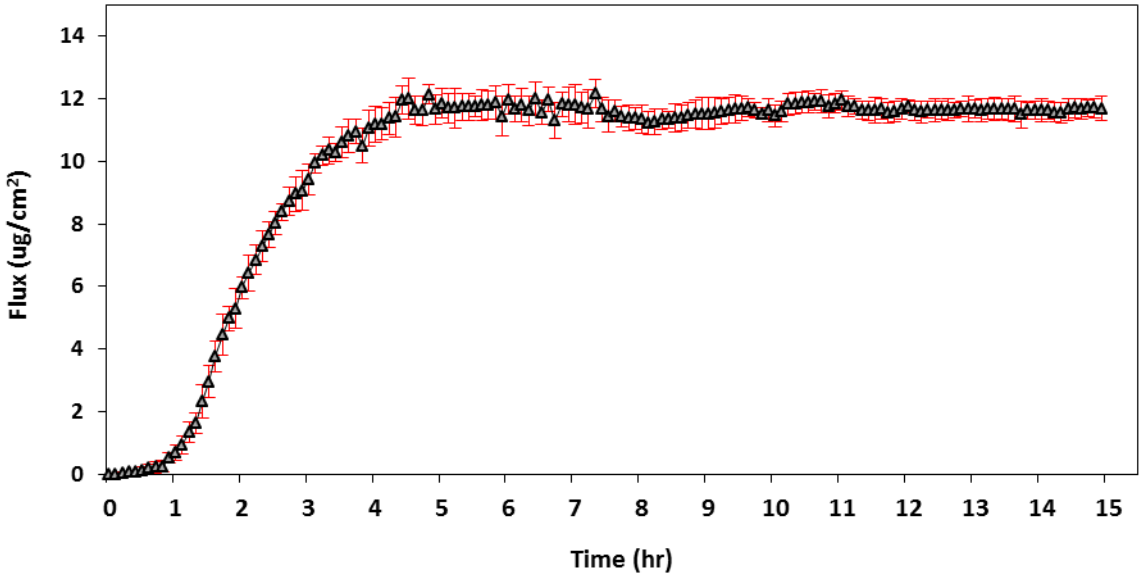

Figure 4.1: Flux of dioxane across human stratum corneum (n =5)

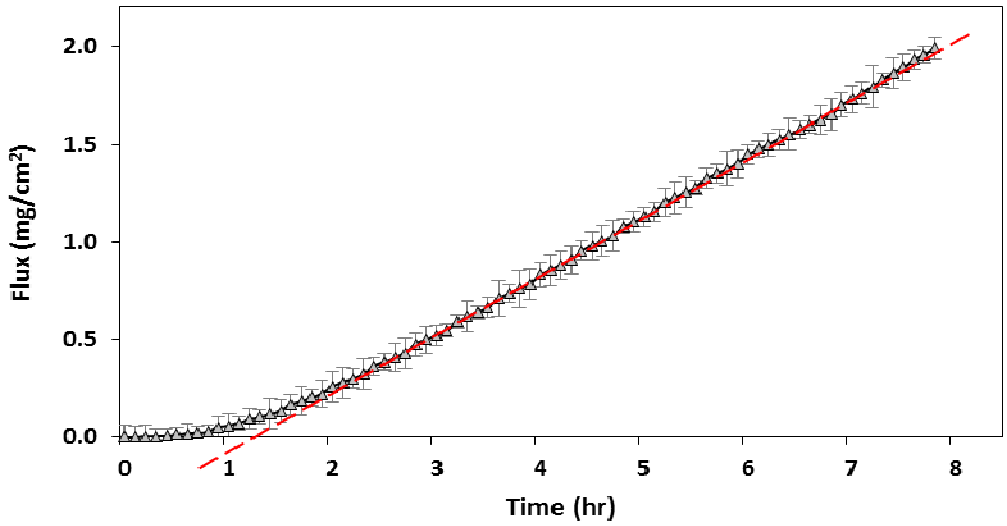

Figure 4.2: Cumulative absorption versus time plot for dioxane following topical application to human stratum cornem in *in vitro* flow-through diffusion cells. The best- fitted straight line was used to calculate the steady state flux (n =5)

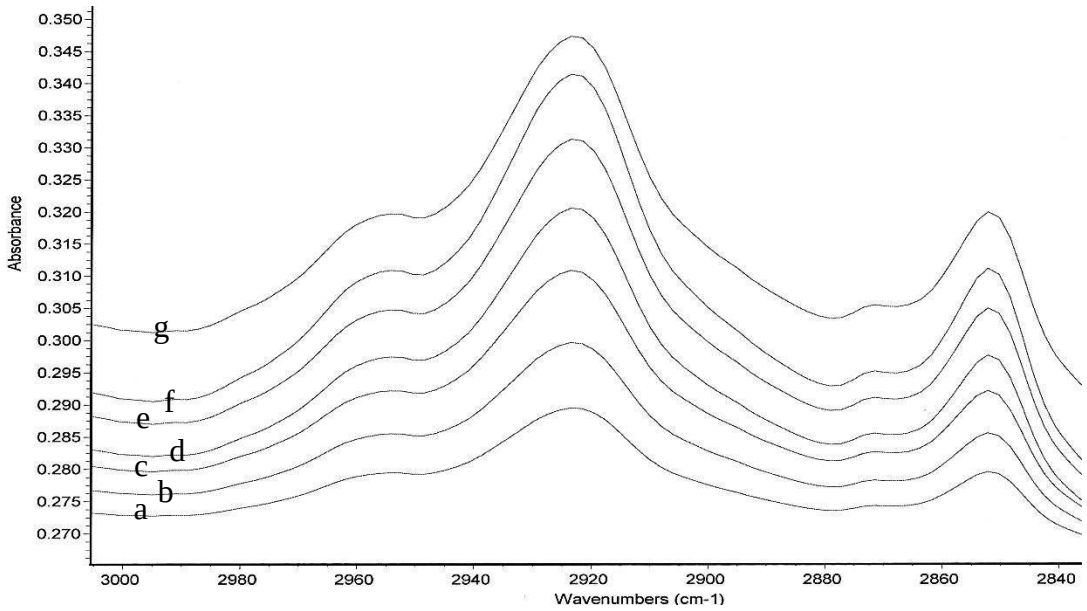

Figure 4.3: FT-IR absorbance spectra of human stratum corneum before (a) and after 12 hr exposure to water (b) 10% Propylene glycol (c) 30% Propylene glycol (d) 50% Propylene glycol (e) 70% Propylene glycol (f) 100% Propylene glycol (g)

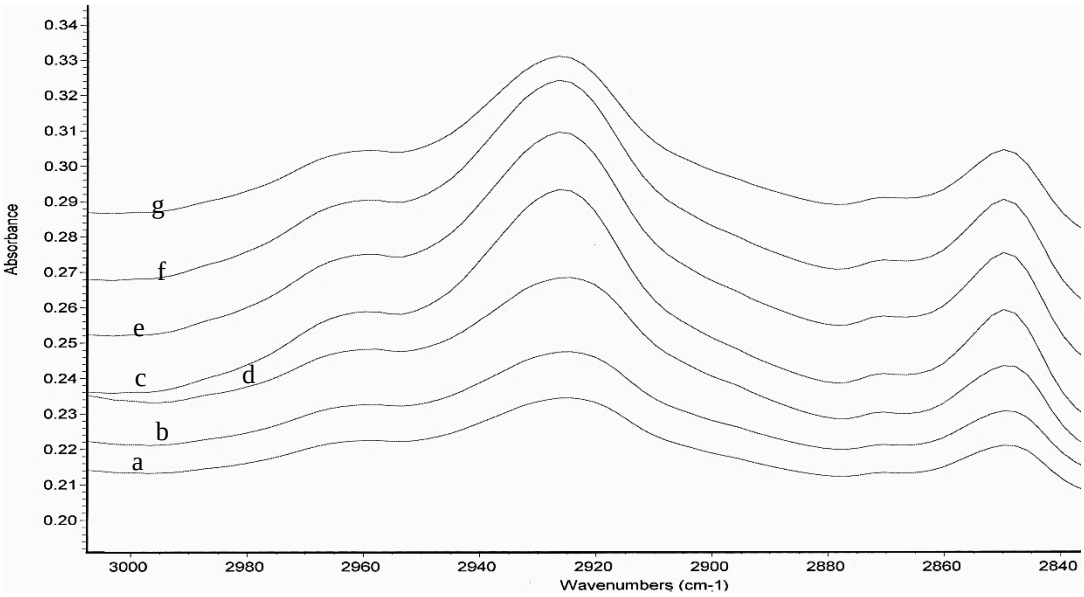

Figure 4.4: FT-IR absorbance spectra of human stratum corneum before (a) and after 12 hr exposure to water (b) 10% ethyl acetate (c) 30% ethyl acetate (d) 50% ethyl acetate (e) 70% ethyl acetate (f) 100% ethyl acetate (g)

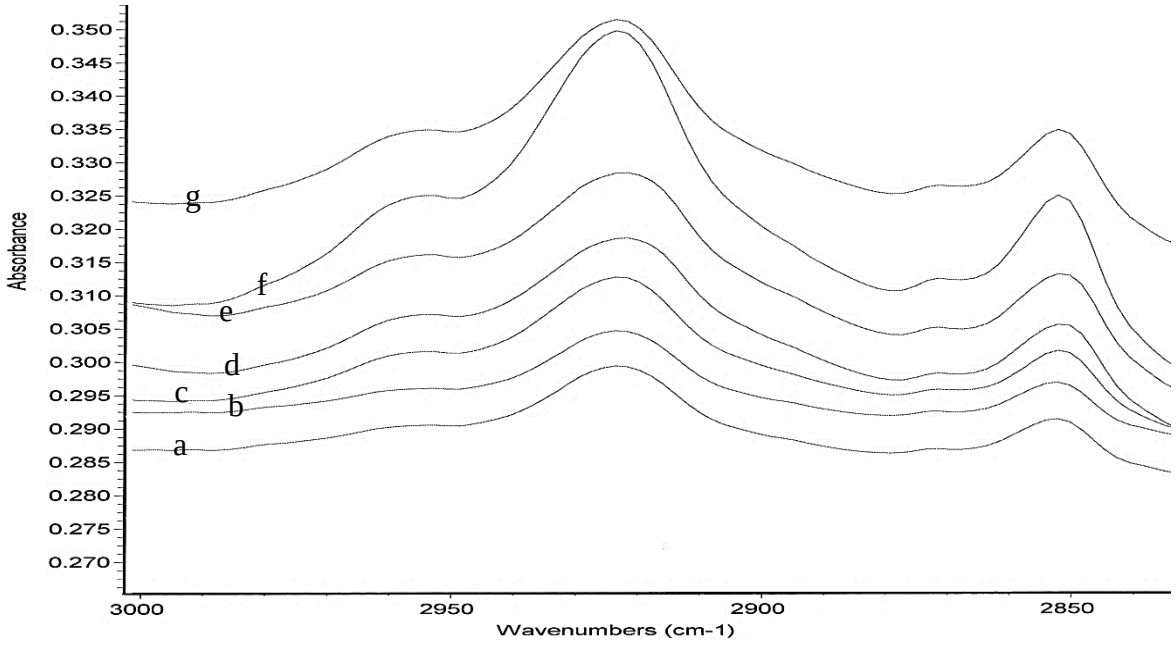

Figure 4.5: FT-IR absorbance spectra of human stratum corneum before (a) and after 12 hr exposure to water (b) 10% ethanol (c) 30% ethanol (d) 50% ethanol (e) 70% ethanol(f) 100% ethanol (g)

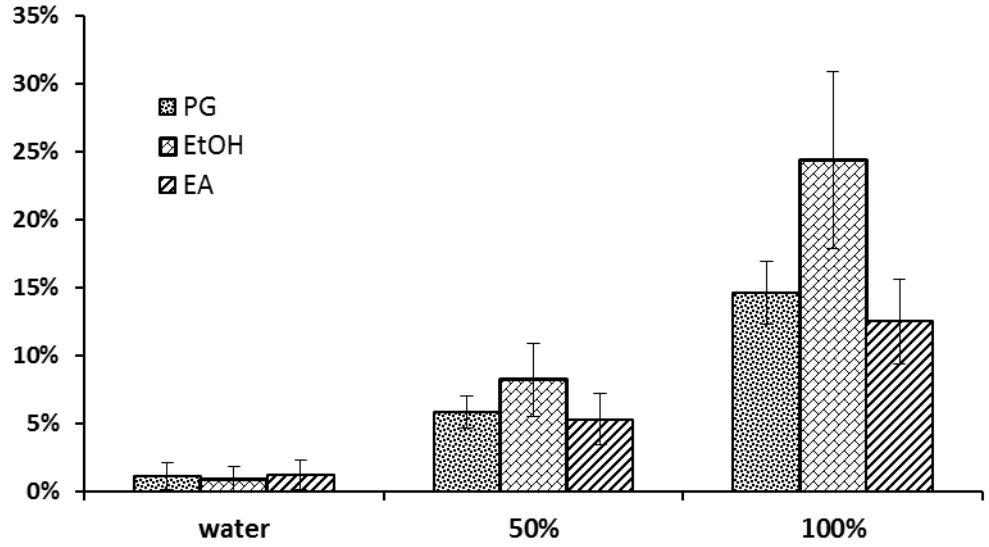

Figure 4.6: Percentage stratum corneum weight loss after 24 hr extraction using water, 50%, and 100 % solvents (n =5)

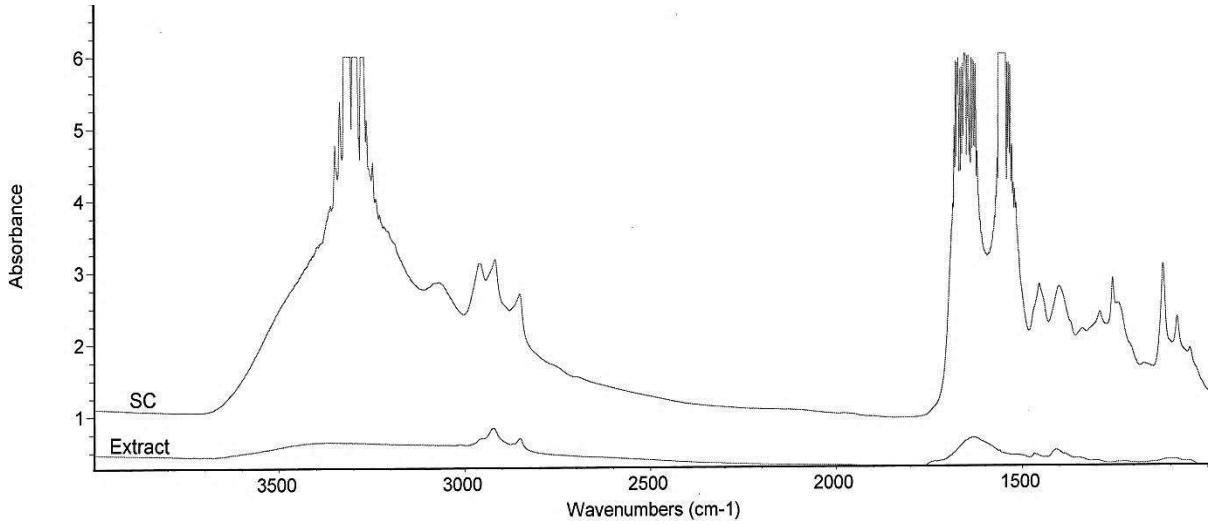

Figure 4.7: FT-IR absorbance spectra of typical stratum corneum and the precipitate from ethanol extract of stratum corneum. The peaks between 2800 cm^{-1} and 3000 cm^{-1} are due to IR absorbance at H-C-H bonds

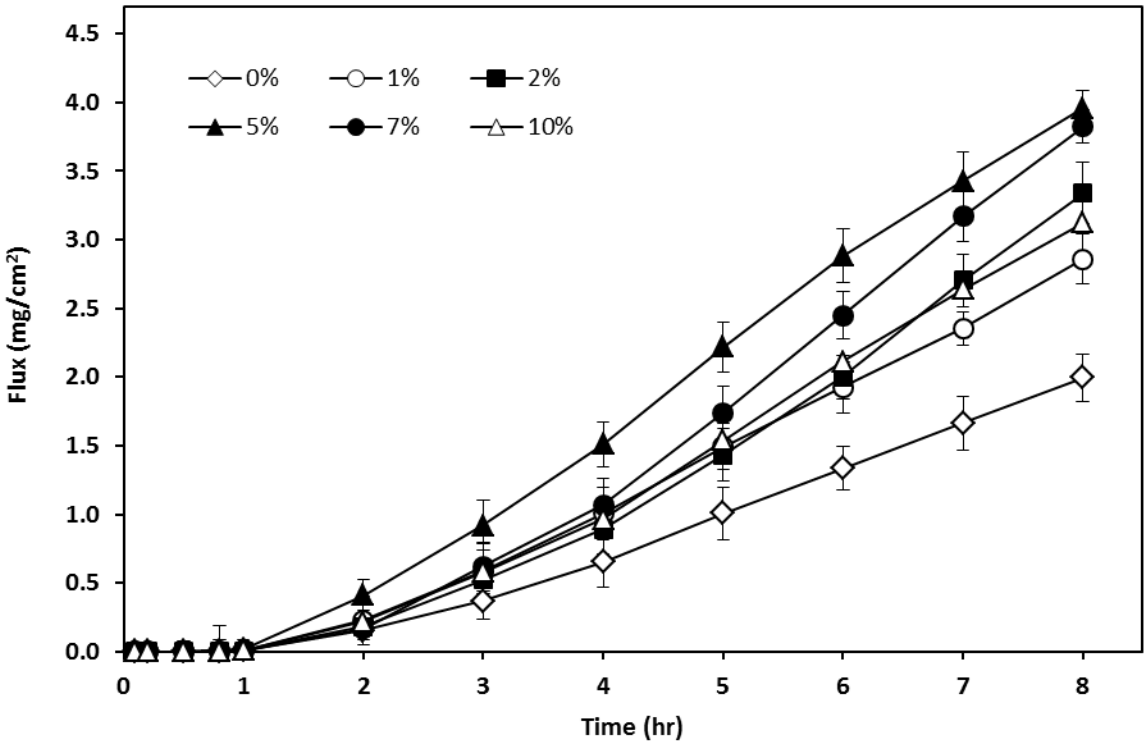

Figure 4.8: The effect of sodium lauryl sulphate concentrations on the *in vitro* cumulative permeation of dioxane through human stratum corneum (n =5)

References

ASTDR, 2012: Toxicological Profile for 1,4-Dioxane. U.S. Department of Health and Human Services Public Health Service, Agency for Toxic Substances and Disease Registry., http://www.atsdr.cdc.gov/toxprofiles/tp187.pdf.

Aungst, B. J., N. J. Rogers and E. Shefter, 1986: Enhancement of naloxon penetration through human skin *in vitro* using fatty acids, fatty alcohols, surfactants, sulfoxides and amides. J. Pharm, 33, 225-234.

Barrett, C. W., J. W. Hadgraft, G. A. Caron and I. Sarkany, 1965: The effect of particle size and vehicle on the percutaneous absorption of fluocinolone acetonide. The British journal of dermatology, 77, 576-578.

Barry, B. W., 1983: Properties that influence percutaneous absorprtion. In: Barry, B.W. (Ed.), Dermatological Formu lations. Marcel Dekker, New York pp. 127-233.

Baynes, R. E., J. D. Brooks, M. Mumtaz and J. E. Riviere, 2002: Effect of chemical interactions in pentachlorophenol mixtures on skin and membrane transport. Toxicological sciences : an official journal of the Society of Toxicology, 69, 295-305.

Berner, B., R. H. Juang and G. C. Mazzenga, 1989a: Ethanol and water sorption into stratum corneum and model systems. Journal of pharmaceutical sciences, 78, 472-476.

Berner, B., G. C. Mazzenga, J. H. Otte, R. J. Steffens, R. H. Juang and C. D. Ebert, 1989b: Ethanol: water mutually enhanced transdermal therapeutic system II: skin permeation of ethanol and nitroglycerin. Journal of pharmaceutical sciences, 78, 402-407.

Black, J. G., 1993: Interactions between anaionic surfactants and skin. in Pharmaceutical Skin Pentration Enhancement (K. A. Walter and J. Hadgraf Eds). Marcel Dekker, New York. pp. 145-173.

Bommannan, D., R. O. Potts and R. H. Guy, 1991: Examination of the effect of ethanol on human stratum corneum in vivo using infrared spectroscopy. Journal of Controlled Release, 16, 299-304.

Borrás-Blasco, J., A. López, M. J. Morant, O. Díez-Sales and M. Herráez-Domínguez, 1997: Influence of sodium lauryl sulphate on the *in vitro* percutaneous absorption of compounds with different lipophilicity. European Journal of Pharmaceutical Sciences, 5, 15-22.

Bouwstra, J. A., L. J. C. Peschier, J. Brussee and H. E. Boddé, 1989: Effect of N-alkylazocycloheptan-2-ones including azone on the thermal behaviour of human stratum corneum. Int. J. Pharm, 52, 47–54.

Bronaugh, R. L., 1982: Percutaneous absorption of cosmetic ingredients. Principles of Cosmetics for the Dermatologist 1982 Edited by P Frost, SN Horwitz. St. Louis, CV Mosby. pp. 277–284.

Bronaugh, R. L. and H. I. Maibach, 1999: Percutaneous Absorption: Drugs--Cosmetics--Mechanisms--Methodology: Drugs--Cosmetics--Mechanisms--Methodology, Third Edition. Taylor & Francis.

Catz, P. and D. R. Friend, 1990: Effect of cosolvents on ethyl acetate enhanced percutaneous absorption of levonorgestrel. Journal of Controlled Release, 12, 171-180.

Chowhan, Z. T. and R. Pritchard, 1978: Effect of surfactants on percutaneous absorption of naproxen I: comparisons of rabbit, rat, and human excised skin. Journal of pharmaceutical sciences, 67, 1272-1274.

CPSC, 2014: Consumer Product Safety Commission. http://www.cpsc.gov (accessed 04.12.2014).

Dennerlein, K., D. Schneider, T. Goen, K. H. Schaller, H. Drexler and G. Korinth, 2013: Studies on percutaneous penetration of chemicals - Impact of storage conditions for excised human skin. Toxicology *in vitro* : an international journal published in association with BIBRA, 27, 708-713.

EWG, 2007: Environmental Working Group. EWG research shows 22 percent of all cosmetics may be contaminated with cancer-causing impurity . http://www.ewg.org/news/news-releases/2007/02/08/ewg-research-shows-22-percent-all-cosmetics-may-be-contaminated-cancer ((accessed 04.12.2014).

Fairley, A., E. C. Linton and A. H. Ford-Moore, 1934: The toxicity to animals of 1,4-dioxane. The Journal of Hygiene, 34, 486-501.

Faucher , J. A. and E. D. Goddard, 1978: Interaction of keratinous substrates with sodium lauryl sulfate: I. sorption. J. Soc. Cosmet. Chem., 29, 323-337.

Florence, T., I. G. Tuker and K. A. Walters, 1994: Interaction of non-ionic alkeyl and aryl ethers with membranes and other biological systems. In: Rosen, M.J. (Ed.), Structure Performance Relationships in Surfactants, ACS Symposium Series, 253, pp. 189–207.

Flynn, G. L., 1990: Physicochemical determinants of skin absorption. IN: Garrity, TR, Henry, CJ (Eds) Principles of route-to route extrapolation for risk assessment. Elsevier, New York, pp 93-127.

Friend, D. R., 1991: Transdermal delivery of levonorgestrel. Medicinal research reviews, 11, 49-80.

Friend, D. R., S. J. Phillips and J. R. Hill, 1991: Cutaneous effects of transdermal levonorgestrel. Food and chemical toxicology : an international journal published for the British Industrial Biological Research Association, 29, 639-646.

Ghanem, A.-H., H. Mahmoud, W. I. Higuchi, P. Liu and W. R. Good, 1992: The effects of ethanol on the transport of lipophilic and polar permeants across hairless mouse skin: Methods/validation of a novel approach. International Journal of Pharmaceutics, 78, 137-156.

Gibson, W. T. and M. R. Teall, 1983: Interactions of C12 surfactants with the skin: changes in enzymes and visible and histological features of rat skin treated with sodium lauryl sulphate. Food and chemical toxicology : an international journal published for the British Industrial Biological Research Association, 21, 587-594.

Gingell, R., R. J. Boatman, J. S. Bus, T. J. Cawley, J. B. Knack, W. J. Krasavage, H. P. Skoulis, C. R. Stack and T. R. Tyler, 1994: Glycol ethers and other selected glycol derivatives. In: Clayton, G.D. & Clayton, F.E., eds., Patty's Industrial Hygiene and Toxicology, 4th ed., Vol. IID, New York, John Wiley & Sons, Inc. . pp. 2816- 2818.

Gloxhuber, C. and K. Kunstler, 1992: Anionic surfactants: Biochemistry, toxicology, dermatology. Surfactant science series. 2nd ed. New York:Marcel Dekker.

Goates, C. Y. and K. Knutson, 1994: Enhanced permeation of polar compounds through human epidermis. I. Permeability and membrane structural changes in the presence of short chain alcohols. Biochimica et biophysica acta, 1195, 169-179.

Hoelgaard, A. and B. Møllgaard, 1985: Dermal drug delivery — Improvement by choice of vehicle or drug derivative. Journal of Controlled Release, 2, 111-120.

IARC, 1999: International Agency for Research on Cancer ; 1,4-Dioxane. In: IARC Monographs on the Evaluation of Carcinogenic Risks to Humans, Vol. 71,Re-evaluation of some organic chemicals, hydrazine and hydrogen peroxide. International Agency for Research on Cancer, Lyon, France 71 part 2 589-602.

Jakasa, I., M. M. Verberk, A. L. Bunge, J. Kruse and S. Kezic, 2006: Increased permeability for polyethylene glycols through skin compromised by sodium lauryl sulphate. Experimental dermatology, 15, 801-807.

Johnstone, R. T., 1959: Death due to dioxane? A.M.A. archives of industrial health, 20, 445-447.

Kadir, R., D. Stempler, Z. Liron and S. Cohen, 1987: Delivery of theophylline into excised human skin from alkanoic acid solutions: a "push-pull" mechanism. Journal of pharmaceutical sciences, 76, 774-779.

KAI, T., V. H. W. MAK, P. R. O. and R. H. GUY, 1990: Mechanism of percutaneous penetration enhancement: effect of n-alkanols on the permeability barrier of hairless mouse skin. Journal of Controlled Release, 12, 103-112.

Kano, H., Y. Umeda, T. Kasai, T. Sasaki, M. Matsumoto, K. Yamazaki, K. Nagano, H. Arito and S. Fukushima, 2009: Carcinogenicity studies of 1,4-dioxane administered in drinking-water to rats and mice for 2 years. Food and chemical toxicology : an international

journal published for the British Industrial Biological Research Association, 47, 2776-2784.

Kurihara-Bergstrom, T., K. Knutson, L. J. DeNoble and C. Y. Goates, 1990: Percutaneous absorption enhancement of an ionic molecule by ethanol-water systems in human skin. Pharmaceutical research, 7, 762-766.

Lee, C. K., T. Uchida, K. Kitagawa, A. Yagi, N. S. Kim and S. Goto, 1994: Skin permeability of various drugs with different lipophilicity. Journal of pharmaceutical sciences, 83, 562-565.

Levang, A. K., K. Zhao and J. Singh, 1999: Effect of ethanol/propylene glycol on the *in vitro* percutaneous absorption of aspirin, biophysical changes and macroscopic barrier properties of the skin. Int J Pharm, 181, 255-263.

Liu, P., T. Kurihara-Bergstrom and W. R. Good, 1991: Cotransport of estradiol and ethanol through human skin *in vitro*: understanding the permeant/enhancer flux relationship. Pharmaceutical research, 8, 938-944.

Lopez, A., F. Llinares, C. Cortell and M. Herraez, 2000: Comparative enhancer effects of Span20 with Tween20 and Azone on the *in vitro* percutaneous penetration of compounds with different lipophilicities. Int J Pharm, 202, 133-140.

Mautone, A. J., K. E. Reilly and R. Mendelsohn, 1987: Fourier transform infrared and differential scanning calorimetric studies of a surface-active material from rabbit lung. Biochimica et biophysica acta, 896, 1-10.

Megrab, N. A., A. C. Williams and B. W. Barry, 1995: Oestradiol permeation across human skin, silastic and snake skin membranes: The effects of ethanol/water co-solvent systems. Int. J. Pharm., 116, 101-112.

Modamio, P., C. F. Lastra and E. L. Marino, 2000: A comparative *in vitro* study of percutaneous penetration of beta-blockers in human skin. Int J Pharm, 194, 249-259.

Mohr, T. K. G., W. H. DiGuiseppi and J. A. Stickney, 2010: Environmental Investigation and Remediation: 1,4-Dioxane and other Solvent Stabilizers. Book News, Inc., Portland - United States, 34.

Moore, D. J., M. E. Rerek and R. Mendelsohn, 1997: Lipid domains and orthorhombic phases in model stratum corneum: evidence from Fourier transform infrared spectroscopy studies. Biochemical and biophysical research communications, 231, 797-801.

Naik, A. and R. H. Guy, 1997: Infrared spectroscopic and differen tial scanning calorimetric investigations of the stratum corneum barrier function. In: Potts, R.O., Guy, R.H. (Eds.), Mechanisms of Transdermal Drug Delivery.Marcel Dekker, New York pp. 87-162.

NICNAS, 1998: National Industrial Chemicals Notification and Assessment Scheme;1,4-Dioxane Priority Existing Chemical No. 7, Full Public Report,. Commonwealth of Australia, ISBN 0 642 47104 5.

Nicolazzo, J. A., T. M. Morgan, B. L. Reed and B. C. Finnin, 2005: Synergistic enhancement of testosterone transdermal delivery. Journal of controlled release : official journal of the Controlled Release Society, 103, 577-585.

Nielsen, J. B., 2005: Percutaneous penetration through slightly damaged skin. Archives of dermatological research, 296, 560-567.

NIOSH, 1984: National Occupational Exposure Survey (1981-83). Cincinnati, OH: U. S. Department of Health and Human Services. http://www.cdc.gov/noes/noes3/empl0003.html.

Nokhodchi, A., J. Shokri, A. Dashbolaghi, D. Hassan-Zadeh, T. Ghafourian and M. Barzegar-Jalali, 2003: The enhancement effect of surfactants on the penetration of lorazepam through rat skin. Int J Pharm, 250, 359-369.

Ostrenga, J., C. Steinmetz, B. Poulsen and S. Yett, 1971: Significance of vehicle composition. II. Prediction of optimal vehicle composition. Journal of pharmaceutical sciences, 60, 1180-1183.

Panchagnula, R., P. S. Salve, N. S. Thomas, A. K. Jain and P. Ramarao, 2001: Transdermal delivery of naloxone: effect of water, propylene glycol, ethanol and their binary combinations on permeation through rat skin. Int J Pharm, 219, 95-105.

Parker, F. S., 1983: Applications of Infrared, Raman and Resonance Raman Spectroscopy in Biochemistry. Plenum, New York.

Poet, T. S. and J. N. McDougal, 2002: Skin absorption and human risk assessment. Chemico-biological interactions, 140, 19-34.

Potts, R. O. and M. L. Francoeur, 1993: Infrared spectroscopy of stratum corneum lipids: *in vitro* results and their relevance to permeability. In: Walters, K.A., Hadgraft, J. (Eds.), Pharmaceutical Skin Permeation Enhancement. Marcel Dekker, New York. pp. 269-291.

Potts, R. O. and R. H. Guy, 1992: Predicting skin permeability. Pharmaceutical research, 9, 663-669.

Rastogi, S. C., 1990: Headspace analysis of 1,4-dioxane in products containing polyethoxylated surfactants by GC-MS. Chromatographia, 29, 441-445.

Raykar, P. V., M. C. Fung and B. D. Anderson, 1988: The role of protein and lipid domains in the uptake of solutes by human stratum corneum. Pharmaceutical research, 5, 140-150.

Reiger, M. M. and L. D. Rhein, 1997: Surfactant in Cosmetics, Vol 68 New York:Marcel Dekker.

Rhein, L. D., C. R. Robbins, K. Fernee and R. Cantore, 1986: Surfactants structure effects on swelling of isolated human stratum corneum. .J. Soc. Cos. Chem. , 37, 127–139.

Ribaud, C., J. C. Garson, J. Doucet and J. L. Leveque, 1994: Organization of stratum corneum lipids in relation to permeability: influence of sodium lauryl sulfate and preheating. Pharmaceutical research, 11, 1414-1418.

Rosado, C., S. E. Cross, W. J. Pugh, M. S. Roberts and J. Hadgraft, 2003: Effect of vehicle pretreatment on the flux, retention, and diffusion of topically applied penetrants *in vitro*. Pharmaceutical research, 20, 1502-1507.

Rowe, E. S., 1983: Lipid chain-length and temperature-depen dence of ethanol phsphatidylcholine interactions. Biochemistry 22, 22, 3299-3305.

Shah, J. C., 1993: Analysis of permeation data: evaluation of the lag time method. International Journal of Pharmaceutics, 90, 161-169.

Shokri, J., A. Nokhodchi, A. Dashbolaghi, D. Hassan-Zadeh, T. Ghafourian and M. Barzegar Jalali, 2001: The effect of surfactants on the skin penetration of diazepam. Int J Pharm, 228, 99-107.

Somasundaran, P. and A. Hubbard, 2006: Encyclopedia of Surface and Colloid Science. Pezron I. 2nd ed. New York: Taylor and Francis.

Sonneck, H. J., 1964: Contact dermatitis caused by dioxane (German). Dermatol Wochenschr, 1, 24–27.

USEPA, 1992: Dermal exposure assessment: Principles and applications. U.S. Environmental Protection Agency, , Office of Health and Environmental Assessment, Washington D.C.

Vaddi, H. K., P. C. Ho and S. Y. Chan, 2002: Terpenes in propylene glycol as skin-penetration enhancers: permeation and partition of haloperidol, Fourier transform infrared spectroscopy, and differential scanning calorimetry. Journal of pharmaceutical sciences, 91, 1639-1651.

van der Merwe, D. and J. E. Riviere, 2005a: Comparative studies on the effects of water, ethanol and water/ethanol mixtures on chemical partitioning into porcine stratum corneum and silastic membrane. Toxicology *in vitro* : an international journal published in association with BIBRA, 19, 69-77.

van der Merwe, D. and J. E. Riviere, 2005b: Effect of vehicles and sodium lauryl sulphate on xenobiotic permeability and stratum corneum partitioning in porcine skin. Toxicology, 206, 325-335.

VCCEP, 2007: Voluntary Children's Chemical Evaluation Program. Tiers 1, 2, and 3 pilot submission for 1,4-dioxane. The Sapphire Group, Inc.

Walters, K. A., 1989: Surfactants and percutaneous absorption. In: Scott, R.C., Guy, R.H., Hadgraft, J. (Eds.), Prediction of Percutaneous Penetration: Methods, Measurements, Modelling. Ibc Technical services, London pp. 148 - 162.

Watkinson, R. M., C. Herkenne, R. H. Guy, J. Hadgraft, G. Oliveira and M. E. Lane, 2009: Influence of ethanol on the solubility, ionization and permeation characteristics of ibuprofen in silicone and human skin. Skin pharmacology and physiology, 22, 15-21.

Wester, R. C. and H. I. Maibach, 2000: Understanding percutaneous absorption for occupational health and safety. International journal of occupational and environmental health, 6, 86-92.

Wirth, W. and O. Klimmer, 1937: 1,4-Dioxan (Toxicity of organic solvents) (German). Int Arch Gewerbepath Gewerbehyg, 7, 192–206.

Zenker, M. J., R. C. Borden and M. A. Barlaz, 2003: Occurrence and treatment of 1,4-dioxane in aqueous environments. Environmental Engineering Science, 20, 423-432.